# Streamflow developments in western-Europe: are trends actually trends?

David Stouten
December 2023
Delft University of Technology

1st Supervisor: M. Hrachowitz
2nd Supervisor: E. Abraham

Faculty of Civil Engineering and Geosciences

# Abstract

This study aims to establish a framework for the growing number of trend analyses that have been performed on river flows in Europe. Most studies apply statistical trend test to fixed periods with relatively short records. Fixed periods are crucial for trend testing, as they provide an appropriate visualisation in a geographical sense. However, short-term changes can often be inconsistent with long-term trends. This study adopts two methods of trend testing. First, a trend analysis is performed over five fixed periods with an identical end year, on a varying number of stream gauges based on record length availability. Afterwards, a temporal sensitivity analysis is performed, whereby trends are estimated on all combinations of start and end year. This method is performed on stream gauges with at least 60 years of record length. These two methods are performed on an encompassing set of hydrological signatures, with the intent to capture the temporal sensitivity in all aspects of the streamflow regime. The results of the fixed period analysis display distinct but coherent spatial patterns for each signature. Furthermore, the results reveal a considerable amount of temporal variability in all signatures. This temporal sensitivity is elucidated further by the results of the temporal sensitivity analysis, which shows that trend analyses are extremely sensitive to the choice of both the start and end year of the considered period. The study provides a reference for comparison of both past, present and future studies. The temporal sensitivity analysis is shown to be a powerful tool and is recommended for future trend analysis studies to contextualize the short-term trends.

# Executive summary

Water can be considered the most crucial element of life on Earth. All living organisms require water for their survival. Thus, effective water management is one of the most important scientific fields. Additionally, water management has become significantly more topical in the past decades. There has been a growing global concern that the hydrological cycle is intensifying as a direct result of anthropogenic climate change. River floods and droughts are already among the costliest natural hazards, and they will become more frequent as a result of the intensifying of the hydrological cycle. Understanding changes in the hydrological cycle, and more specifically streamflow has become one of the most important challenges in modern hydrology. Reliable information on patterns in these changes enables the identification of changes in the streamflow regime influenced by large scale processes such as climate change. Hydrological changes occur in many different forms, spanning a wide range of both time scales and spatial dimensions. The present study aims to analyse past trends in various aspects of the streamflow regime. The main objective of this research is to analyse spatial and temporal patterns and trends in the entire streamflow regime.

An extensive literature review has been conducted to gain sufficient knowledge of the overall topic and the scientific areas relevant to this research. The fundamental aspects of the streamflow regime, and the overarching hydrological cycle are analysed. From there, the existing literature regarding the two largest concerns of water management is explored. These two concerns are fluvial flooding and droughts. The most important aspects of the streamflow regime are researched and the hydrological signatures that are relevant to these aspects are investigated.

An encompassing set of hydrological signatures is drafted. This set aims to capture the most important aspects of the streamflow regime, across all stages of flow. These hydrological signatures are then determined on a dataset of nearly 1200 stream gauges in western Europe. These stream gauges vary greatly in both record length and contributing catchment area. Trends in these signatures are analysed using the Mann-Kendall test and the Theil-Sen slope estimator. First on five fixed periods with an identical end year, this provides a good visualisation of both spatial and temporal patterns in these trends. Finally, a temporal sensitivity analysis is conducted to contextualise the consistency of short-term trends with long-term trends.

The results show that most signature display a high degree of variability in both the magnitude and direction of trends. This variability can be seen on both the spatial-and-temporal scale. Similarities across different signatures are also found. The most recent years of the analyses (i.e., 2015 – 2019) show a relatively high degree of consistency of short-term trends in long-term trends. This implies that signatures of these years are significantly high or low, that trends are consistent. The results of the temporal sensitivity analysis visualise the patterns of the variability in trends, both in magnitude and direction.

The research concludes that the interpretation of trend analyses has to be well substantiated. This is done by highlighting the intricate patterns of temporal variability across various signatures in the streamflow regime. In order to correctly interpret hydrological trend studies, one must investigate the large number of influencing factors. Examples of these factors are climate change, multidecadal oscillation patterns and anthropogenic influences. The results in this study can be used for future studies which intend to delve deeper into more specific parts of the streamflow regime to indicate how the streamflow has broadly changes and how these changes are highly variable in both the spatial and temporal scale. Future research should expand on this research by attempting to explain the driving mechanisms of the temporal variability and thereby developing more sophisticated and innovative methods of trend detection that consider temporal variability and its driving mechanisms.

# Table of Contents

# 1. Introduction

Effective water management is one of the most vital aspects to life on Earth. River floods are one of the costliest natural hazards, with the global annual average losses being estimated at $104 billion (’Desai et al., 2015). Additionally, droughts are among the costliest and recurring natural hazards as well (Peña-Angulo et al., 2022). There is a growing global concern that the hydrological cycle is intensifying as a direct result of anthropogenic climate change (Allan et al., 2020). This intensifying of the hydrological cycle is causing changes to the streamflow regime. Therefore, there is a growing demand for observational streamflow data which can be used to identify emerging trends in river flows. This streamflow data and emerging trends should also be compared with future projections from climate models.

This demand has led to a large number of hydrological studies being focused on trend analyses using observational streamflow data. Over the past decade there has been a surge of studies that have investigated different aspects of streamflow across a wide variety of regions and spatial scales. Studies such as (Blöschl et al., 2019; Mangini et al., 2018) have investigated trends in the magnitude of floods across Europe over the past decades. (Berghuijs, Woods, et al., 2016; Blöschl et al., 2017) have studied the timing and seasonality of flooding across the United States and Europe respectively. Fluvial flooding has received significantly more attention than fluvial droughts due to its more direct and visible impact, but research on droughts has been conducted. (Barker et al., 2016; Hisdal et al., 2001; Peña-Angulo et al., 2022) are examples of studies investigating patterns of hydrological droughts.

There has been a large increase in the number of hydrological studies that focus exclusively on networks of near-natural catchments with long high-quality data. The purpose of this focus is to connect trends to climate change and/or variability rather than direct anthropogenic influences (e.g. dams, water removal for irrigation or domestic consumption). These disturbances can obscure the climate change signal. Studies by (Frei et al., 2015; Stahl et al., 2010) are focused on networks of near-natural catchments in the United States and Europe respectively. There also exist studies that focus on the impact of anthropogenic influences, such as (Vorogushyn & Merz, 2013). These studies are often focused on a single catchment or river to assess the impact of anthropogenic disturbances.

One fundamental problem with observational streamflow data is the relatively short duration of most streamflow records. (Kundzewicz & Robson, 2004) states that at least 50 years of record is necessary for proper climate change detection. In Europe, the majority of streamflow records are 50 years or shorter, starting from the 1970s or later. Combined with the desire of using only near-natural catchments this leads to relatively low spatial coverage. In trend analyses this means that study periods are selected to maximize both the spatial and temporal coverage (Mangini et al., 2018).The most recent periods provide the greatest spatial coverages and are therefore given the most attention.

One crucial consideration in the interpretation of the results from these studies is the fact that a trend in any fixed period, however long it might be, may not be representative. Trends can be heavily influenced by multi-decadal variability and/or oscillations. The underlying reasons for these oscillations in streamflow are not immediately clear. They are often not actively sought after or only briefly mentioned in studies. Furthermore, there is a widespread belief that the past is no longer indicative of the future. This is represented by the statement “stationarity is dead” (Milly et al., 2008). This statement is questioned by both (KOUTSOYIANNIS, 2003; Montanari & Koutsoyiannis, 2014), which show that streamflow generally shows long-term persistence. The physical interpretation of this long-term persistence may prove to be difficult. However, it is visible that trends can be influenced by (multi) decadal scale variations that are driven by physical process which are often well understood. For example, (Steirou et al., 2017) provides a literature review of links between large scale circulation

pattern and streamflow in Central Europe. The review paper displays the abundance of studies linking atmospheric circulation patterns to streamflow variability in various parts of the world.

As a result of the sensitivity of linear trends to these multidecadal oscillations or other influencing patterns, the idea of conducting multi temporal trend analyses has gained more attention in the recent years. (Hisdal et al., 2001) investigates four different time periods with a similar ending year to detect spatial and temporal changes in streamflow droughts. Both (Frei et al., 2015; Stahl et al., 2010) have investigated multiple fixed periods to detect interdecadal variability in streamflow developments.

However, there does not exist a recent study that applies a multi-temporal trend testing method at a larger scale in Europe. As mentioned previously, past studies have mainly focused on flooding rather than each aspect of the streamflow regime and the different stages of flow (low, average and high flow). This study aims to investigate spatial patterns and temporal trends in a number of hydrological signatures that represent all aspects of the streamflow regime, during each stage of flow. Furthermore, patterns of multidecadal variability in these signatures are characterized to examine its impact on the observed linear trends in fixed periods. The present study is meant to serve as a benchmark against which the findings of past and future studies can be evaluated.

This paper is organized in the following way. Section 2 provides the research framework, providing a more detailed description of the problem statement and stating the research objectives. Section 3 gives a review of the literature study that was performed to properly conduct this research. Section 4 describes the methodology of the trend testing. Section 5 presents the results and section 6 provides a discussion on the implications of these results. Finally, conclusions are drawn.

# 2. Research framework

This section elaborates on the underlying motivation and structure of this study. It provides a clear roadmap of the entire research. A comprehensive exposition is provided of the problem statement, which serves as the motivation for this research, elucidating its context and significance. Based on this problem statement, multiple research objectives are drafted. These research objectives are then supported by several research questions which are formulated to help achieve the research objectives.

## 2.1 Problem statement and societal relevance

Water can be considered the most crucial element of life on this planet. All organisms on earth, including humans, require water for their survival. Therefore, it is vital to ensure that there is an adequate supply and availability of freshwater resources. Since a few decades, water scarcity has become a major threat to livelihood and a large confining factor to socio-economic developments in increasing parts of the world (Liu et al., 2017). There has been a large increase in water demand globally, mainly due to factors such as rapid population growth and economic development. On the other hand, climate change has led to higher concerns regarding the increase in river floods. This increase is a result from the increased water holding capacity of a warmer atmosphere (Field, 2012). Fluvial flooding is among the costliest natural hazards globally. The estimated global annual average losses due to fluvial flooding are $104 billion (’Desai et al., 2015), and these are expected to increase with the rapid population growth, economic development and urbanization. The main factor of these increases being rapid climatic changes.

So it is known that there are ever more increasing concerns regarding many aspects of global water. Due to these concerns, the scientific fields of water management and hydrology is becoming more and more relevant as time passes. The key to effective water management is a deep understanding of the hydrological cycle, which describes the continuous movement, or circulation, of water in the Earth-Atmosphere system. Figure 1 displays the many processes, fluxes and storages of the hydrological cycle.

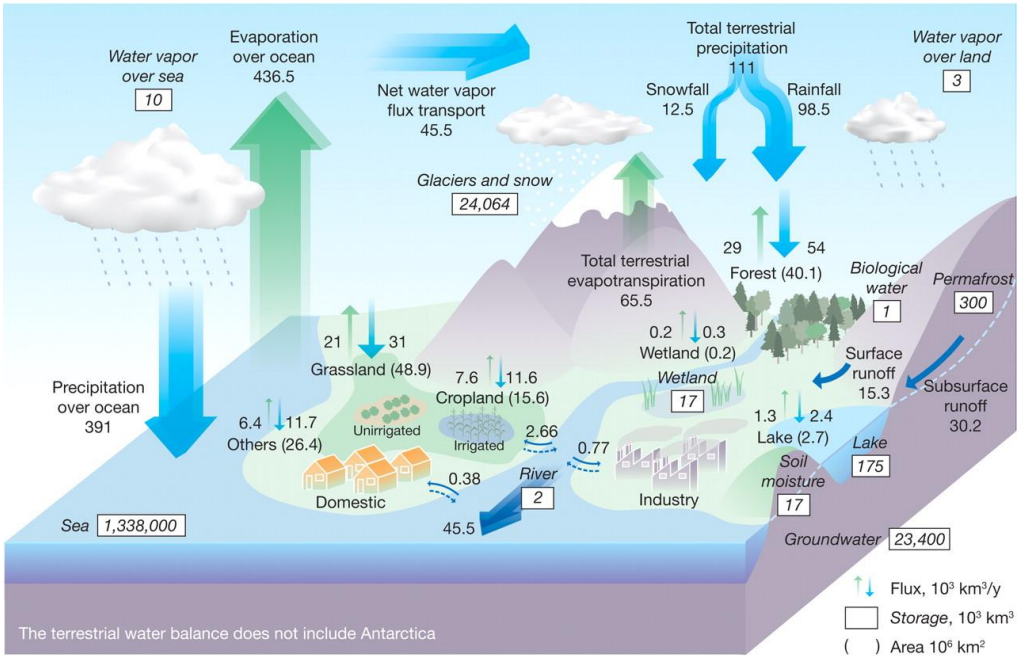


*Figure 1: Global hydrological fluxes (1000 km3/year) and storages (1000 km3) with natural and anthropogenic cycles from (Oki & Kanae, 2006). Big vertical arrows show total annual precipitation and evapotranspiration over land and ocean (1000 km3/year), which include annual precipitation and evapotranspiration in major landscapes (1000 km3/year) presented by small vertical arrows; parentheses indicate area (million km2).The direct groundwater discharge, which is estimated to be about 10\% of total river discharge globally, is included in river discharge.*

About 2.5 % of the total water on Earth is considered to be fresh water, and most of this fresh water is stored as either glaciers or deep groundwater. Figure 1 shows that the amount of water stored in rivers is just 2000 $km^3$, which is significantly less than the annual water withdrawal of 3800 $km^3$/year. However, the total water storage in rivers is not an appropriate measure. This is because, unlike most other natural resources, water has a closed circular nature. This means that when water evaporates from the sea or open water surfaces, it changes from liquid form to gas form. This gas form is commonly known as clouds. The water within these clouds eventually recondenses as precipitation and, through different pathways, will find its way back into the rivers. From there it flows into the sea and open water surfaces, where it will evaporate again, restarting the cycle once again. Thus creating a closed hydrological cycle. This indicates that using the 45500 $km^3$/year of annual river discharge would be a more accurate measure of water availability.

As mentioned previously, there are also the growing concerns regarding fluvial flooding. (Field, 2012) critically assessed the scientific literature focusing on climate change and the global impact resulting from these events. The IPCC report defines many different types of floods, including fluvial (river) floods, coastal floods, flash floods and urban floods. Each of these floods are often hazardous, not only to human life, but also to flora, fauna and the overall environment. Floods are affected by several aspects of the climate system (Kundzewicz et al., 2014; Kundzewicz & Robson, 2004). The largest influencing factor is precipitation. The intensity, duration and timing of precipitation all influence streamflow and floods. Temperature patterns, which can cause phenomena such as snow/ice melt and soil freezing are large are also large influencing factors. Floods are also affected by the environmental, or drainage basin conditions, such as the soil moisture content. All of these phenomena are in a way affected by climate changes and have led to flood regime changes around the globe.

When considering the annual river discharge, also known as streamflow, as the most relevant measure for water resources and water management, extensive and deep knowledge about the hydrological and streamflow regimes is crucial. The streamflow regime is the characteristic pattern of a river's flow, timing, quantity and variability (Poff et al., 1997). In simpler terms, it is the description of how water flows through the river. In modern hydrology, elucidating temporal and spatial patterns of hydrological change has become one of the most essential challenges (Stahl et al., 2010). Elucidating these temporal and spatial patterns provides an understanding of trends which have occurred over the past decades. Comparing trends over different time periods gives insight into whether short-term changes are consistent with long-term changes. These trends and patterns can be linked to observed climate forcing data from the same period to better understand the relationship between climate forcings and changes in the streamflow. Analysing and visualising trends in the streamflow regime of the past decades and subsequently linking them to climate forcings is essential for appropriately predicting future trends. This better understanding can thus serve as a baseline for future water management.

Hydrological changes occur in many different forms, spanning a wide range of both time scales and spatial dimensions. The most common method to investigate these changes is by defining and determining hydrological signatures, such as the annual maximum flow . These hydrological signatures in turn can be used on a wide range of applications. In order to obtain sufficient knowledge about the hydrological state of rivers, hydrological signatures should be selected that encapsulate the entire streamflow regime. (McMillan, 2020) provides an extensive review of various hydrological signatures and their respective applications and (Olden & Poff, 2003) examines a large number of hydrological signatures, analysing them on both relevance and redundancy. Many studies often tend to focus on one aspect of the streamflow regime and select signatures which are relevant to that specific aspect. There seems to be a lack in studies which create an encompassing set of hydrological signatures to characterize the entire streamflow regime and subsequently analyse these signatures on spatial and temporal patterns.

## 2.2 Research objectives and research questions

As mentioned above, understanding the hydrological state of rivers and potential changes in this state is essential for effective water management. A broad and deep knowledge of both the hydrological cycle and the streamflow regime is crucial. This can be achieved by analysing past trends in various aspects of the streamflow regime. The main objective of this research is to analyse spatial and temporal patterns and trends in the entire streamflow regime. As mentioned above, there appears to be a lack of an encompassing and parsimonious set of hydrological signatures to characterize the entire streamflow regime. This research also aims to fill this knowledge gap and create an appropriate set of hydrological signatures to characterise the streamflow regime. This second research objective will support and substantiate the main research objective. Finally, this research aims to identify potential decadal-scale variability in streamflow trends over multiple overlapping time periods. This will be done to demonstrate the sensitivity of a trend analysis to the choice of time period. In summary, the research objectives can be written down as one main objective, with two underlying and supporting objectives. The objectives are defined as:

- Analyse spatial patterns and temporal and trends in river flows, considering the entire streamflow regime.
    - Create a proper set of hydrological signatures to characterize the streamflow regime.
    - Identify decadal-scale variability in streamflow trends across the streamflow regime.

In order to accomplish these research goals, multiple research questions have been drafted, these research questions are divided over the three research objectives. The research objectives will be accomplished by answering the following questions:

- Analyse spatial and temporal patterns and trends in river flows
    - Can change be detected in the river flow characteristics over the past decades?
    - How have the river flow characteristics changed over the past decades?
    - What spatial patterns can be detected regarding the changes in flow characteristics?

- Create a proper set of hydrological signatures to characterize the streamflow regime.
    - What are the most important aspects of the streamflow regime?
    - What are the most commonly used hydrological signatures?
    - How to select a sufficient number of signatures, whilst avoiding redundancy?

- Identify decadal-scale variability in streamflow trends across the streamflow regime.
    - Do differences in trends occur when analysing them across different time periods?
    - How consistent are trends in different signatures across different time periods?
    - Are short-term changes representative of the magnitude and direction of long-term change?

A crucial aspect of this research is that no expectations and/or hypotheses are stated, the aim is not to answer specific questions about hydrological changes. The aim of this research is to show how the entire streamflow regime in Western Europe has changed. This is done over several time periods to show whether these trends are sensitive to the choice of time period.

# 3. Literature review

In order to gain sufficient knowledge of the overall topic and the scientific areas relevant to this research, an extensive literature review is carried out. This section describes the phenomena found during the literature review. The findings of this study are important to the research in a number of ways. Firstly, they are intended to provide an adequate level of knowledge of the methods commonly applied in hydrological trend analysis studies. This will ensure that, for example, decisions regarding assumptions and methods are well founded. Secondly, this literature review serves as an inspiration for this research. Whilst all the methods, concepts and phenomena that have been analysed in the past can be found in this literature review, it is also important to identify potential gaps in knowledge that can be filled by this research.

## 3.1 Hydrological cycle in the changing climate

Water is unique among natural resources due to its circular nature (Allan et al., 2020; Oki & Kanae, 2006). Evaporation from oceans and other open water surfaces converts liquid water to a gas form, which then recondenses and returns to the oceans or other water surfaces through various pathways. An overview of the hydrological cycle has already been shown in Figure 1.

The hydrological cycle is influenced by natural factors, such as variations in solar activity and volcanic eruptions, as shown by (Allan et al., 2020). Furthermore, paleoclimatic records demonstrate significant changes in the past. (Buckley et al., 2010; Haug et al., 2003). However, it is evident that anthropogenic activities increasingly dominate changes in the hydrological cycle (Allan et al., 2020; Oki & Kanae, 2006). This is occurring indirectly through climate response to greenhouse gas emissions and directly from groundwater extractions and land surface interference (Abbott et al., 2019). While global mean precipitation changes are mainly determined by changes in the global energy, regional changes can be attributed to the transport of water vapor and dynamic processes. Changes in weather patterns are dependent on heating and cooling patterns in Earth's atmosphere and across the planet's surface. Future climate project (Field, 2012; Intergovernmental Panel on Climate Change, 2014) suggest that precipitation frequency, intensity and duration, among other water cycle characteristics will undergo changes.

Precipitation is the primary source of water for rivers, and changes in precipitation variability directly impact the amount of water flowing into rivers. Understanding changes in precipitation variability is crucial for comprehending the hydrological cycle's response to global warming and its effects. Precipitation variability refers to the fluctuations in the amount, intensity, and frequency of rain, snow, or other forms of precipitation over a particular area and time period. These fluctuations have major societal, agricultural and environmental relevance (Pendergrass et al., 2017). Precipitation variability also connects the extreme precipitation events (i.e. floods and droughts). It is commonly assumed that precipitation variability remains unaffected in a warming climate (Hawkins & Sutton, 2011; Thompson et al., 2015). Or that the precipitation mean and variability change at the same pace (Gellens & Roulin, 1998).

The aim of (Pendergrass et al., 2017) is to formulate a complete theory on how precipitation is affected by a warming climate. Precipitation variability is quantified by its standard deviations and analysed through a set of model simulations that were subject to a single forcing scenario. The analysis focuses on model simulations driven by a significant increase in greenhouse gas forcing along with changes in aerosol forcing. In the majority models the precipitation variability increases robustly over almost all land areas in response to anthropogenic warming. For longer timescales (i.e. interannual and longer) the forced increase may be compensated for or amplified by natural variability. In the majority of the models, the change in precipitation variability is more significant than the change in mean precipitation and less significant than the change in moisture and extreme precipitation. Over large spatial and temporal scales, the increased precipitation variability is a robust emergent aspect of the hydrological cycle that is changing due to anthropogenic climate warming. Further research in both theoretical work

and impact studies is needed to enhance and link the comprehension of changes in mean precipitation, variability, and extremes. These extreme precipitation events are further elaborated on in the following sections of this report.

## 3.2 Fluvial flooding

As mentioned in section 2.1, river floods are among the costliest natural risks. The study by (Blöschl et al., 2020) examines the current flood rich period from a long perspective. It is shown that the past three decades were among the most flood-rich periods in Europe in the past 500 years. The risks and costs are expected to increase due to phenomena such as climate change, rapid urbanization and economic growth (Winsemius et al., 2016). Due to these growing concerns and risks, there has been a large number of studies focused on a variety of aspects of fluvial flooding.

Understanding studies on fluvial flooding starts with the most basic concept: the definition of a flood. A flood, in layman terms, is defined as an overflow of water into normally dry land. (Field, 2012; Kundzewicz et al., 2014) define floods as: *"the overflowing of the normal confines of a stream or other body of water or the accumulation of water over areas that are not normally submerged. Floods include river (fluvial) floods, flash floods, urban floods, pluvial floods, sewer floods, coastal floods, and glacial lake outburst floods."* Both of these definitions give the physical definition of flooding.

A flood is a physical phenomenon. This presents several challenges when analysing flooding. The main reason is that these physical events hold little to no statistical significance. Consequently, floods are commonly characterised using specific quantitative criteria or thresholds associated with hydrological parameters. These definitions serve as a foundation for analysing historical flood data, identifying trends and investigating the impact of floods. As floods can vary significantly in terms of magnitude, duration and frequency, these statistical definitions provide a mean to analyse and compare different flood events.

In general, two statistical methods are used to define floods and derive time series of flood events. The first method is the annual maximum flow (AMF) (Blöschl et al., 2019). The second method is the peak over threshold approach (POT) (Mangini et al., 2018; Petrow & Merz, 2009). A comparison of the two methods is outlined by (Cunnane, 1973; Madsen et al., 1997). The AMF method consists of determining the highest yearly discharge values, creating the AMF time series. The primary benefit of this method is the fact that two successive flood events can be considered independent. However, the AMF method has a disadvantage in that it can neglect smaller flood events as they are not the highest flow event in that respective year (Mangini et al., 2018). These smaller events can still hold a significant societal relevance. The POT approach establishes a threshold value which is considered as a flood event. The POT series then consists of flood peaks exceeding this predefined threshold. With this method it is important to ensure that POT events are independent, i.e. that events do not occur on the recession curve of the preceding event. The POT approach allows for the detection smaller flood events and the detection of trends in the mean number of flood events per year. The POT approach is also denoted as the partial duration series (PDS) method.

Flood studies generally concentrate on one of these two methods. The most common approach is the AMF method. This is largely due to the availability of records. A disadvantage, that both the AMF method and the POT approach share is that these statistical events are not necessarily large enough to physically inundate the floodplains. These two methods have limited usefulness for characterizing actual overbank floods because these physical flood events occur, on average less frequently than once per year (Wolman & Miller, 1960). An alternative method is therefore proposed by (Collins et al., 2022) wherein the 10 largest AMF flows observed in a 50-year period. These flood events have empirical return periods ranging from approximately 5 years ($10^{th}$ largest event) to 50 years (largest event). This method aims to identify the actual overbank flows and therefore the river flows which are the most relevant for actual damages.

Regardless of how a flood is defined, there is a wide variety of types of analysis and corresponding methods for studying fluvial flooding. There are several aspects of fluvial flooding, each of which has received different levels of attention from researchers. The aspect that has been researched the most is the magnitude of flooding, which is also the most straightforward characteristic.

An example of a study conducting analyses on the magnitude of fluvial flooding is given by (Blöschl et al., 2017). It claims to be the first study to provide coherent large-scale observational evidence of flood discharge changes at the continental scale (European continent). Previous studies were not representative of Europe, as stream gauges were mainly concentrated in Western-Europe. Therefore, a trend analysis is performed on the most comprehensive dataset of flood observations in Europe (Hall et al., 2015). (Bertola et al., 2020) further extends this magnitude trend analysis, using the same database and developing selection criteria to ensure comparability with (Blöschl et al., 2017). While the first study only examines changes in the magnitude of the AMF events, this study aims to assess the changes in small versus big floods by looking at the corresponding flood quantiles. In addition to this, the effect of catchment area is also assessed by comparing changes in flood quantiles for different catchment areas. The results from (Blöschl et al., 2017) & (Bertola et al., 2020) are given by Figures 2 and 3 respectively.

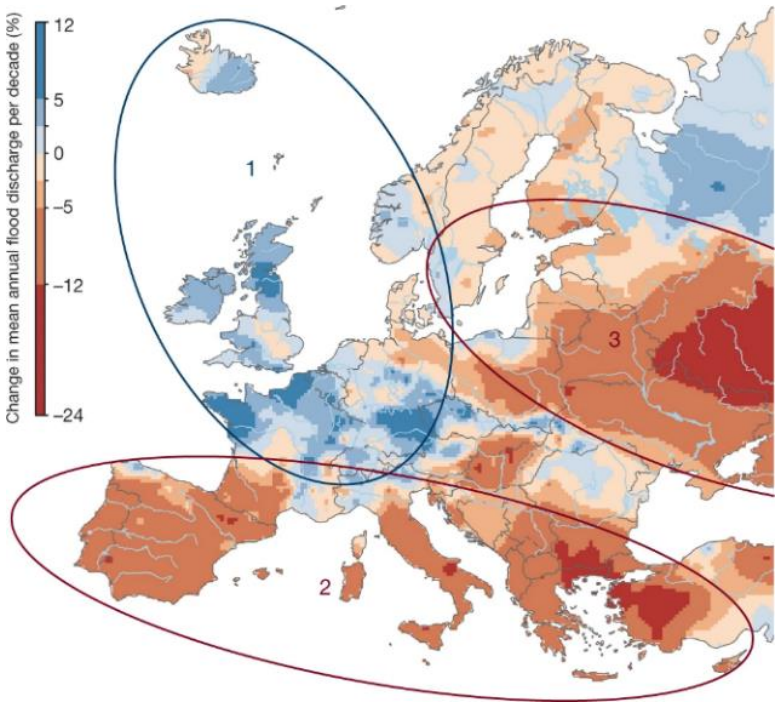


*Figure 2: Observed regional trends of river flood discharges in Europe (1960 - 2010) by (Blöschl et al., 2019). Blue indicates increasing flood discharges and red denotes decreasing flood discharges (in per cent change of the mean annual flood discharge per decade).*

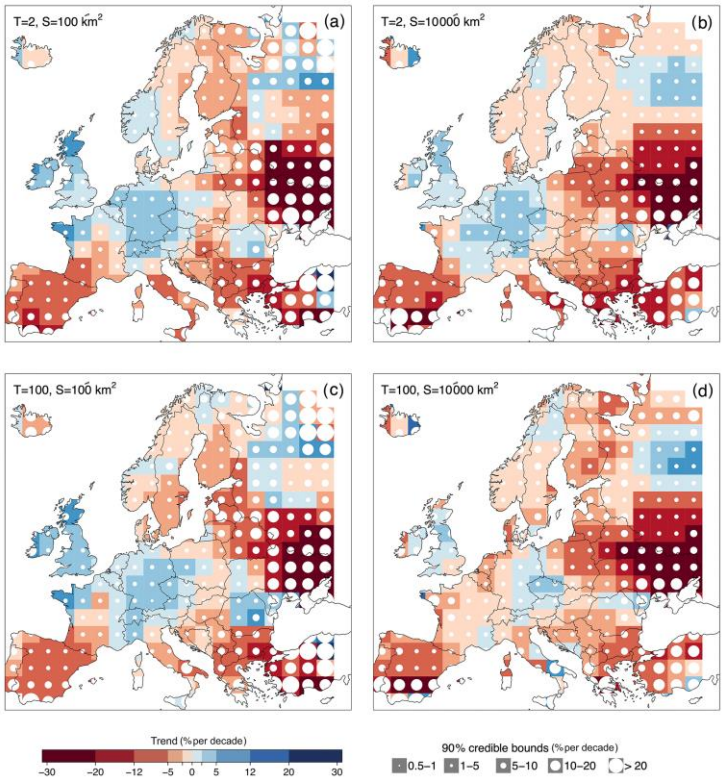


*Figure 3: Flood trends in Europe: small vs big floods by (Bertola et al., 2020). The panels show the median of the posterior distribution of the regional relative trends of flood quantiles in time (i.e. the percentage change in per cent per decade). Positive trends in the magnitude of flood quantiles are shown in blue, and negative trends in red. Circle size is proportional to the width of the 90 % credible intervals. Results are shown for the median flood (i.e. T = 2 years), in panels (a, b), and for the 100-year flood, in panels (c, d). Flood trends refer to a small catchment area (i.e. 100 km2 ) in (a, c) and to a large catchment area (i.e. 10 000 km2 ) in panels (b, d).*

Looking at the two figures, the similarity is very clear. The data show a clear regional pattern in flood magnitude trends across Europe, with increasing floods in north-western Europe and decreasing floods in eastern Europe. In smaller catchments the 100-year flood increases more than the median flood, while the opposite is observed in medium and large catchments.

Another aspect of fluvial flooding that is often studied is the timing of floods. There are several ways to study the timing of floods. (Blöschl et al., 2017) investigates the timing of the AMF events in a year to assess whether the timing of river floods has shifted. Circular statistics are then used to determine the average date of occurrence, the concentration of events around that date, and to estimate trends in the timing of river floods based on Julian dates for each stream gauge. (Bayliss & Jones, 1993; Mardia, 1975) This approach accounts for the cyclical nature of annual flood occurrence and provides valuable insights into temporal patterns of hydrological phenomena.

A common method to study the timing of floods is to analyse the river flood seasonality. River flood seasonality refers to the recurring patterns of timing of river floods within a year. It involves identifying when in the year a river is most likely to experience increased water levels that result in flooding. The river flood seasonality reflects the relative importance of different flood-generating mechanisms (Collins, 2019). Changes in flood seasonality can indicate and explain changes in flood-generating mechanisms. Inferring these different flood-generating mechanisms is crucial for understanding past, present and future flood risks. (Berghuijs, Hartmann, et al., 2016; Berghuijs, Woods, et al., 2016) provide such analyses for Europe and the United States respectively. Both studies follow roughly the same approach. First, the mechanisms that can cause flooding are defined. The mechanisms are (i) extreme precipitation, (ii) soil moisture excess and (iii) snowmelt. These mechanisms are then described by simple process descriptions to characterise the seasonality. The seasonality statistics of floods and the

driving mechanisms are then calculated are calculated by using the circular statistics mentioned above. An example of the seasonality characteristics floods and flood-generating mechanisms characterized by circular statistics is shown in Figure 4.

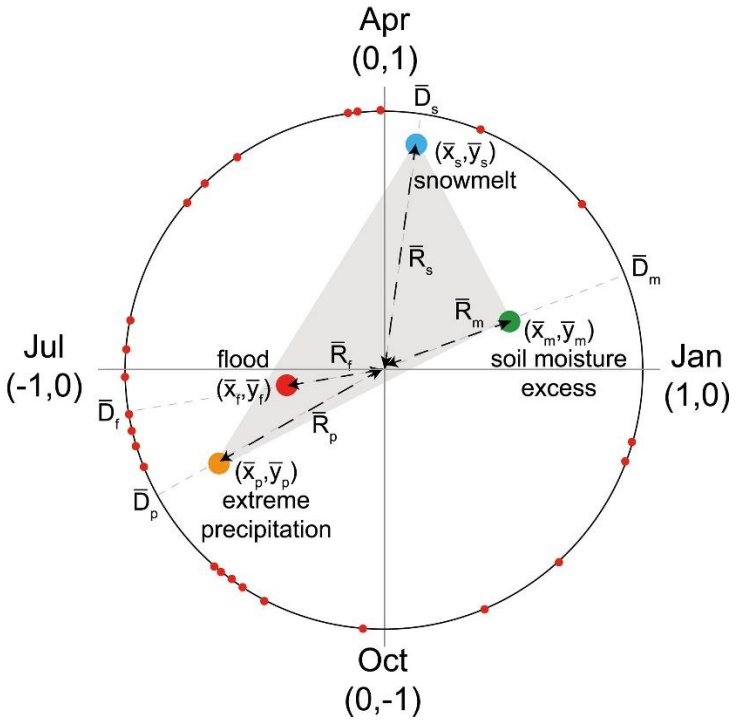


*Figure 4: The seasonality characteristics of floods and flood-generating mechanisms characterized by circular statistics for the Reuss river by (Berghuijs et al., 2019) . The dates of occurrence of each year, Di,k (day of year), fall on the unit circle (here only shown for floods). These dates are used to derive the mean cosine and sine components, xi and yi and thus to estimate the mean date of flooding. The concentration, Ri (dimensionless), expresses how tightly occurrences are clustered around the mean date, and the subscripts indicate the process of interest (f = flood, p = precipitation, m = soil moisture excess, and s = snowmelt). The cosine and sine components of the flood generating mechanisms are used to infer their relative importance as flood drivers by comparing their seasonality statistics.*

With these seasonality statistics, the final step is to estimate the relative importance of each mechanism by solving the following set of linear equations:

$$\alpha_p \bar{x}_p + \alpha_m \bar{x}_m + \alpha_s \bar{x}_s = \bar{x}_f,$$

$$\alpha_p \bar{y}_p + \alpha_m \bar{y}_m + \alpha_s \bar{y}_s = \bar{y}_f,$$

$$\alpha_p + \alpha_m + \alpha_s = 1,$$

where $\alpha_i$ indicates the relative importance of each flood driver (with $[0 \leq \alpha_i \leq 1]$), and $x_i$ and $y_i$ are the average cosine and sine components of the dates of occurrence.

## 3.3 Droughts

Droughts are also among the most damaging and most costly recurring natural hazards, with devastating economic, ecological and political impacts (Ide, 2018; von Uexkull et al., 2016; D. A. Wilhite & Pulwarty, 2017). Changes in drought severity, frequency, duration and timing will have major implications for water management. With the projected global temperature increase, scientists agree that extreme droughts will become more frequent. Drought can be considered as a normal, recurrent climatic phenomenon (Hisdal et al., 2001).

Drought is by definition a relative term, which is applicable to any climate region. Like floods, droughts can also be defined in a variety of ways. Droughts are most commonly defined as streamflow or precipitation deficits relative to average conditions. However, this is not the only definition of droughts,

and a discussion of different drought definitions can be found in (Dracup et al., 1980; D. A. Wilhite & Glantz, 1985). Characterising droughts, both in terms of severity and risk is a difficult task. This is because droughts are rarely confined to a single location. Instead, droughts often affect large regions and extend over long periods such as months, years or even decades (Van Loon & Laaha, 2015).

Another reason why droughts are difficult to characterise is the fact that drought evolution is influenced by a wide variety of hydrometeorological variables, such as precipitation, runoff, evaporation, transpiration and antecedent soil moisture content (Mishra & Singh, 2010; Sheffield et al., 2012). Four types of droughts are given by (Peña-Angulo et al., 2022) : agricultural droughts, hydrological droughts, meteorological droughts and socioeconomic droughts. Among these four types, hydrological droughts are the most relevant for policy makers and hydrologists due to the societal reliance on water availability in river systems (Van Loon & Laaha, 2015).

The first pan-European study on droughts was conducted by (Briffa et al., 1994), who examined summer (June-August) moisture variability across Europe for 1892-1991 using the Palmer Drought Severity Index (PDSI) (Palmer, 1965). Prior to the publication of (Briffa et al., 1994) the PDSI had been widely used to study the nature of drought over the United States, but there had been no studies based on the method outside of the US. This work was largely prompted by the extensive nature of the drought that affected large parts of Europe from 1988 to 1992 (Marsh & Monkhouse, 1993; Tselepidaki et al., 1992). Despite its title, the PDSI represents the full range of moisture conditions, from extremely wet to extremely dry. It was created as a meteorological index expressing regional moisture supply, standardised in relation to local climatological norms. It therefore does not represent effective drought in absolute terms. The PDSI is based on a water balance calculation and requires a number of arbitrary assumptions (Palmer, 1965). Using a principal component analysis (Jolliffe & Cadima, 2016), nine regions are identified based on the spatial coherence of the PDSI. The study concludes that there has been a slight, but consistent increase in moisture supply over the entire period, although this is not statistically significant. The PDSI data which is described by (Briffa et al., 1994) was meant to serve as a useful resource for further climate studies.

The first data and trend analysis study based on actual streamflow data in Europe is conducted by (Hisdal et al., 2001). In this study, a pan-European dataset of more than 600 daily streamflow records is analysed to detect spatial and temporal patterns in streamflow droughts. The two different methods described in the previous section, being AMS and PDS are studied over four different time periods. The aim of this paper was to answer the question of whether hydrological droughts have become more severe or more frequent. The paper states that for a consistent analysis of droughts, it is necessary to distinguish between summer and winter droughts. Summer droughts are caused by a lack of precipitation and high evaporation. Winter droughts are by precipitation that is being stored as snow. The distinction is made because these types of droughts have different implications for water management. Five drought parameters are defined in the study, being annual maximum drought duration (AMD), annual cumulated duration of all drought events (ACD), annual maximum deficit volume standardised by seasonal mean flow (AMV), annual cumulated deficit volume standardised by seasonal mean flow (ACV) and number of drought events per year (NV). In most of the catchments no significant trends are found, but distinct regional different are found across all time periods. Large areas where less severe drought conditions can be explained by an increase in precipitation are found and more severe drought conditions due to a decrease in precipitation. In addition to the trend analysis, the influence of the chosen time period is investigated. The temporal scale of a trend analysis is important when assessing the trend. What appears to be an increasing trend over a ‘short’ period of observation may be part of a long- term fluctuation and therefore cannot be seen as evidence of anthropogenic climate change, nor can it be used as a baseline for future predictions. It is concluded that, despite several reports of droughts in Europe at the time, there is no clear evidence that drought conditions have generally become more or less severe.

This study dates back than two decades. A similar, more recent study is given by (Peña-Angulo et al., 2022). In this study a hydrological drought is defined as a period with streamflow below a predetermined

threshold. The Standardised Streamflow Index (SSI) is used to identify hydrological drought events (Barker et al., 2016). This index compares hydrological droughts irrespective of streamflow magnitude or river system characteristics. The study identifies six homogeneous regions representing the changes in monthly streamflow across Europe. The differences observed in these clusters are expected to correspond to different physical mechanisms controlling the climate and streamflow variability in the regions. The findings of the study indicate that there are no homogeneous streamflow trends in space nor over months at the continental scale. Again the findings of the study show that there are large spatial and temporal differences in streamflow across Europe. In general, the monthly streamflow as characterised by the SSI showed a negative trend in southern and central Europe. A positive trend was observed in northern Europe. The study also reveals distinct patterns at the monthly scale. These changes in streamflow are generally consistent with the spatial patterns of changes in hydrological droughts. This suggests that hydrological droughts in Europe are not homogeneous, and therefore result from different driving mechanisms.

## 3.4 Natural flow regime (Streamflow regime)

The natural flow regime, also known as the streamflow regime, is a fundamental aspect of river ecosystems. Understanding the streamflow regime is vital for water management and maintaining the river ecosystem health. The streamflow regime refers to the variation in streamflow over different timescales. More precisely, the streamflow regime describes exactly how a river flows. The importance of streamflow in the hydrological cycle has been mentioned in section 2.1. Thus, understanding the streamflow regime is essential for a better understanding of the hydrological cycle. (Poff et al., 1997) provides a detailed and comprehensive study on the streamflow regime. The natural flow of a river can vary on time scales from hours to years, or even decades. A deep understanding of this regime requires many years of observational data from a stream gauge. Streamflow regimes show regional patterns, which are largely determined by factors such as river size and by geographic variation in climate, geology, topography, and vegetative cover. There are five critical components of the streamflow regime that regulate processes in river ecosystems: the magnitude frequency, duration, timing and rate of change of hydrological conditions (Poff & Ward, 1989; Richter et al., 1996; Walker et al., 1995).

**The magnitude** of discharge at a given time interval is the amount of water moving through the river at a given location per unit of time. The magnitude can be either absolute or relative discharge.

**The frequency** of occurrence refers to the number of times the streamflow is above or below a certain threshold. Frequency of occurrence is inversely related to magnitude of discharge (Poff et al., 1997). The higher the magnitude, the lower the frequency of occurrence. For example, a 50-year flood is exceeded on average once every 50 years resulting in a frequency of 0.02. The magnitude of the average or median flow from a timeseries has a frequency of occurrence of 0.5.

**The duration** is the period of time is associated with a specific flow condition. Duration can also be an absolute period (hours, days) or relative period (% of year).

**The timing**, also known as the predictability, of streamflow refers to the regularity with which a specific flow event occurs. This regularity can be defined informally or formally and with respect to different timescales (POFF, 1996). This means that flow events can occur with a low or high seasonal predictability.

**The rate of change,** also known as the flashiness, of streamflow refers to the rate at which the streamflow changes from one magnitude to another. Flashy rivers have rapid rates of change, while stable rivers have slow rates of change.

All streamflow is ultimately derived from precipitation, but will always be a combination of surface water, groundwater and subsurface water. Climate, geology, topography, soils, and vegetation influence

both the supply of water and the pathways by which precipitation reaches the river channel. Hydrograph peaks, which are the river's response to precipitation events, are generated collectively by overland flow and shallow subsurface flow. In contrast, baseflow, which is the supply of water to a river during periods of low precipitation, is generated by deeper groundwater flows. Variability in precipitation intensity, timing and duration, combined with the effects of terrain, soil texture and plant evapotranspiration on the hydrological cycle combine to create diverse local and regional flow patterns.

## 3.5 Hydrological signatures

Hydrological signatures are metrics that are created to quantify aspects of the streamflow response. Linking these signatures to the actual underlying hydrological processes enables many applications such as analysis of hydrological change, selection hydrological model structure and identification of dominant processes. A comprehensive literature review is provided by (McMillan, 2020). The review states that many hydrological signatures are not process-based and that knowledge of signature-process relationships is scattered among studies. Rather than being linked to hydrological processes, signatures often focus on capturing elements of the streamflow regime that are relevant to ecological applications (Clausen & Biggs, 2000). The review paper catalogues more than 50 hydrological signatures representing processes seen in the hydrological cycle such as evapotranspiration, snowmelt, infiltration excess and baseflow. The majority of signatures reviewed demonstrate how signatures can enable hydrologists to make the most out of streamflow data. Without requiring data which is less widely available, such as soil moisture. The review is structured using hydrological process classes (Anderson & McDonnell, 2005). For each process class, hydrological signatures are found in the existing literature. The review is restricted to hydrological signatures that can be derived using only streamflow and precipitation data, where rainfall data is used to interpret the signatures, but not used by itself. These data types are selected because they are the most commonly available to hydrologists. It is recognised that more complex findings can be derived from experimental catchments with detailed datasets, including tracers and soil moisture data. However, as such data sets are typically not available for large scales, both temporally and spatially, these are not considered in the review. Figure 5 shows a summary of all the signatures considered in the review, their distribution across over the processes and timescales and whether they quantify the process or test for its occurrence.

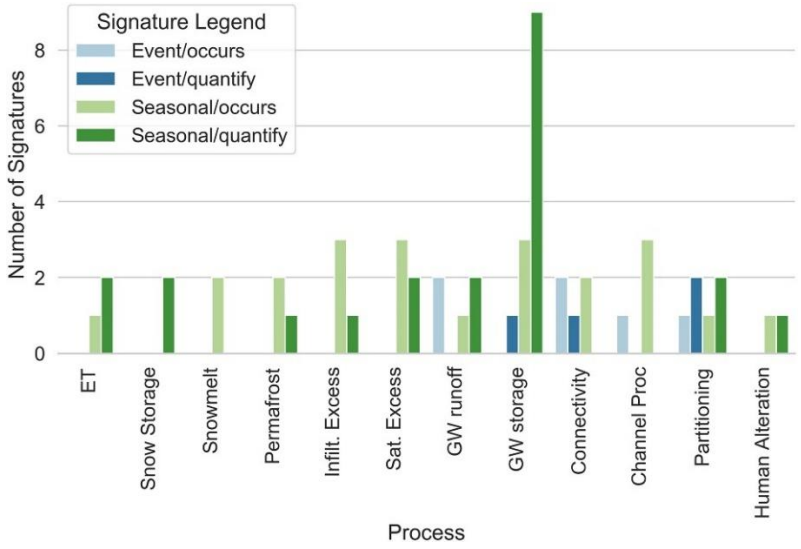


*Figure 5: Numbers of signatures available to characterize each process, split by timescale (event or seasonal), and whether the signature quantifies the process or tests for its occurrence by (McMillan, 2020)*

Figure 5 shows a significant variability in signature coverage. Surface processes, i.e. ET, snow, permafrost, infiltration and saturation excess have no signatures on the event timescale. Groundwater storage, connectivity and partitioning all benefit from a diverse range of signatures. These processes are related to the split between fast and slow hydrological processes. In general, there are more signatures

related to the seasonal scale than to the event scale. In addition to these findings, the review also proposes a new signature typology. The 5 proposed types are:

1. Time series visuals
2. Quantified event dynamics
3. Quantified seasonal dynamics
4. Seasonal statistics
5. Mini-model

The review also shows that a hydrological signature is often related to multiple processes, making it difficult to use signature values to characterise catchment processes. On the other hand, there are also many signatures that focus on similar characteristics of the streamflow regime. Given the number of different ways in which streamflow can be characterised, hydrologists have adopted a variety of approaches, resulting in a large number of competing hydrological signatures (Olden & Poff, 2003). Hydrologists are faced with the difficult task of choosing from an abundance of available hydrological signatures. Creating the question: What minimum subset of hydrological signatures is required to adequately describe the most important aspects of the streamflow regime?

(Olden & Poff, 2003) undertakes a comprehensive review of the available hydrological signatures for characterising the streamflow regime. The review examines 171 published hydrological signatures in search of a reduced set to describe the streamflow regime. The 171 signatures are grouped into the five categories discussed in the previous section of this report. A principal component analysis (Jolliffe & Cadima, 2016) (PCA) extracted from the 171 x 171 correlation matrix is used to examine the intercorrelation patterns of the hydrological signatures. Figure 6 shows the two-dimensional ordination, which illustrates the major intercorrelation patterns between the signatures. The correlation between any two indices is related to the cosine of the angle between their index axes, i.e. between the vectors joining the origin and the index positions in Euclidean space.

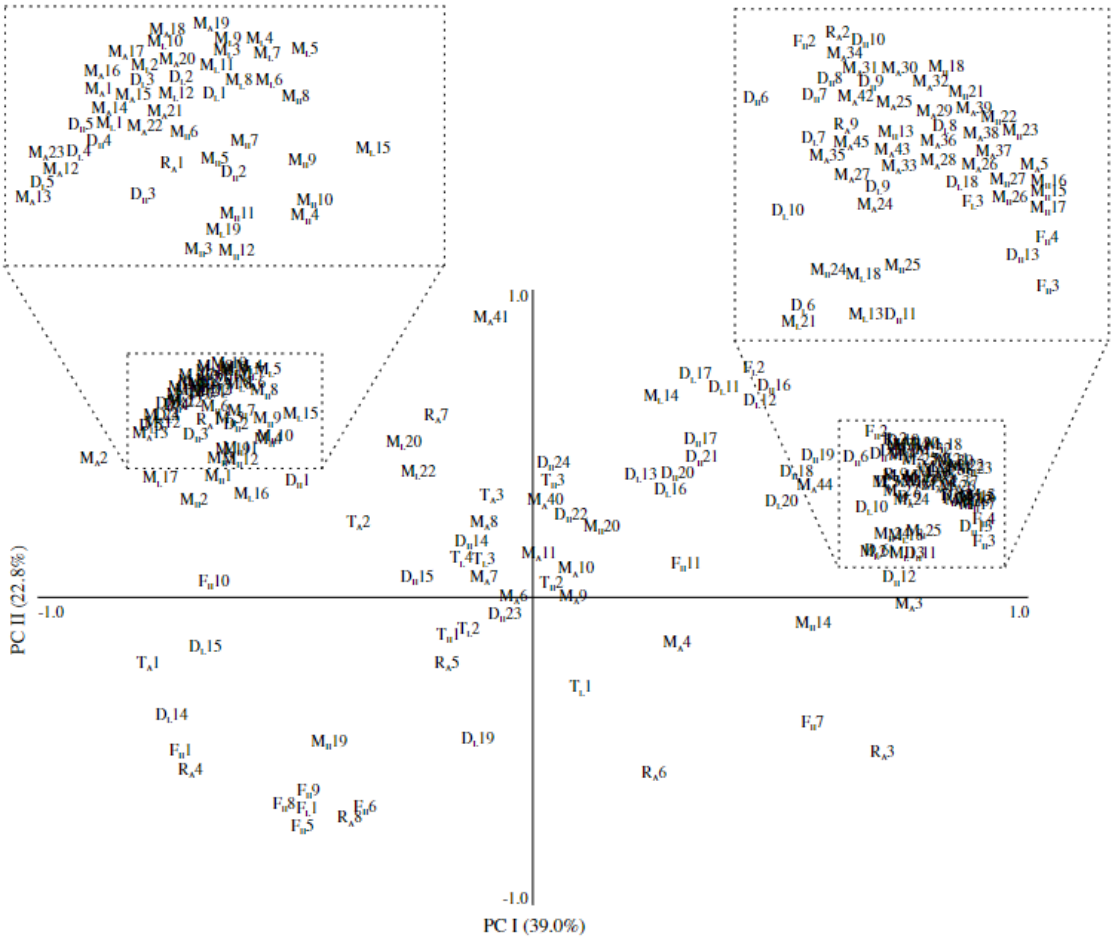


*Figure 6: Ordination from the principal component analysis by (Olden & Poff, 2003). Correlations between indices are interpreted as the cosine of the angle between their index-axes (i.e. between the vectors joining the origin and the index positions in Euclidean space)*

Figure 6 demonstrates a large variability in the degree of correlation between the signatures, although the majority of the signatures are highly correlated (either negatively or positively). A large number of signatures are located in the upper left and upper right quadrants. The transferability of the signatures is assessed by identifying signatures that consistently describe dominant patterns of variation for 'stream types' with distinctly different streamflow characteristics. The ten streamflow types of (POFF, 1996) are reduced to six distinctive types to capture a range of streamflow regimes that occur around the globe. The six types are:

1. Harsh intermittent
2. Intermittent flashy or runoff
3. Snowmelt
4. Snow and rain
5. Stable groundwater
6. Perennial flashy or runoff

This review provides a statistically based framework to aid in the selection of hydrological signatures. By focusing on intercorrelation between signatures hydrologists can select a subset of optimal signatures based on the hydroclimatic region, or stream type. Using this framework will maximise the information provided by the subset of signatures while minimising the degree of redundancy. However, this approach should only be used as an aid in the selection of hydrological signatures. It should be used in conjunction with more intuitive selection criteria based on the particular research questions of interest.

# 4. Methodology

In order to answer the research questions and achieve the research objectives, a research plan is carefully drawn up. As mentioned in section 2.1, this research is a data and trend analysis study. Data analysis is the process of inspecting, modelling and transforming data with the aim of discovering meaningful information (Kudyba, 2014). This meaningful information is then used for a wide variety of purposes, such as supporting decision making or drawing conclusions. The entire research process for this specific study is roughly visualised in Figure 7.

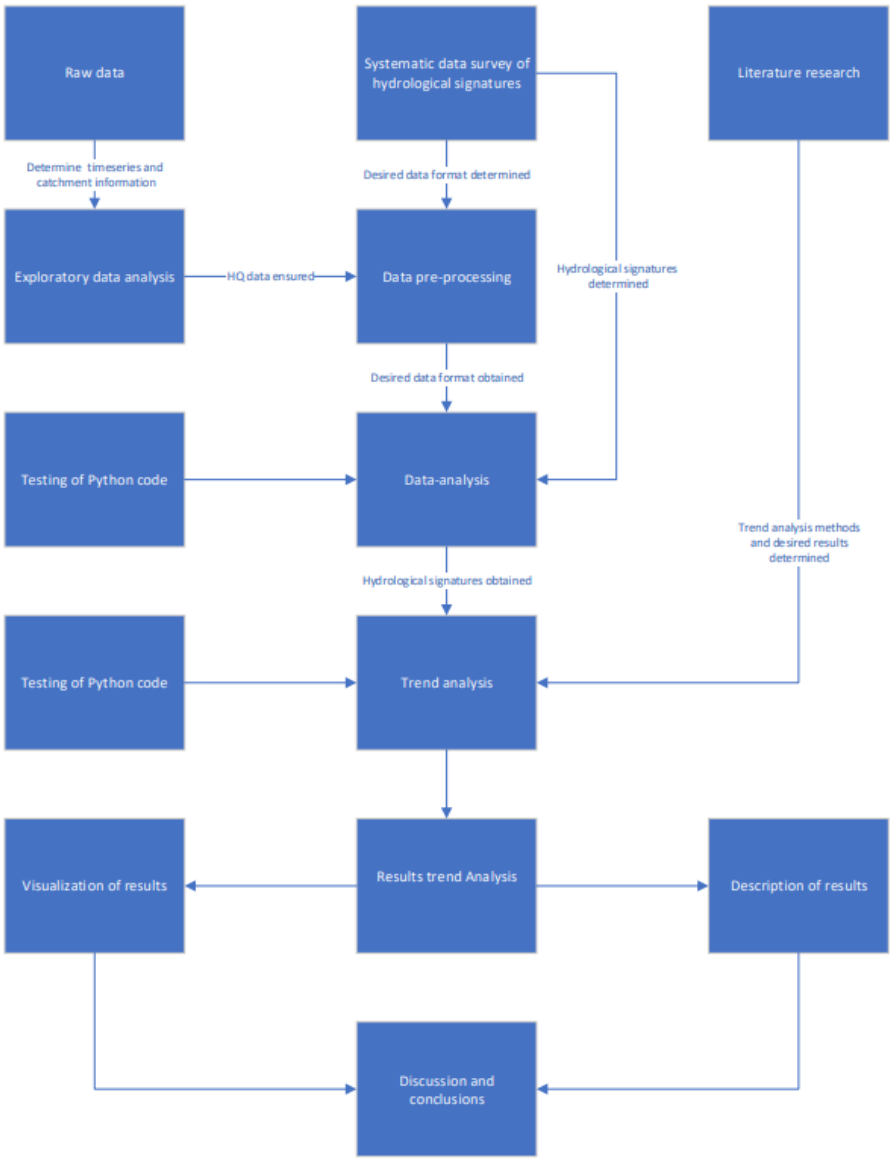


*Figure 7: General flowchart of the research plan*

## 4.1 Data collection

Typically, data analysis studies begin with data collection. Hydrological studies can often be quite spread out spatially and temporally (McMillan, 2020). These large spatial and temporal scales can make the actual generation of data practically impossible, especially with the desire for time series of at least 50 years. Fortunately, the process of measuring streamflow has been performed for centuries, making it possible to perform hydrological analyses over periods as long as 500 years such as (Blöschl et al., 2020; Glaser et al., 2010). However, as mentioned in chapter 1, the most recent periods provide the greatest spatial coverage.

As mentioned in chapter 1, the importance of measuring hydrological data is immense. Effective water management would not be possible without proper data measurement (Stewart, 2015). Many datasets containing either hydrological data or climate data have been created in recent decades. Examples of this include the Global Runoff Data Centre (GRDC) dataset (Stahl et al., 2010), the E-OBS dataset (Cornes et al., 2018) and the European Flood Database (Hall et al., 2015). A crucial part of the management of these datasets are the FAIR (Findable, Accessible, Interoperable and Researchable) principles. These principles have been formulated to improve the infrastructure that supports the reuse of data. The intent of these principles is to act as a guideline for stakeholders to ensure the reusability of their data (Wilkinson et al., 2016).

For this study a dataset was provided by my supervisor. This decision was made because the process of data collection, although an important part of any data analysis study, was considered to be outside the scope of this study. Mainly because the process of data collection can be very time consuming. Even though the dataset has been provided, steps still need to be taken to gather information about the dataset and the individual time series, which are described in section 4.2.

## 4.2 Exploratory data analysis and data pre-processing

It is crucial to work with highest quality data possible. Problems such as instrument errors, changes in measurement techniques or typographical errors can cause apparent changes in a data series. An exploratory data analysis (EDA) is used to identify potential problems in the data. The concept of EDA was first formulated by (Tukey, 1962). An exploratory data analysis looks at the data from as many angles as possible with the aim of uncovering interesting features or possible problems in the data (Morgenthaler, 2009).

The main use of the EDA in this study is to examine the raw data to identify features such as data problems (outliers, missing data) , temporal patterns (seasonality, trends) and the data structure (date format, units). A detailed visual examination of each data series is unfeasible and unnecessary for this study, due to the sheer number of time series in the dataset. For each country two data series are selected at random and visually examined. In addition to gaining a better understanding of the dataset as a whole, there were three main conclusions can be drawn from the EDA. Firstly, some time series have missing data, i.e. no data was measured on certain dates. Secondly, there are different writing dates in the data structure. And finally, all the time series have different temporal ranges, meaning that the record lengths of the time series. These problems are all dealt with during data pre-processing.

Data preprocessing is one of the essential steps in a data analysis study (García et al., 2016). Data preprocessing is also the first step in the Knowledge Discovery from Datasets process (KDD) (Han et al., 2022). Data preprocessing is performed in the programming language Python, using the integrated development environment PyCharm. All of the preprocessing steps are elaborated on in this chapter, the actual Python code is shown in Appendix B

Data preprocessing is one of the essential steps in a data analysis study (García et al., 2016). Data preprocessing is also the first step in the Knowledge Discovery from Datasets process (KDD) (Han et al., 2022). All of the data pre-processing steps, as well as with the data and trend analyses are performed in the Python programming language, using the PyCharm integrated development environment. All of the preprocessing steps are explained in this chapter, the actual Python code is presented in Appendix B

First, each individual time series is given an identifier in Python. This is done to facilitate further analyses and to organise the data properly. The most common and well supported method of writing date entries is in the datetime format. However, a number of time series have the dates written in serial datetime. This format uses integers to indicate the number of days that have elapsed since the first of January 1900. These serial datetime values are converted to regular datetime values to facilitate the analysis.

Once the date values have been converted to the desired format, the data series are checked for temporal coverage. The phenomenon of missing data has been discussed extensively for a long period of time (Schafer & Graham, 2002). A review on the processing of missing hydrological data is given by (Gao et al., 2018). The study proposes a number of methods for the imputing of missing data, such as singular spectrum analysis (SSA) and autoregressive and moving average models (ARMA). It is decided that implementing these methods is outside the scope of this study. Instead of these data imputation methods, a data coverage threshold of 300 days is set. 300 days is about 80% of a year. This means that years with less than 300 days of data are not considered in the data-and-trend analysis.

## 4.3 Catchment characteristics and time series information (Study area and time series overview)

The dataset contains hydrological data from a total of 1184 stream gauges in five countries. The hydrological data is expressed in mean daily discharge in cubic metres per second [$m^3/s$]. The contributing catchment area is the region from which surface water drains into the river. This contributing catchment area is necessary for the normalization of streamflow, which is described in section 4.5. For 1160 of the stream gauges, the contributing catchment area is known. The distribution of the stream gauges and their contributing catchment areas is shown in Table 1

| Area <km2 | Belgium | France | Germany | Luxemburg | Netherlands | Total |
|---|---|---|---|---|---|---|
| **1** | 0 | 0 | 0 | 0 | 0 | 0 |
| **10** | 5 | 3 | 3 | 0 | 0 | 11 |
| **25** | 9 | 6 | 25 | 0 | 0 | 40 |
| **50** | 5 | 25 | 55 | 0 | 3 | 88 |
| **100** | 37 | 48 | 97 | 2 | 2 | 186 |
| **250** | 49 | 115 | 178 | 3 | 0 | 345 |
| **500** | 21 | 82 | 89 | 7 | 1 | 200 |
| **1000** | 7 | 48 | 46 | 3 | 0 | 104 |
| **2500** | 7 | 50 | 38 | 2 | 1 | 98 |
| **5000** | 1 | 23 | 15 | 2 | 0 | 41 |
| **10000** | 0 | 11 | 2 | 0 | 0 | 13 |
| **25000** | 3 | 6 | 6 | 0 | 1 | 16 |
| **50000** | 0 | 5 | 1 | 0 | 1 | 7 |
| **100000** | 0 | 1 | 4 | 0 | 0 | 5 |
| **250000** | 0 | 0 | 5 | 0 | 1 | 6 |
| ***Total*** | *144* | *423* | *564* | *19* | *10* | *1160* |

*Table 1: Streamflow dataset catchment area distribution*

To gain insight about the temporal ranges of all of the stream gauges, all of the years contained within each individual time series. This provides information on the number of available time series for each year, as well as the record lengths and the start years of the time series. The histograms of these distributions are plotted in Figure 8.

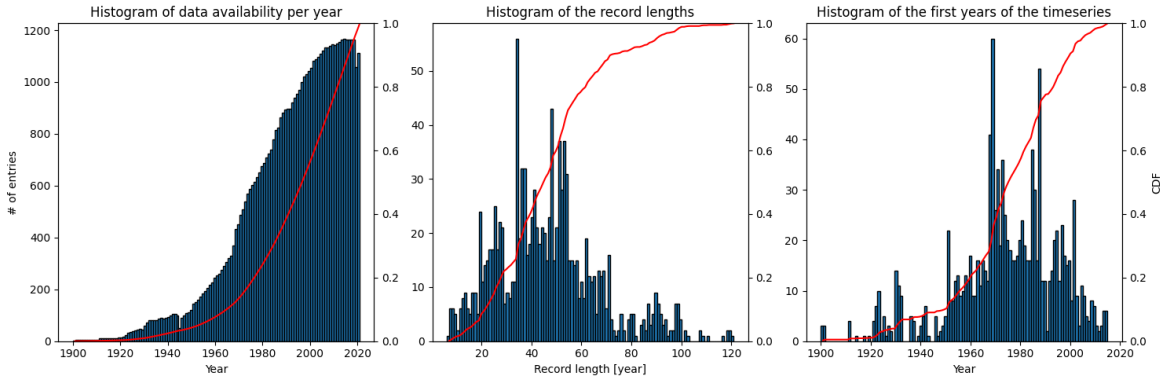


*Figure 8: Histograms showing the distribution of: data availability per year, record lengths of the time series, start years of the time series. The cumulative distribution function (CDF) is given by the orange lines. The number of time series is given by the left y-axis and the CDF by the right y-axis.*

The choice is made to perform the trend analysis on five fixed time periods. Period 1 is the so-called reference period has a temporal range from 2000-2019. From this reference period, each period adds a decade to the temporal range. This results in the periods: Period 1 (2000-2019), period 2 (1990 – 2019), period 3 (1980 - 2019), period 4 (1970 - 1980) and period 5 (1960 – 2019). The spatial coverage of each period is shown in Figure 9

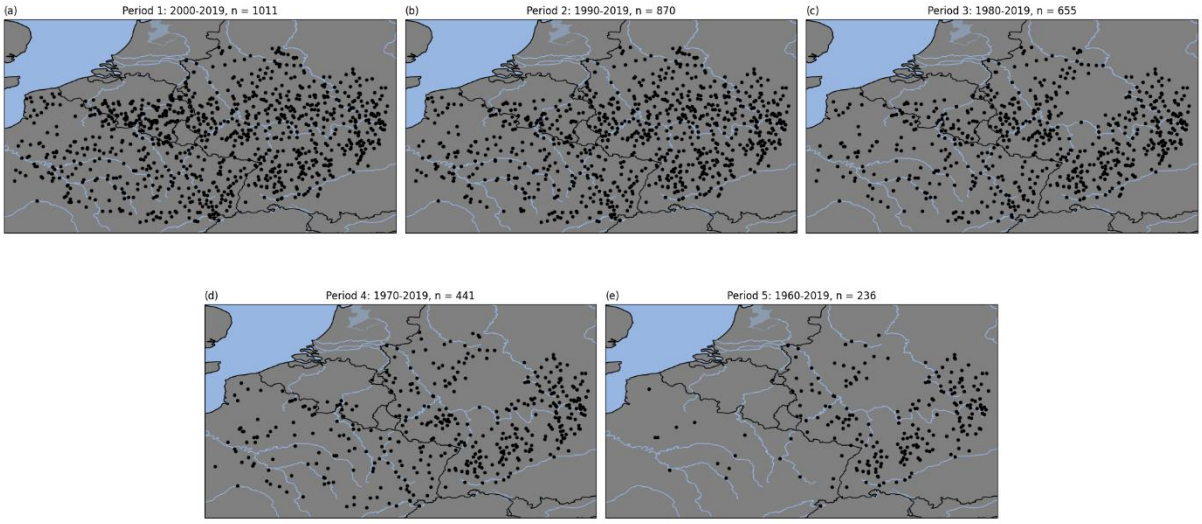


*Figure 9: Spatial coverage of each respective period. (n is the number of stream gauges)*

## 4.4 Selection of hydrological signatures

Hydrological signatures are metrics that quantify aspects of streamflow response (McMillan, 2020). There are many different aspects regarding streamflow response, and the utility of hydrological signatures for describing these aspects has led to increased application in riverine studies. Another result of this is the increase in the amount of existing hydrological signatures (Gao et al., 2009). Many of these signatures are often focused on the same aspect of the streamflow regime, becoming redundant relative to each other. (Olden & Poff, 2003) addresses this this issue and provides a comprehensive review of 171 hydrological signatures. The paper highlights patterns of redundancy among these signatures. With these concerns in mind, a list of hydrological signatures is drafted. These are the signatures which are calculated in the data analysis part of this research. This section substantiates not only the final selection of hydrological signatures, but also the selection process.

As mentioned in section 2.2, the main objective of this research is to provide an overview of the temporal changes and spatial differences in streamflow in western Europe. In order to achieve this objective, the final selection of hydrological signatures should be representative of the entire streamflow regime. (Poff et al., 1997) and (Richter et al., 1996) state that there are five main aspects that describe the streamflow regime. These are: magnitude, frequency, duration, timing and rate of change. These aspects "can be used to characterise the entire range of flows and specific hydrologic phenomena, such as floods or low flows, which are critical to the integrity of river ecosystems". Four of these aspects are selected as being relevant to this research. The rate of change is determined to be irrelevant for this research, as the main application of this component is ecosystem influence (Richter et al., 1998), which is outside the scope of this research. To fully capture the streamflow regime, the distinction is made between the three stages of fluvial flow. These stages are low flow, medium flow and high flow. Combining the four aspects of the hydrological regime with the three stages of river flow would result in a selection of 12 hydrological signatures. However, the frequency, timing and duration of average flow are not feasible signatures to analyse and are therefore not considered. This results in a selection of 9 hydrological signatures which describe the full hydrological regime for this study.

- Annual Minimum Flow of 7 consecutive days (AmF7) [mm/year]
- Average Daily Flow (ADF) [mm/year]
- Annual Maximum Flow (AMF) [mm/year]
- Low Flow Pulse Count (LFPC) [counts/year]
- High Flow Pulse Count (HFPC) [counts/year]
- Low Flow Pulse Duration (LFPD) [days]
- High Flow Pulse Duration (HFPD) [days]
- Julian date of AmF7 [-]
- Julian date of AMF [-]

**Annual Minimum Flow of 7 consecutive days (AmF7)**

This signature represents the annual minimum total flow over any 7 consecutive days in mm/year. This signature is determined annually.

**Average Daily Flow (ADF)**

This signature represents the average daily flow in mm/year. This signature is determined annually.

**Annual Maximum Flow (AMF)**

This signature represent the annual maximum flow on a single day in mm/year. This signature is determined annually.

**Low Flow Pulse Count and Duration (LFPC & LFPD)**

These signatures represent the frequency and duration of the low flow stage. Low flow pulses are defined as periods where the streamflow drops below the $25^{th}$ percentile. Both the number of occurrences and the mean duration of these periods are determined annually.

**High Flow Pulse Count and Duration (HFPC &HFPD)**

These signatures represent the frequency and duration of the high flow stage. High flow pulses are defined as periods where the streamflow rises above the $75^{th}$ percentile. Both the number of occurrences and the mean duration of these periods are determined annually.

**Julian date of AmF7 and AMF**

These signatures are the dates of occurrence of the AmF7 and AMF events. They are also determined annually.

## 4.5 Data analysis (calculation of signatures)

In this section the calculation of each signature is briefly explained. Several Python functions are written to calculate all the signatures. In order to ensure smooth computation, all of the functions have a similar structure and the input for all of the functions is identical. Every function takes a single pre-processed timeseries as input. The complete Python code can be found in Appendix B.

The AmF7 magnitude signature occurs over seven consecutive days. So each data entry is checked to see if it is surrounded by 'data containing days'. If this is the case, a list is created containing the streamflow of 7 consecutive days. The minimum value is determined for each year. This value is saved as the AmF7 magnitude signature and the date of occurrence as the AmF7 timing. The AMF is somewhat easier to determine as it occurs over only one day. The maximum value of daily streamflow is determined annually, and the date of occurrence is saved as the AMF timing. The ADF value is calculated by taking the average of the data each year.

The pulse signatures are somewhat more complicated to determine. Over the entire length of the time series, the 1$^{st}$ and 3$^{rd}$ quartile are determined. These values represent the low flow threshold and high flow threshold respectively. A low flow pulse is defined as a period when the streamflow magnitude reaches below the 1$^{st}$ quartile and a high flow pulse is defined as a period when the streamflow magnitude reaches above the 3$^{rd}$ quartile. For both low-and-high flow pulses, the number of pulses and the average duration of these pulse are determined annually.

All of the signatures are determined using Python and stored in a data frame for each individual time series. The magnitude signatures are normalised by dividing by the catchment area and converted to units of mm/year. These data frames are then used to perform the trend analyses. All of the Python code related to the data analysis is shown in Appendix B

## 4.6 Trend analysis

As mentioned above, the trend analysis is performed on five fixed periods. Therefore, the data frames are filtered according to their temporal coverage. If a time series contains both the start and end year of the period, it is used for the trend analysis of that period.

The non-parametric Mann-Kendall (MK) test, combined with the Theil-Sen slope estimator for trend estimation (KENDALL, 1938; Mann, 1945; Sen, 1968). The MK test is considered to be a robust non-parametric test. (Kunkel et al., 1999) states that "This non-parametric test is particularly useful for analysis of extreme climate events that are not necessarily normally distributed". The MK test is based on the number of pairs of data entries within the time series for which the difference is either positive (increasing) or negative (decreasing) rather than on the actual magnitude of these differences. This minimises the effect of extreme values in the data. A brief summary of the MK test will be given later in this section.

The Theil-Sen slope estimator is given by:

$$\beta = median\left(\frac{x_j - x_i}{j - i}\right)$$

This is a non-parametric slope estimator. The choice is made for a non-parametric slope estimator because it does not assume a distribution of the data, but only that the data is independent. Since the signatures are determined annually, it is safe to assume that the data is independent. This estimator is also chosen for robustness and insensitivity to missing data and outliers(Rousseeuw & Leroy, 1987). The trend estimator β is given by the median of the slopes between all possible pairs in the time series.

The two timing signatures have to be treated differently than the other signatures because they are circular in nature and can occur throughout the year. Because of this circularity, all calculations relating to the trend analysis of the timing signatures are performed using circular statistics (Bayliss & Jones, 1993; Mardia, 1975). Circular statistics is a specialised sub-discipline of statistics used to analyse data with cyclical or angular properties. Circular statistics is tailored to data sets that repeat in a circular manner, which is the case for the timing signatures as these signatures wrap around the period of a year. For circular statistics, the Theil-Sen slope estimator is given by:

$$\beta = \text{median}\left(\frac{D_j - D_i + k)}{j - i}\right) \text{ with } k = \begin{cases} -\bar{m} \text{ if } D_j - D_i > \bar{m}/2 \\ \bar{m} \text{ if } D_j - D_i < -\bar{m}/2 \\ 0 \text{ otherwise} \end{cases}$$

Where $k$ makes the adjustment for the circular nature of the dates, ensuring that the smallest slope is selected between the pairs.

## 4.7 Temporal sensitivity analysis

In addition to the trend analyses with the different fixed periods, the MK test is used on all possible combinations of start and end years. The original Mann-Kendall statistic $S$ is given by:

$$S = \sum a_{ij} b_{ij} \, [-], \; a_{ij} = sgn(x_j - x_i), b_{ij} = sgn(y_j - y_i)$$

The S statistic denotes sum of the differences between all possible pairs in the data values. The range of S is dependent on the amount of data values within the time series. Under the null hypothesis that there is no trend within the time series:

$$E(S) = 0,$$
$$\text{Var}(S) = n(n-1)(2n+5)/18.$$

The Z score is the standardised value, given by:

$$Z = \begin{cases} \frac{S-1}{\sqrt{\text{Var}(S)}} & \text{if } S > 0 \\ 0 & \text{if } S = 0 \\ \frac{S+1}{\sqrt{\text{Var}(S)}} & \text{if } S < 0 \end{cases}$$

This Z score is determined for each signature, using stream gauges that contain at least 60 years of data. This selection corresponds with the stream gauges of the fifth fixed period, as shown in Figure 9(e). The number of stream gauges for this analysis is n = 236 The Z score is averaged across all stream gauges.

The entire trend analysis is performed in Python using the Python package pyMannKendall, written by (Hussain & Mahmud, 2019). The Python code is shown in Appendix B.

# 5. Results

As mentioned in the previous chapter, the trend analysis is performed on nine signatures over five different time periods with an identical end year. The spatial coverage of each period is shown in Figure 9. To keep the presentation of the results as consistent as possible, all the results of the trend slope estimation are presented and described in an identical manner. First, the results of each period are presented in a scatter plot with an underlying map of western Europe. The location of each point represents the location of the stream gauge, and the colour of the bubble represents both the magnitude and direction of the trend. Positive trends are presented as blue circles and negative trends as presented as red circles. The meaning of positive and negative trends is unique for each signature and will therefore be given at each signature, as well as the units of the estimated slope.

Additionally, a violin plot showing the distribution of the trends is given. A violin plot is a statistical graphic for comparing probability distributions. It is like a box plot, with the addition of a rotated kernel density estimation on each side (Hintze & Nelson, 1998). For each trend analysis, the total range of the estimated trend values is given. The first quartile, median and third quartile are represented by vertical lines in the violin plot. The range of the violin plot is determined based on the maximum absolute trend values for each period. This means that the range will be different for each period. This choice was made in order to show the shape of the trend distribution, rather than the magnitude of trends. The percentage of positive and negative trends is given. The trends are tested for statistical significance at a significance level of ($\alpha = 0.10$) but since the focus of this research is analysing variability in trends, they are not actively mentioned. The distributions between positive-and-negative trends for each trend analysis are shown in the tables of Appendix A

To appropriately compare the results between the periods, the trend analysis is also performed on only gauges with at least 60 years of record length. These gauges are selected and then the analysis is performed over the five different time periods. The methodology described above is applied on these analyses as well to maintain consistency.

## 5.1 AmF7 timing

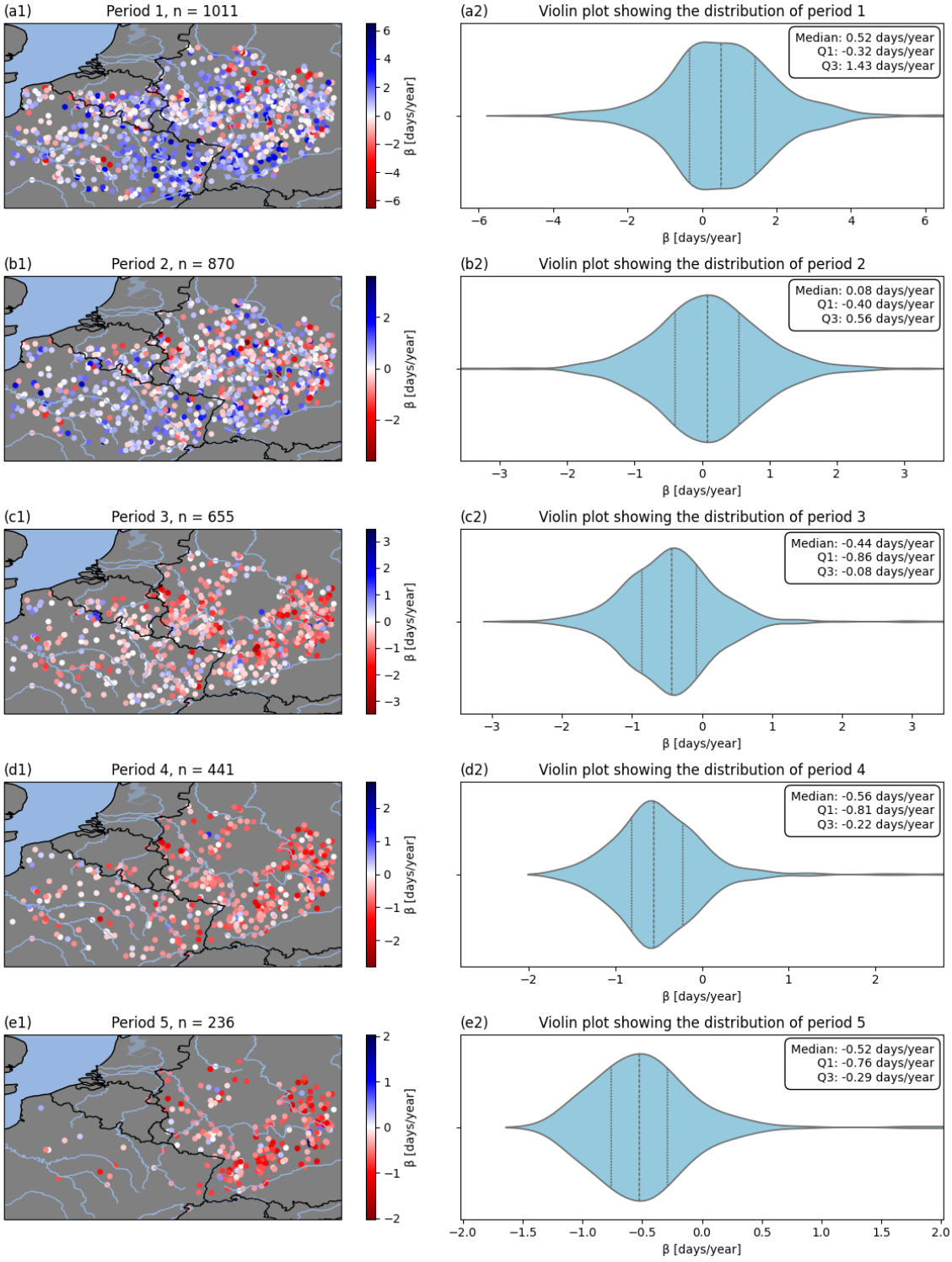


*Figure 10: Trend results for the timing of the AmF7 event. Scatterplot on the left shows the location of the trends and the violin plot on the right shows the distribution of trends over the entire study area. Blue circles represent positive trends and red circles represent negative trends. Period 1: 2000-2019, period 2: 1990-2019, period 3: 1980-2019, period 4: 1970-2019, period 5: 1960-2019.*

These graphs show the trends in the timing of the AmF7 event for the different time periods in [days/year]. Negative trends, which are shown by the red circles, represent an ‘earlier in year’ trend. Positive trends, which are shown by the blue circles indicate a positive (forwards in time).

Period 1 shows more positive trends than negative trends, with the percentage of positive trends being 63.9 % and the percentage of negative trends being 34.2 %. The trend slopes range from -5.1 days/year to 6.5 days/year with a median value of 0.5 days/year. Over the entire period, this translates to -100 days and 130 days. Most parts of the study area show mainly positive trends, which is also visible from the histogram. A decreasing pattern can be seen from south to north for the entire study area. The southern parts of the study area display the largest positive trends. The further north in the study area, the smaller these trends become, with the most northern parts also showing more negative trends.

Looking at the graphs of the second period, it can be seen from both the histogram and the map plot that the distribution between positive and negative trends is more evenly distributed compared to the first period. The percentage of positive trends being 52.0 % and the percentage of negative trends being 43.4%. The absolute trend values are smaller for the second period, ranging from -3.6 days/year to 3.3 days/year. As noted before, the area generally shows an even distribution between positive and negative trends. However, the western part of the study area shows slightly more positive trends and the eastern / northeastern parts show slightly more negative trends.

The graphs of the third period are significantly different than the first two periods. There are now significantly more negative trends than the first periods, with the percentage of positive trends being 18.5 % and the percentage of negative trends being 78.2 %. In addition to this shift in trend direction, the absolute values of the trends have remained the same. The trends range from -2.8 days/year to 3.5 days/year with a median value of -0.4 days/year.

The graphs of the fourth period are similar to those of the third period, showing again the dominant negative trend pattern. The percentage of positive trends being 10.7 % and the percentage of negative trends being 87.5 %. The trends range from -1.7 days/year to 2.8 days/year with a median value of -0.6 days/year.

The graphs of the fifth period are again similar to those of the third and fourth period. The percentage of negative trends being 8.9 % and the percentage of negative trends being 89.8 %. The trends range from -1.4 days/year to 2 days/year with a median value of -0.5 days/year.

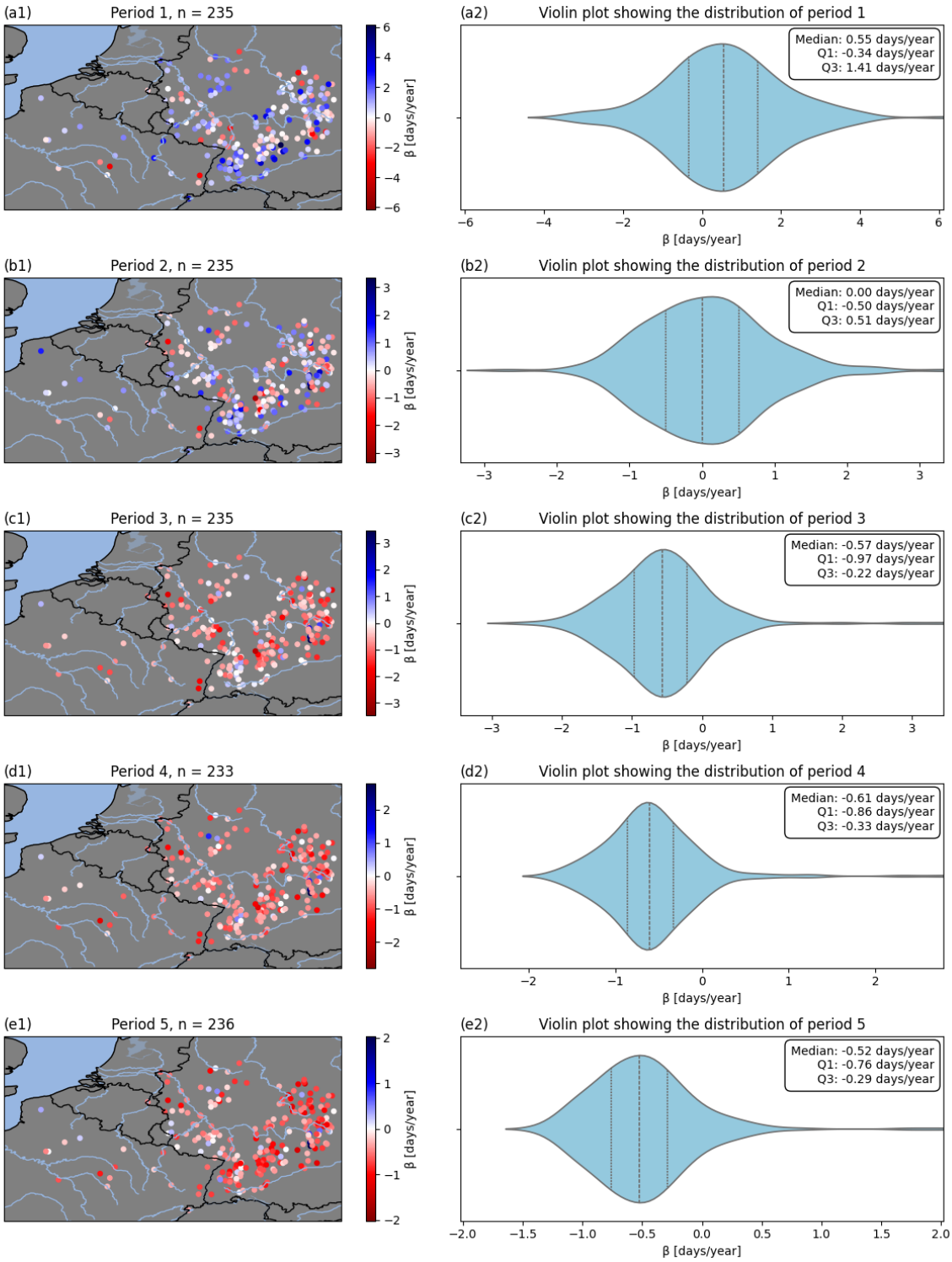


*Figure 11: Trend results for the timing of the AmF7 event, using only stream gauges with record length of at least 60 years. Scatterplot on the left shows the location of the trends and the violin plot on the right shows the distribution of trends over the entire study area. Blue circles represent positive trends and red circles represent negative trends. Period 1: 2000-2019, period 2: 1990-2019, period 3: 1980-2019, period 4: 1970-2019, period 5: 1960-2019.*

These graphs show the trends in the timing of the AmF7 event, using only the gauges which are available for the fifth period. These graphs are meant to the show the impact of the selected temporal range on a trend analysis.

The results of the first period show mostly positive trends, with the percentage of positive trends being 65.1 % and the percentage of negative trends being 33.6 %. The trends range from -3.4 days/year to 6.1 days/year with a median value of 0.6 days/year.

The results of the second period are similar to those of the first period, with a more even distribution of positive and negative trends. The percentage of positive trends being 49.4 % and the percentage of negative trends being 46.4 %. The absolute values of the trends have become smaller, ranging from -2.7 days/year to 3.3 days/year with a median value of 0.0 days/year.

The results of the third period are significant different from the two preceding periods. The entire study area shows mostly negative trends for the third period/ The percentage of positive trends being 11.9 % and the percentage of negative trends being 86.0 %. In addition to this, the absolute values have not become smaller. The trends range from -2.6 days/year to 3.5 days/year with a median value of -0.6 days/year.

The results of the fourth period are similar to those of the third period, showing an even higher percentage of negative trends. The percentage of positive trends being 7.7 % and the percentage of negative trends being 91.0 %. The absolute values of the trends have become slightly smaller. The trends range from -1.7 days/year to 2.8 days/year with a median value of -0.6 days/year.

Finally, the results of the fifth period are similar to those of the two preceding periods. Showing mostly negative trends, the percentage of positive trends being 8.9 % and the percentage of negative trends being 89.8 %. The absolute values of the trends have become slightly smaller, ranging from -1.4 days/year to 2.0 days/year.

When comparing the results across all periods there are significant differences between the results and a coherent pattern can be found. The first period shows mostly positive trends. When moving further back in time, the trends become predominantly negative for all of the gauges considered. In addition to this, the trend values become smaller when moving back in time. This is mainly because the temporal range increases, and the trends are determined in slope values (i.e. over time unit). The temporal range of the trends in the first period is -3.4 days/year to 6.1 days/year, which translates to -70 days to 120 days over the entire period. For the fifth period,  the temporal range translates to -90 days to 120 days over the entire period.

## 5.2 AMF timing

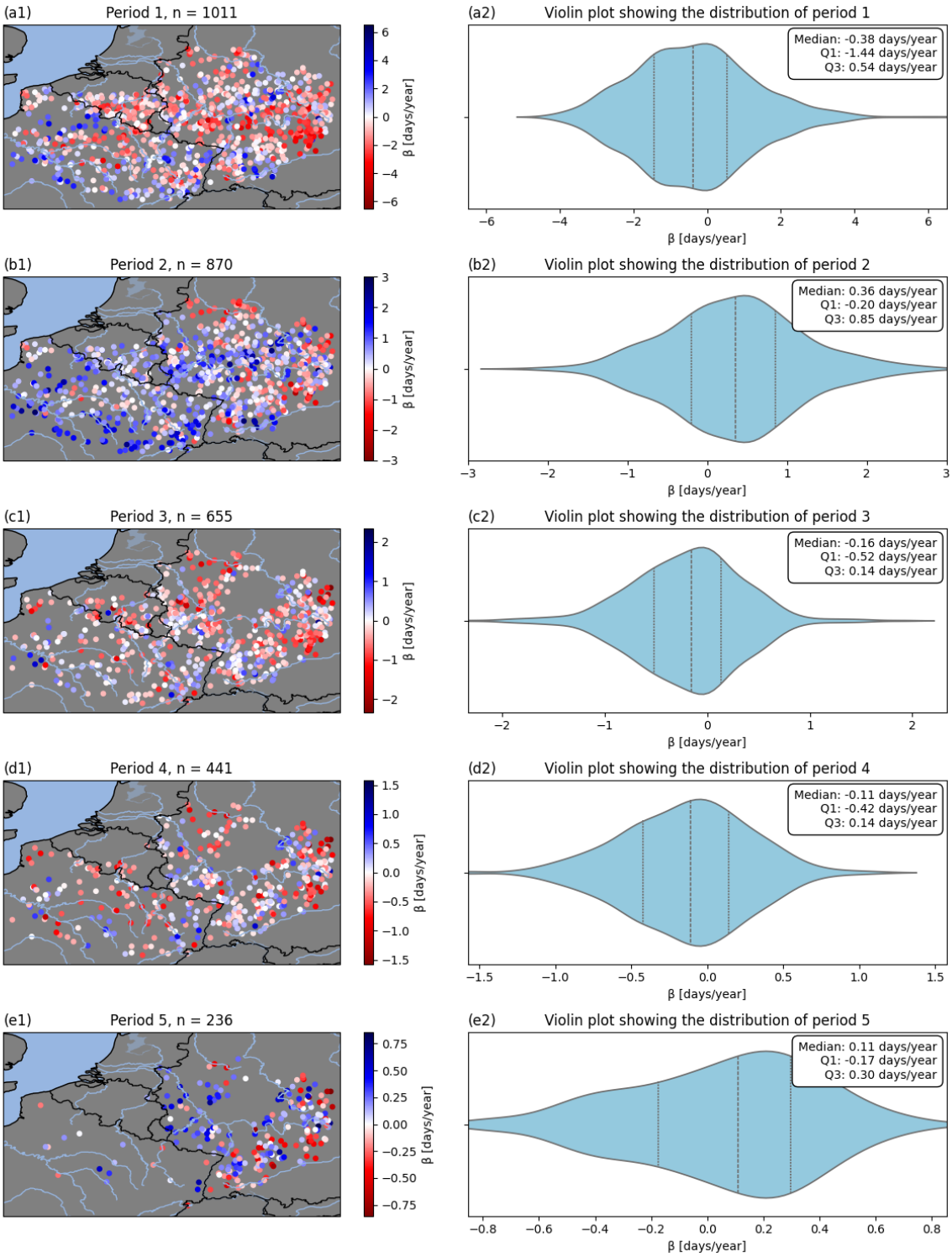


*Figure 12: Trend results for the timing of the AMF event. Scatterplot on the left shows the location of the trends and the violin plot on the right shows the distribution of trends over the entire study area. Blue circles represent positive trends and red circles represent negative trends. Period 1: 2000-2019, period 2: 1990-2019, period 3: 1980-2019, period 4: 1970-2019, period 5: 1960-2019.*

These graphs show the trends in the timing of the AMF event for the different time periods in [days/year]. Negative trends, which are shown by the red circles, represent an 'earlier in year' trend. Positive trends, which are shown by the blue circles indicate a positive trend (forwards in time)

Period 1 shows slightly more negative trends than positive trends ranging from -4.4 days per year to 6.5 days/year and a median value of -0.4 days/year. Over the entire period this translates to -90 days and 130 days. It is difficult to see a clear spatial pattern in the trends, as they are quite evenly distributed across the study area. The Southern and Western parts of the study area show mostly positive trends, along with a small area in the North-Eastern part of the study area. The central and eastern parts of the study area show mostly negative trends, especially the smaller area in the east. The percentage of positive trends for period 1 is 39.4 %. The percentage of negative trends for period 1 is 59.2 %

When looking at the graph of the second period, distinct differences can be seen when comparing it to the second. The first major difference which is clearly visible from the plotted map is the fact that the entire study area now displays dominantly positive trends, especially in the central and western part. Secondly, looking at the histogram it can be seen that the trends are overall smaller compared to the first period. The trends range from -2.4 days/year to 3.0 days per year with a median value of 0.4 days/year. The percentage of positive trends for period 2 is 65.3 %. The percentage of negative trends for period 2 is 31.6 %

From the results of the third period, it is difficult to see a clear spatial pattern in the trends, similar to the results of the first period. There are more negative trends than positive trends, especially in the central and Eastern parts of the study area. Also more white circles are noticeable when compared to the first two periods, indicating more trends which are close to 0. This can also be seen from the distribution portrayed by the histogram. In addition to this, the values of the slope have again become smaller. The trends for the third period range from -2.3 days/year to 1.9 days/year with a median value of -0.2 days/year. The percentage of positive trends for period 3 is 33.4 %. The percentage of negative trends for period 3 is 60.5 %

The fourth period displays mostly negative trends, except for a small area in the central part of the study area. When looking at the spatial distribution of trends, the fourth and the third period show a similar pattern, with again a more noticeable number of white circles when compared to the first two periods. The absolute values of the trends have again become smaller, the trends in the fourth period range from -1.6 days/year to 1.1 days/year. The percentage of positive trends for period 4 is 34.0 %. The percentage of negative trends for period 4 is 59.2 %

The fifth period displays a clear spatial pattern. The trends are mostly positive, especially in the central part of the study area, or in this case the western part of Germany since the spatial coverage is mostly in Germany for this period. The Eastern part shows more negative trends, which is consistent with the first four periods for this area. The absolute values have again become smaller, now ranging from -0.8 days/year to 0.9 days/year. The percentage of positive trends for period 5 is 59.3 %. The percentage of negative trends for period 5 is 36.0 %

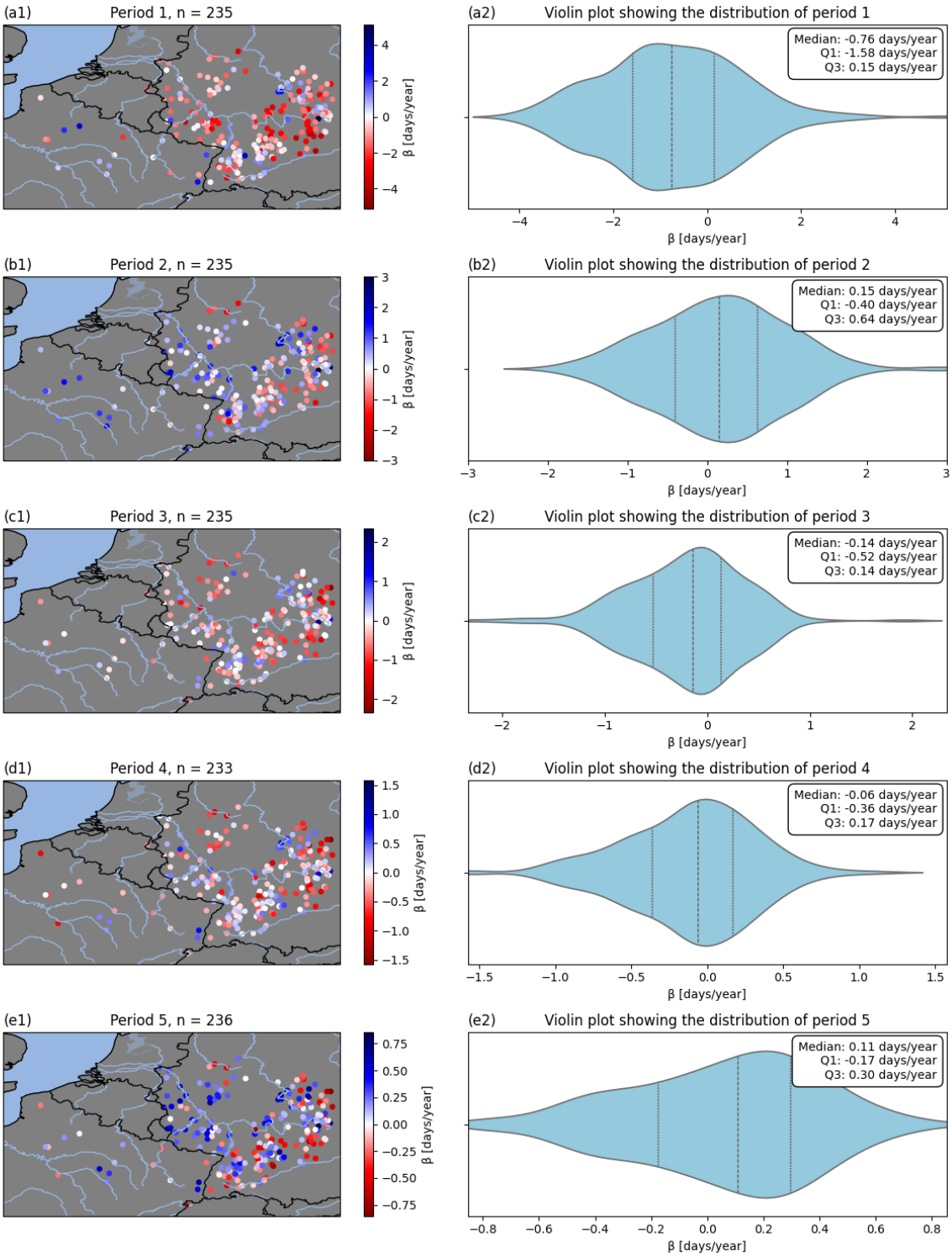


*Figure 13: Trend results for the timing of the AMF event, using only stream gauges with record length of at least 60 years. Scatterplot on the left shows the location of the trends and the violin plot on the right shows the distribution of trends over the entire study area. Blue circles represent positive trends and red circles represent negative trends. Period 1: 2000-2019, period 2: 1990-2019, period 3: 1980-2019, period 4: 1970-2019, period 5: 1960-2019.*

These graphs show the trends in the timing of the AMF event, using only the gauges with a record length > 60 years. These graphs are meant to the show the impact of the selected temporal range on a trend analysis.

The results of the first period show mostly negative trends, both the histogram and map plot. The percentage of positive trends for period is 30.2 % and the percentage of negative trends being 68.9 %. The trends range from -4.0 days/year to 5.1 days/year with a median value of -0.8 days/year.

The results of the second period differ significantly from those of the first period, with the trends being more evenly distributed, even having slightly more positive trends. The percentage of positive trends for period 2 is 57.4 % with the percentage of negative trends being 38.3 %. The absolute trend values have become smaller. The trends range from -2.0 days/year to 3.0 days/year with a median value of 0.2 days/year.

The results of the third period then show again more negative trends over the stream gauges. The percentage of positive trends being 33.2 % and the percentage of negative trends being 59.6 %. The absolute values of the trends have decreased, but only for the positive trends. The trends range from -2.3 days/year to 1.9 days/year with a median value of -0.1 days/year.

The results of the fourth period are in line with those of the third period, again showing mostly negative trends. The percentage of positive trends being 37.3 % and the percentage of negative trends being 55.8 %. The absolute values of the trends has become smaller, trends range from -1.6 days/year to 1.1 days/year with a median value of -0.1 days/year.

The results of the fifth period show mostly positive trends over the gauges, with the percentage of positive trends being 59.3 % and the percentage of negative trends being 36.0 %. The absolute values of the trends has become slightly smaller compared to the fourth period. The trends range from -0.8 days/year to 0.9 days/year with a median value of 0.1 days/year.

Looking at the results across all periods, there are significant differences between the results but a coherent pattern in these differences is not found. Three periods are found with mostly negative trends, being period 1,3 and 4. Two periods are found with mostly positive trends, being period 2 and 4. One pattern can be found is the fact that the absolute values of the trends become smaller over each period. This is mainly because the temporal range increases, and the trends are determined in slope values (i.e. over time unit). The temporal range of the trends is from -4 days/year to 5 days/year, which translates to -80 days to 100 days over the entire period. For the fifth period the temporal range translates to -60 days to 60 days.

## 5.3 AmF7 magnitude

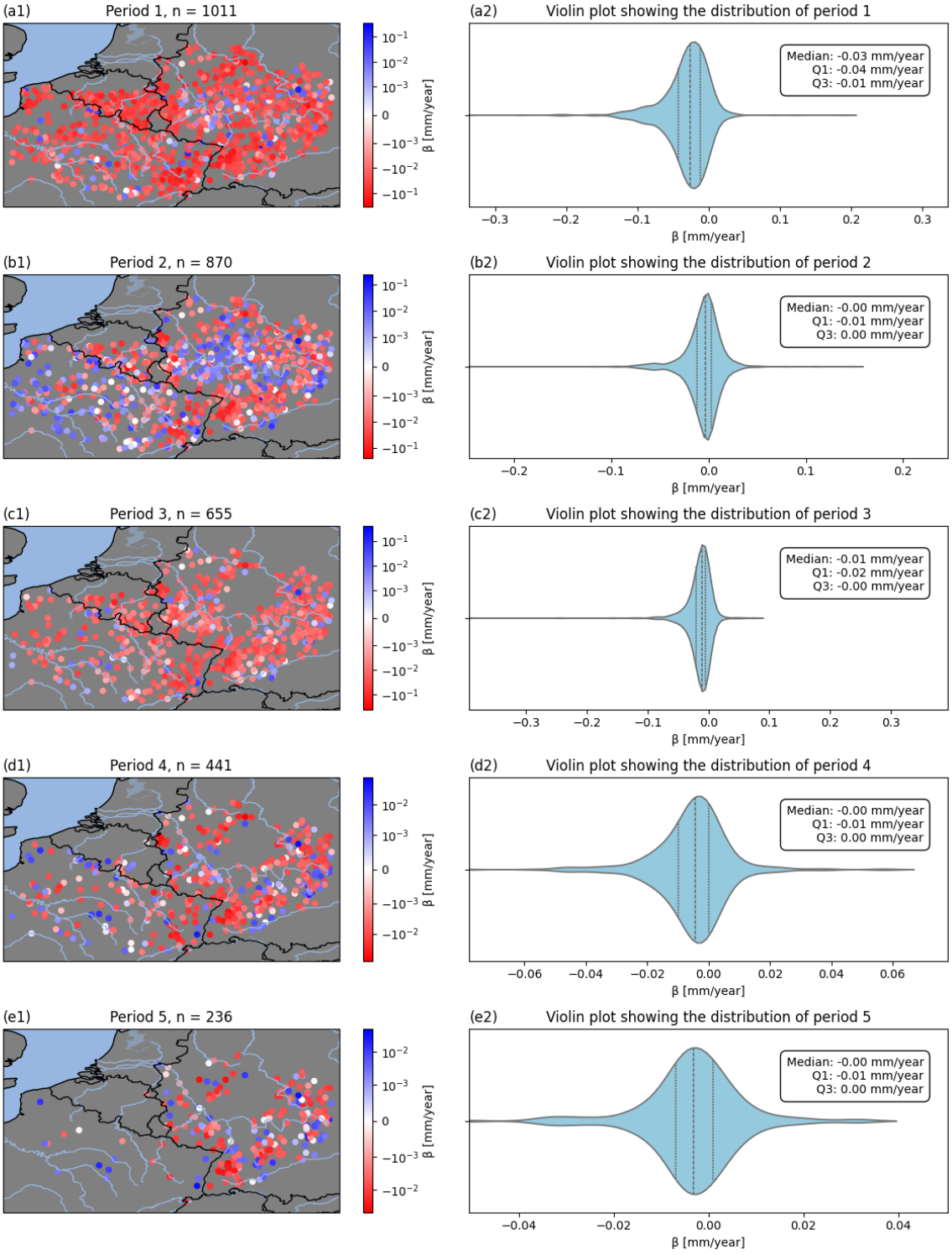


*Figure 14: Trend results for the timing of the AmF7 magnitude. Scatterplot on the left shows the location of the trends and the violin plot on the right shows the distribution of trends over the entire study area. Blue circles represent positive trends and red circles represent negative trends. Period 1: 2000-2019, period 2: 1990-2019, period 3: 1980-2019, period 4: 1970-2019, period 5: 1960-2019.*

These graphs show the trends in the magnitude of the AmF7 event for the different time periods in absolute values [mm/year]. Negative trends, which are shown by the red circles, represent decreasing magnitude. Positive trends, which are shown by the blue circles, represent increasing magnitudes.

The results of the first period show a clear spatial pattern across the entire study area. Nearly of all the trends are negative, with the percentage of significant positive trends being 9.4 % and the percentage of negative trends being 90.5 %. The trends range from -0.34 mm/year to 0.19 mm/year, with a median value of -0.03 mm/year. From the violin plot, it is seen that the vast majority of the trends is relatively close to the median value with q1 = -0.04 mm/year and q3 = -0.01 mm/year. Indicating that 50% of all trends are within this range. These values are significantly smaller than the largest outliers.

The results of the second period show a more even distribution compared to the first period, with the percentage of positive trends being 36.7 % and the percentage of negative trends being 62.2 %. The western part of the study area shows mostly positive trends, along with a small cluster of stream gauges in the north/eastern part of the study area. But most of the area is dominated by negative trends. The absolute values of the trends have become smaller compared to the trends of the first period. The trends range from -0.25 mm/year to 0.15 mm/year with a median value of -0.00 mm/year. From the violin plot it becomes visible that the distribution of the trends has also become more concentrated. The trends are now closer to the median value with q1 = 0.01 mm/year and q3 = 0.00 mm/year.

The results of the third period clearly shows a pattern dominated by negative trends similar to those of the first period. The percentage of positive trends being 11.9 % and the percentage of negative trends being 88.1 %. The absolute values of the trends have stayed the same with the trends ranging from -0.39 mm/year to 0.08 mm/year with a median value of -0.01 mm/year. The shape of the violin plot is also very similar to that of the second period but shifted to the left (i.e. towards more negative trends), with q1 = -0.020mm / year and q3 = -0.00 mm/year.

The results of the fourth period show a bit more positive trends, but the entire study area is still dominated by negative trends. The percentage of positive trends being 27.0 % and the percentage of negative trends being 72.6 %. The absolute values of the trends have become significantly smaller, ranging from -0.08 mm/year to 0.06 mm/year with a median value of -0.00 mm/year. From the shape of the violin plot, it is clearly visible that the distribution of the trends is relatively more dispersed than for the preceding periods, with q1 = -0.01 mm/year and q3 = 0.00 mm/year.

The results of the fifth period are similar to those of the fourth period, with the map plot not showing major differences relative to the fourth period. The percentage of positive trends is 31.4 % and the percentage of negative trends is 68.3 %. This small shift in the distribution is mainly due to the fact that more catchments with negative trends than positive trends were eliminated when moving from period 4 to period 5. The absolute values of the trends have decreased slightly, ranging from 0.05 mm/year to 0.03 mm/year with a median value of -0.00 mm/year. The shape of the violin plot shows that the distribution of the trends has become slightly more dispersed compared to the distribution of the preceding periods, with q1 = -0.01 mm/year and q3 = 0.00 mm/year.

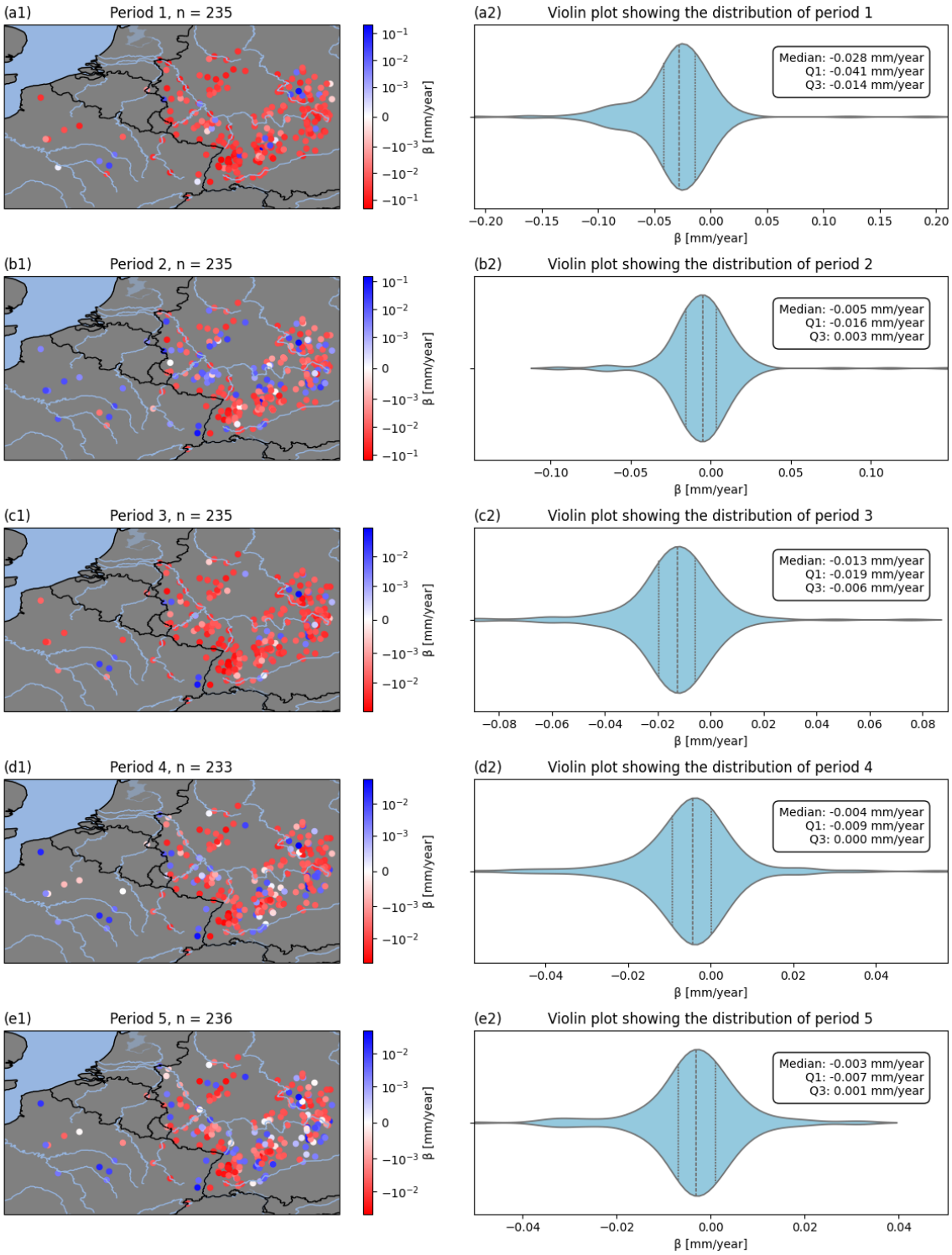


*Figure 15: Trend results for the AmF7 magnitude, using only stream gauges with record length of at least 60 years. Scatterplot on the left shows the location of the trends and the violin plot on the right shows the distribution of trends over the entire study area. Blue circles represent positive trends and red circles represent negative trends. Period 1: 2000-2019, period 2: 1990-2019, period 3: 1980-2019, period 4: 1970-2019, period 5: 1960-2019.*

These graphs show the trends in the magnitude  of the AmF7 event, using only the gauges which are available for the fifth period. These graphs are meant to the show the impact of the selected temporal range on a trend analysis.

The results of the first period show mostly negative trends for the entire study area. The percentage of positive trends is 8.9% and the percentage of negative trends is 91.1 %. The trends range from -0.21 mm/year to 0.19 mm/year with a median value of -0.03 mm/year.  The violin plot shows that the distribution of the trends is quite concentrated, with q1 = -0.04 mm/year and q3 =  = -0.01 mm/year.

The results of the second period show a more even distribution of the trends, both in the map plot and the violin plot. However, most of the trends are still negative, the percentage of positive trends being 34.0 % and the percentage of negative trends being 65.5 %. The absolute values of the trends have become smaller compared to the first period, ranging from -0.10 mm/year to 0.15 mm/year with a median value of -0.005 mm/year. The distribution of the trends is slightly more concentrated than for the first period, with q1 = -0.016 mm/year and q3 = 0.003 mm/year.

The results of the third period are more similar to those of the first period than to those of the second period. The results show mostly negative trends, with the percentage of positive trends being 11.9 % and the percentage of negative trends being 88.1 %. The absolute values of the trends have become slightly smaller compared to the second period, ranging from -0.09 mm/year to 0.08 mm/year with a median value of -0.01 mm/year. The violin plot shows a more dispersed distribution of trends compared to the previous periods, with q1 = -0.02 and q3 = -0.01 mm/year.

The results of the fourth period show slightly more positive trends when compared to the third period. The percentage of positive trends is 26.2 % and the percentage of negative trends is 73.4 %. The absolute values have become significantly smaller when compared to the preceding periods. Trends range from -0.06 mm/year to 0.05 mm/year with a median value of -0.00 mm/year. The relative spread of the distribution has remained similar to that of the third period, as shown by the shape of the violin plot. q1 = 0.01 mm/year and q3 = 0.00 mm/year.

The results of the fifth period again show an increase in positive trends when compared to the previous period. The percentage of positive trends is 31.4 % and the percentage of negative trends is 68.2 %. The absolute values of the trends have decreased very slightly, ranging from -0.05 mm/year to 0.03 mm/year, with a median value of -0.0 mm/year. The distribution of the trends, as shown by the violin plot, has remained has also remained similar, with q1 = -0.01 mm/year and q3 = 0.00 mm/year.

## 5.4 ADF magnitude

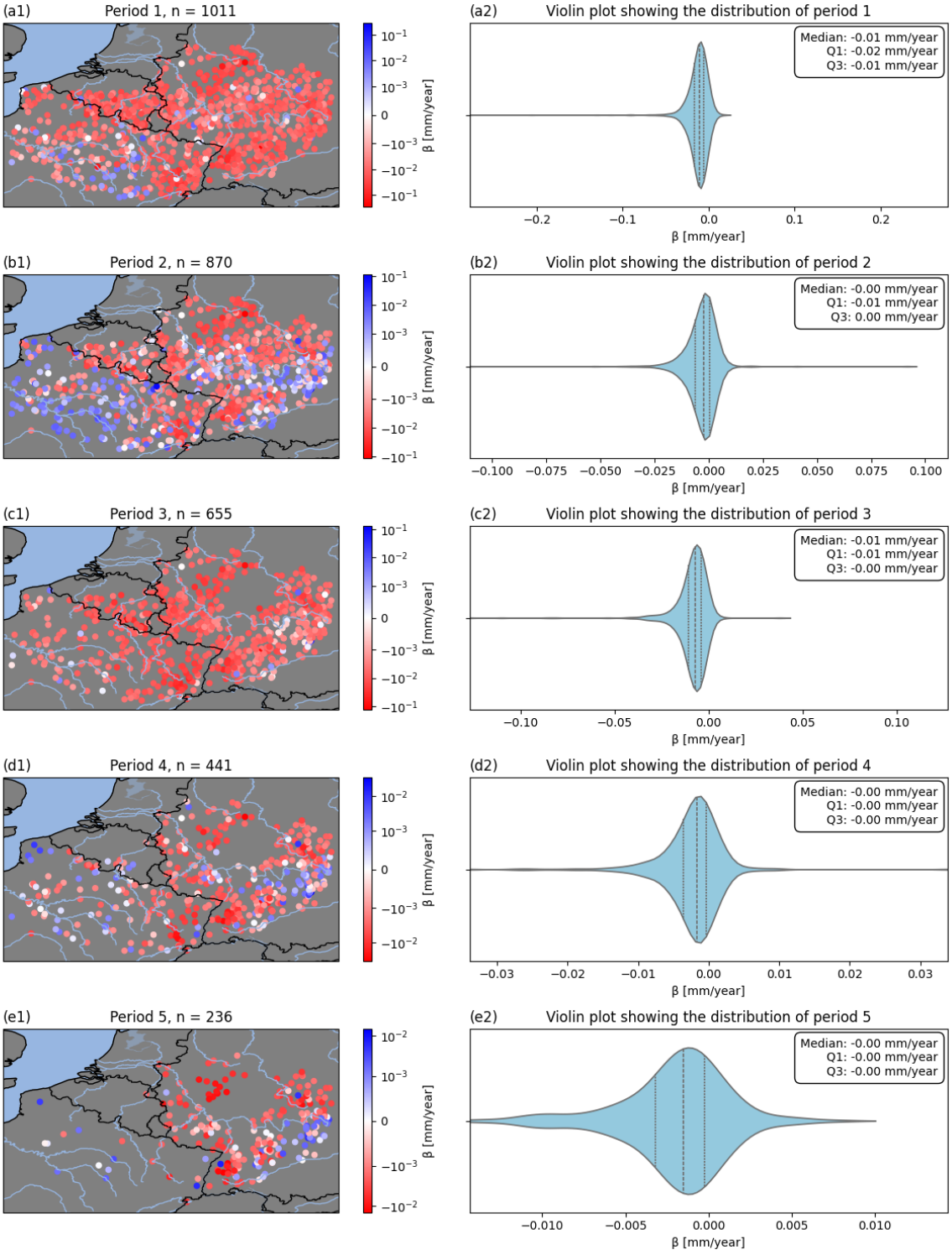


*Figure 16: Trend results for the timing of the ADF magnitude. Scatterplot on the left shows the location of the trends and the violin plot on the right shows the distribution of trends over the entire study area. Blue circles represent positive trends and red circles represent negative trends. Period 1: 2000-2019, period 2: 1990-2019, period 3: 1980-2019, period 4: 1970-2019, period 5: 1960-2019.*

These graphs show the trends in the magnitude of the ADF for the different time periods in absolute values [mm/year]. Negative trends, which are shown by the red circles, represent decreasing magnitude. Positive trends, which are shown by the blue circles, represent increasing magnitudes.

The results of the first period show a very clear pattern in the trends across the entire study area. Almost the entire study area shows mostly negative trends, with the exception being the southwestern part of the study area, where there are slightly more positive trends. The percentage of positive trends is 6.9 % and the percentage of negative trends is 93.1 % Trends range from -0.28 mm/year to 0.02 mm/year with a median value of -0.01 mm/year. This shows, along with the shape of the violin plot that the largest negative outlier is very large compared to the rest of the trend values. When looking at the violin plot, it can be seen that the distribution of trends is actually quite concentrated, with q1 = -0.02 mm/year and q3 = -0.01 mm/year.

The results of the second period shows a large increase in stream gauges displaying a positive trend, with the percentage of positive trends being 30.6 % and the percentage of negative trends being 69.4 %. This increase is visible across the entire southern part of the study area. The trends range from -0.011 mm/year to 0.09 mm/year, with a median value of -0.01 mm/year. The violin plot shows that the distribution of the trends is a bit more dispersed compared to the first period, with q1 = -0.01 mm/year and q3 = 0.00 mm/year.

The results of the third period are similar to those of the first period rather than to the second period. The entire study are shows mostly negative trends with almost no positive trends to be found. The percentage of positive trends is 3.4 % and the percentage of negative trends is 96.6 %. The absolute values of the trends have become slightly smaller, ranging from -0.13 mm/year to 0.04 mm/year, with a median value -0.01 mm/year. The relative spread of the trends is similar to that of the second period but shifted more towards the negative trends. With q1 = 0.01 mm/year and q3 = -0.00 mm/year.

The results of the fourth period show slightly more positive trends compared to the third period. The percentage of positive trends is 22.7 % and the percentage of negative trends is 77.3 %. The absolute values of the trends have become significantly smaller compared to the third period, ranging from -0.03 mm/year to 0.03 mm/year, with a median value of -0.00 mm/year. The violin plot shows that the trends have become relatively more dispersed, with q1 = 0.00 mm/year and q3 = 0.00 mm/year.

The results of the fifth period a similar pattern to the fourth period. The percentage of positive trends is 22.9 % and the percentage of negative trends is 77.1 %. The absolute values of the trends have become smaller compared to the previous periods, ranging from -0.01 mm/year to 0.01 mm/year, with a median value of -0.002 mm/year. The violin plot shows that the trends have become relatively more dispersed, with q1 = 0.003 mm/year and q3 = 0.003 mm/year.

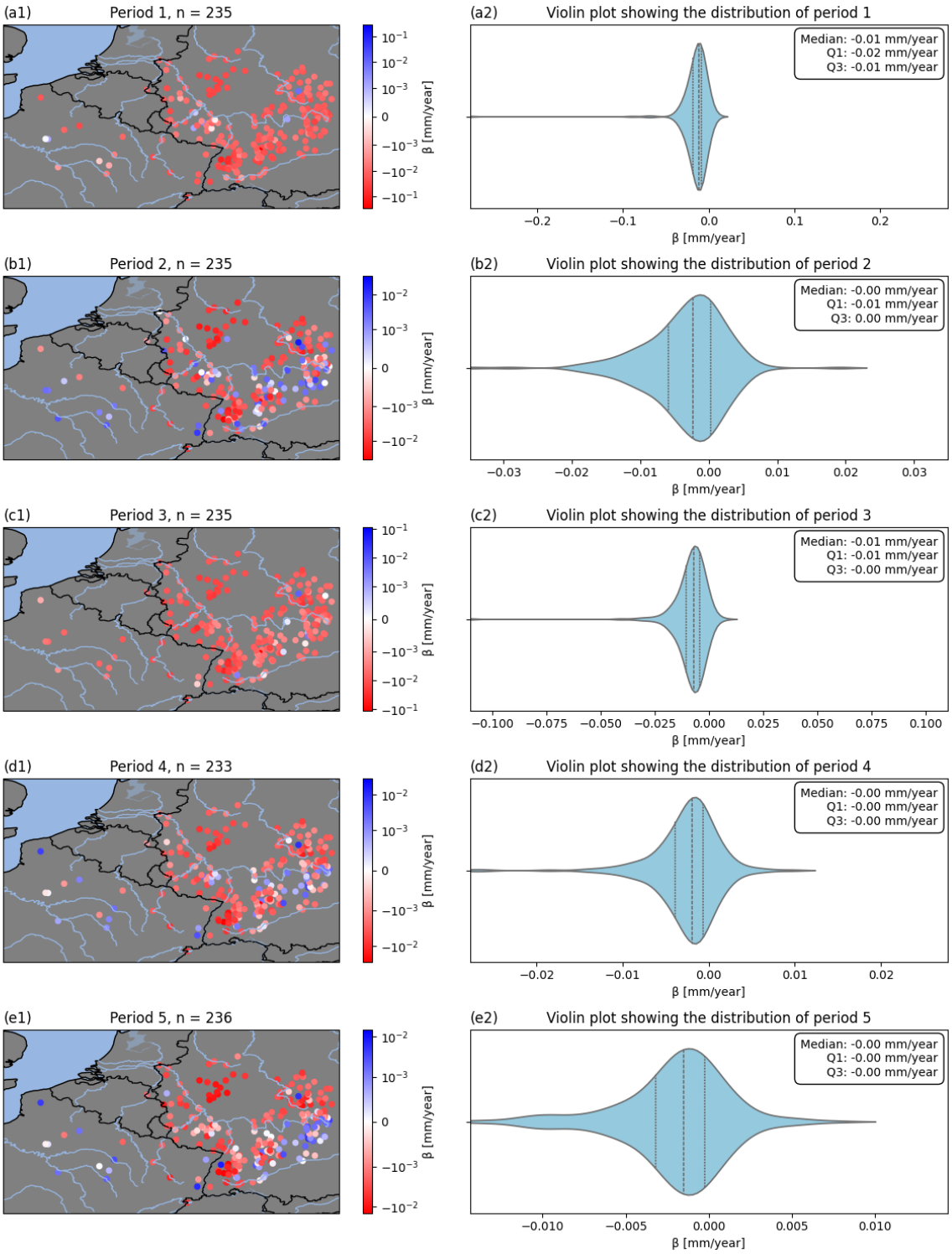


*Figure 17: Trend results for the ADF magnitude, using only stream gauges with record length of at least 60 years. Scatterplot on the left shows the location of the trends and the violin plot on the right shows the distribution of trends over the entire study area. Blue circles represent positive trends and red circles represent negative trends. Period 1: 2000-2019, period 2: 1990-2019, period 3: 1980-2019, period 4: 1970-2019, period 5: 1960-2019.*

These graphs show the trends in the magnitude  of the ADF, using only the gauges which are available for the fifth period. These graphs are meant to the show the impact of the selected temporal range on a trend analysis.

The results of the first period show mostly negative trends over the entire study area. The percentage of positive trends is 3.0 % and the percentage of negative trends is 97.0 %. The violin plot shows that the distribution of the trends is close together. With the exception to this being the large negative outlier, trends range from -0.03 mm/year to 0.01 mm/year with a median value of -0.01 mm/year.

The results of the second period show a large increase in stream gauges showing a positive trend. The percentage of positive trends is 28.1 % and the percentage of negative trends is 71.9 %. So the entire study area is still dominated by negative trends, with the southern parts showing more positive trends compared to the first period. The absolute values of the trends has also become smaller and the shape of the violin plot shows a more dispersed distribution, which is mainly due to the elimination of the large negative outlier of period 1. Trends range from -0.03 mm/year to 0.02 mm/year with a median value of -0.02 mm/year.

The results of the third period are similar to those of the first period, showing almost exclusively negative trends. The percentage of positive trends is 3.4 % and the percentage of negative trends is 96.6 %. An interesting thing which is visible from the violin plot is the fact that there is once again a large negative outlier present in the results. The shape of the violin plot therefore shows a more concentrated distribution. However, the absolute values of the trends have also become larger. Trends range from -0.011 mm/year to 0.01 mm/year, with a median value of 0.01 mm/year.

The results of the fourth period showcase a slight increase in the positive trends across the southern part of the study area. The percentage of positive trends is 17.6 % and the percentage of negative trends is 82.4 %. This shows that there is also an increase in significant negative trends. The absolute values of the trends have become smaller compared to the previous periods, ranging from -0.03 mm/year to 0.01 mm/year, with a median value of -0.00 mm/year.

The results of the fifth period shows a slight increase in positive trends compared to the previous period, along with a small decrease in negative trends. The percentage of positive trends is 22.9 % and the percentage of negative trends is 77.1 %. The shape of the violin plot shows the most dispersed distribution of the trends, but this can mainly be attributed to the smaller absolute values of the trends. Trends range from -0.01 mm/year to 0.01 mm/year, with a median value of -0.002 mm/year.

## 5.5 AMF magnitude

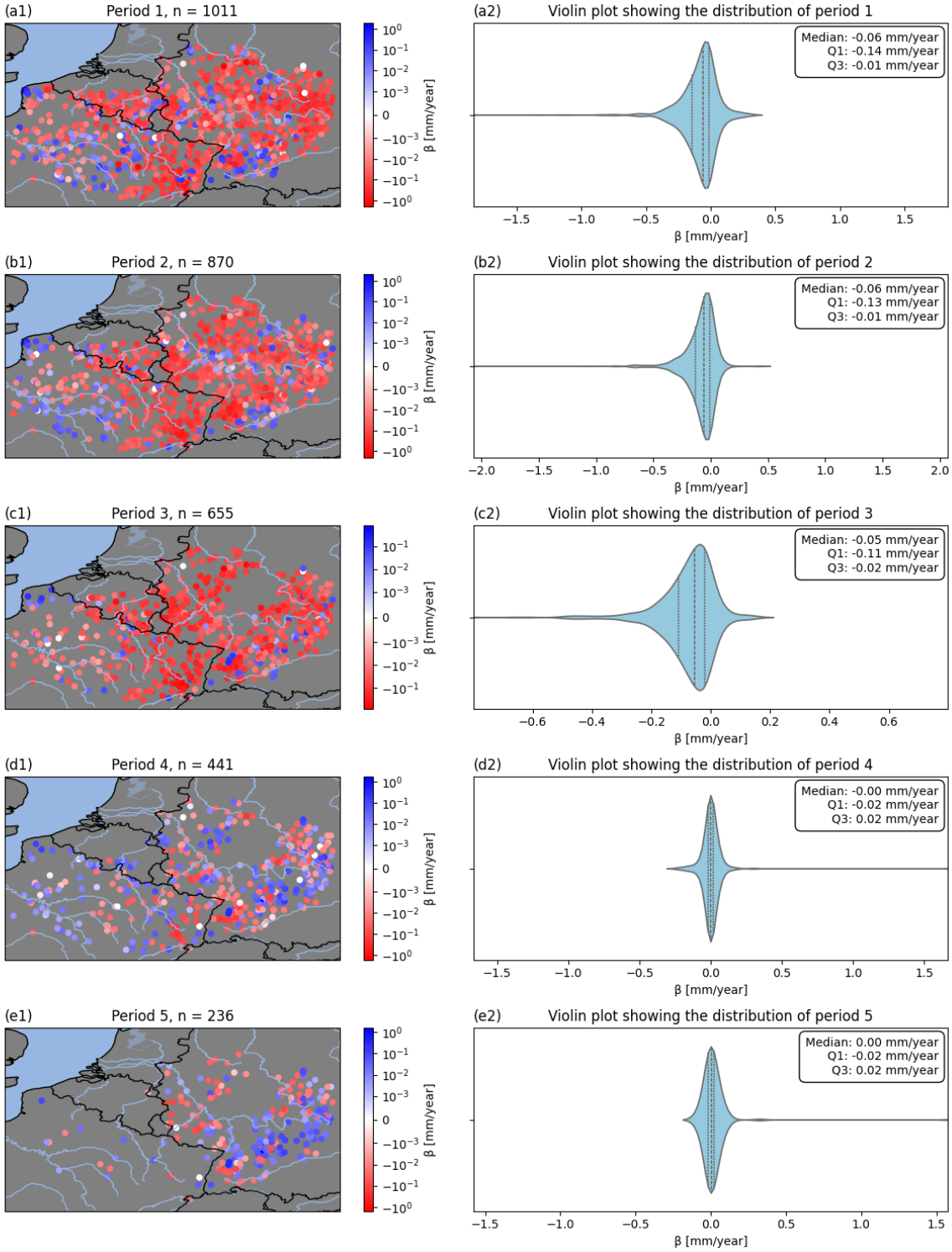


*Figure 18: Trend results for the AMF magnitude. Scatterplot on the left shows the location of the trends and the violin plot on the right shows the distribution of trends over the entire study area. Blue circles represent positive trends and red circles represent negative trends. Period 1: 2000-2019, period 2: 1990-2019, period 3: 1980-2019, period 4: 1970-2019, period 5: 1960-2019.*

These graphs show the trends in the magnitude of the AMF event for the different time periods in absolute values [mm/year]. Negative trends, which are shown by the red circles, represent decreasing magnitude. Positive trends, which are shown by the blue circles, represent increasing magnitudes.

The results of the first period show mostly negative trends, with some clusters of positive trends in the southern parts of the study area. The percentage of positive trends is 18.8 % and the percentage of negative trends is 80.7 %. The shape of the violin plot shows a well concentrated distribution of the trends, with a large negative outlier. The trends range from -1.83 mm/year to 0.32 mm/year, with a median value of -0.059 mm/year.

The results of the second period are almost identical to those of the first period when looking at the map and violin plot. The percentage of positive trends is 17.9 % and the percentage of negative trends is 81.6 %, again confirming the similarity between the results of the two period. Interestingly enough, both the positive and the negative outlier which are already visible in the results of the first period has become larger for the second period. Trends range from -2.07 mm/year to 0.44 mm/year, with a median value of 0.057 mm/year. The shape of the violin plot is also practically identical to the first period.

The results of the third period do show significant differences when compared to the previous periods. The trends have now shifted further into the negative direction, eliminating the positive clusters which are visible in the results of the previous periods. The percentage of positive trends is 9.5 % and the percentage of negative trends is 90.1 %. The absolute values of the trends have become smaller, ranging from -0.080 mm/year to 0.16 mm/year, with a median value of -0.054 mm/year.

The results of the fourth period are vastly different from those of the previous periods. The distribution between positive and negative trends is now nearly even, with the percentage of positive trends being 48.1 % and the percentage of negative trends being 50.8 %. This even distribution is also shown by the shape of the violin plot. The violin plot also shows a very large outlier in the positive direction. The absolute values for the trends have generally become smaller, ranging from -0.25 mm/year to 1.68 mm/year, with a median value of -0.000 mm/year.

The results of the fifth period are similar to those of the fourth period, with a slight increase in positive trends and a decrease in negative trends. The percentage of positive trends being 55.5 % and the percentage of negative trends being 43.6 %. These changes are mainly due to the elimination of catchments from period 4 or 5. Whether these changes hold for the same catchments is further analysed in the next section. The absolute values of the trends have become smaller, with the exception being the large outlier in the positive direction which is also visible in period 4. Trends range from -0.11 mm/year to 1.58 mm/year.

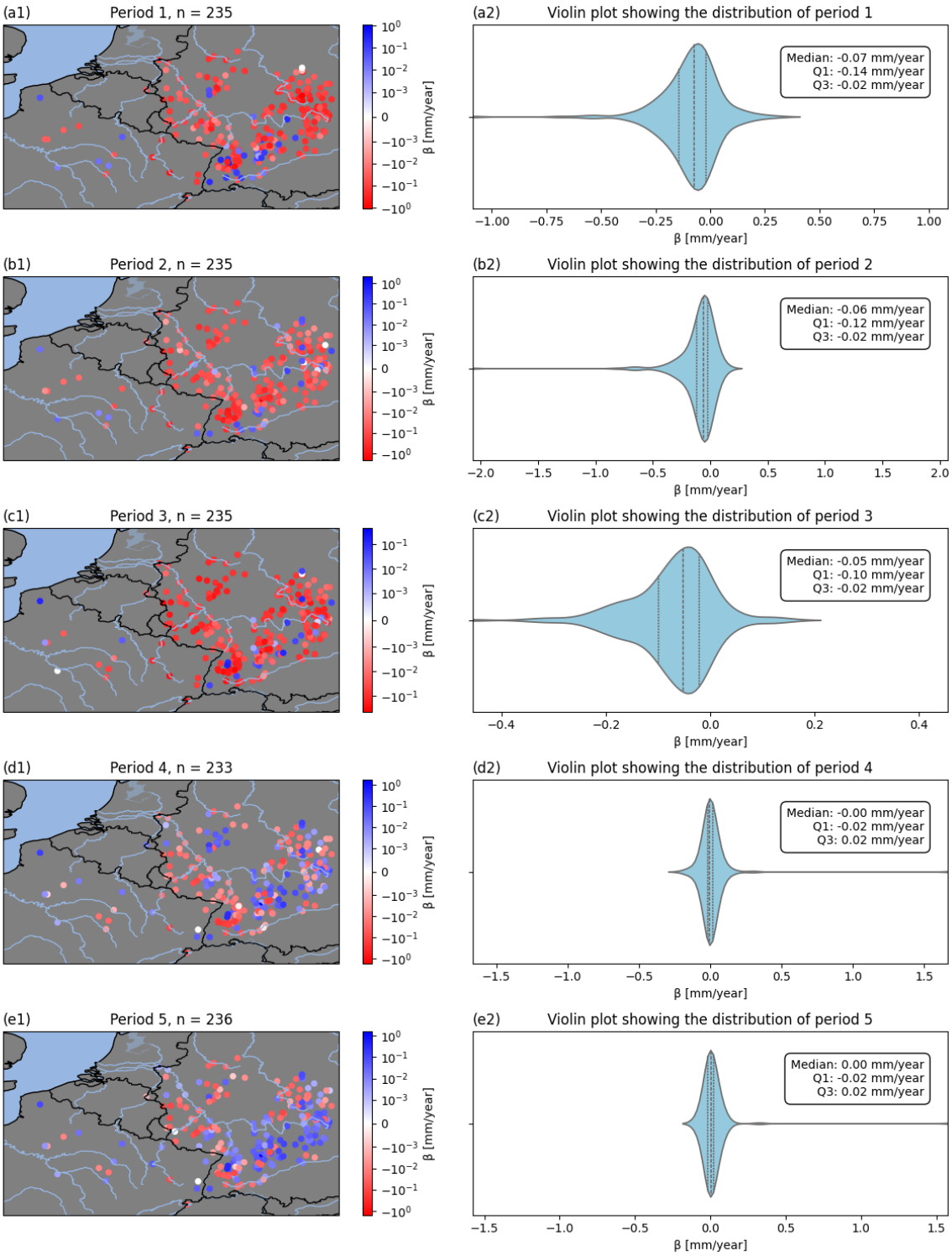


*Figure 19: Trend results for the AMF magnitude, using only stream gauges with record length of at least 60 years. Scatterplot on the left shows the location of the trends and the violin plot on the right shows the distribution of trends over the entire study area. Blue circles represent positive trends and red circles represent negative trends. Period 1: 2000-2019, period 2: 1990-2019, period 3: 1980-2019, period 4: 1970-2019, period 5: 1960-2019.*

These graphs show the trends in the magnitude of the AMF event, using only the gauges which are available for the fifth period. These graphs are meant to the show the impact of the selected temporal range on a trend analysis.

The results of the first period show mostly negative trends, with a small cluster of positive trends in the southern part of the study area. The percentage of positive trends is 15.3 % and the percentage of negative trends is 84.3 %. The shape of the violin plot shows that the trends are quite dispersed, with the exception being the large outlier in the negative direction. The trends range from -1.09 mm/year to 0.31 mm/year, with a median value of -0.07 mm/year.

As in the previous section, the results of the second are very similar to those of the first period, however some more differences can be seen with the smaller number of stream gauges considered. Negative trends have become slightly more dominant over the entire study area, with the percentage of positive trends being 10.6 % and the percentage of negative trends being 86.8 %. The shape of the violin plot shows that the absolute values of the negative trends have become significantly larger and have decreased slightly for the positive trends, further confirming the shift towards negative trends. The trends range from -2.07 mm/year to 0.15 mm/year, with a median value of -0.06 mm/year.

The results of the third period are similar compared to the previous periods, the major difference is the decrease in significant trends, both in the negative and positive direction. The percentage of positive trends is 10.6 % and the percentage of negative trends is 88.5 %. Both the map and the violin plot seem to display more negative trends, but these trends have overall become less significant. In addition to this, the absolute values of the trends have decreased in the negative direction whilst remaining the same in the positive direction. Trends range from -0.46 mm/year to 0.16 mm/year, with a median value of -0.05 mm/year.

The results of the fourth period are, as also described in the previous section, vastly different from those of the previous periods. While the majority of the trends are still negative there is a significant increase in positive trends, as shown by the map and violin plot. The percentage of positive trends is 41.6 % and the percentage of negative trends is 57.5 %. This also indicates a decrease in the significance of all the trends. The violin plot shows a large outlier in the positive direction, while the absolute values of trends in the negative direction have decreased slightly compared to those in period 3. The trends range from -0.21 mm/year to 1.67 mm/year, with a median value of -0.003 mm/year.

The results of the fifth period are similar to those of the fourth period, but now the majority of the trends is positive. The percentage of positive trends is 55.5 % and the percentage of negative trends is 43.6 %. The violin plot is near identical to the one of the fourth period, showing a slight decrease in the absolute values of the trends. Trends range from -0.11 mm/year to 1.58 mm, with a median value of 0.00 mm/year.

## 5.6 Low flow pulse count

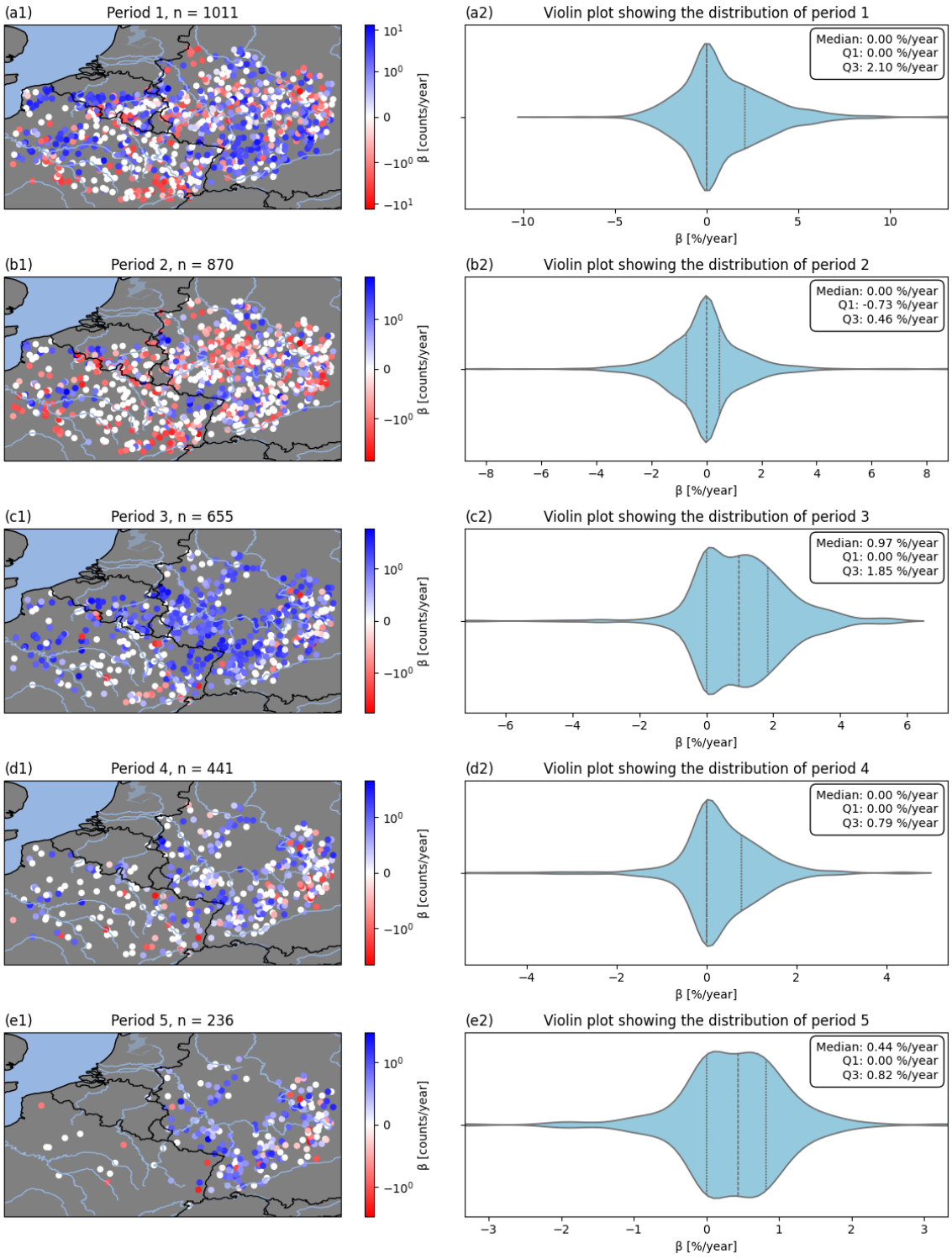


*Figure 20: Trend results for the LFPC. Scatterplot on the left shows the location of the trends and the violin plot on the right shows the distribution of trends over the entire study area. Blue circles represent positive trends and red circles represent negative trends. Period 1: 2000-2019, period 2: 1990-2019, period 3: 1980-2019, period 4: 1970-2019, period 5: 1960-2019.*

These figures show the results from the trend analysis on the LFPC signature. Trends are originally determined in counts per year. In order to make these trends less abstract, they are plotted as the percent change in mean LFPC per year. So for the first period, the mean of the LFPC signature over 20 years is taken and the trends are plotted relative to this value. Negative trends, which are shown by the red circles, represent decreasing counts (i.e. less occurrences). Positive trends, which are shown by the blue circles, represent increasing counts (i.e. more occurrences). White circles represent stream gauges for which the analysis found a trend of zero.

The results of the first period show that there mostly positive trends or no trends over the entire study area. The eastern and northern parts of the study area display dominantly positive trends and the eastern and southern parts display mostly no trends. The percentage of positive trends is 46.4 % and the percentage of negative trends is 23.1 %. The shape of the violin plot supports the fact that there exists mostly positive trends or no trends. Trends range from -9.12 %/year to 13.16% per year with a median value of 0.00 %/year. These 'relative' trend ranges translate to roughly -180 % and 260% of the mean value over 20 years. This seems impossible but it is not. This is further elaborated upon in the discussion. The violin plot also shows the large amount of stream gauges which trend is determined at exactly zero.

The results from the second period show a large increase in negative trends compared to the first period. The entire study area is now dominated by negative and no trends, with a large decrease in positive trends compared to the first period. The percentage of positive trends is 27.4 % and the percentage of negative trends is 33.9 %. This indicates a higher percentage of no trends, which is also visible from the map and violin plot. The relative trend values have become smaller, ranging from -8.26 %/year to 8.77 %/year with a median value of 0.00 %/year.

The results of the third period show a clear pattern across the entire study area. The entire area is dominated by positive trends and compared to the previous periods, a lot of the white circles have disappeared. The percentage of positive trends is 67.5 % and the percentage of negative trends is 7.0 %. The violin plot also demonstrates the clear dominance of the positive trends. The relative trend values have become slightly smaller, ranging from -7.22 %/year to 5.71 %/year with a median value of 0.97 %/year.

The results of the fourth period show a slight decrease in the relative number of positive trends, shifting more towards no trends. Whether this is due to the elimination of stream gauges that display a positive trend from period 3 is investigated in the next section. The percentage of positive trends is 46.7 % and the percentage of negative trends is 12.9 %. The relative values of the trends have become smaller in both directions, ranging from -5.36 %/year to 4.40 %/year with a median value of 0.00 %/year.

The results of the fifth period are similar to those of the fourth period, showing mostly no trends and positive trends across all stream gauges. The percentage of positive trends is 61.4 % and the percentage of negative trends is 13.6 %. The relative values of the trends have become smaller compared to the previous periods, ranging from -3.32 %/year to 3.28 %/year with a median value of 0.44 %/year.

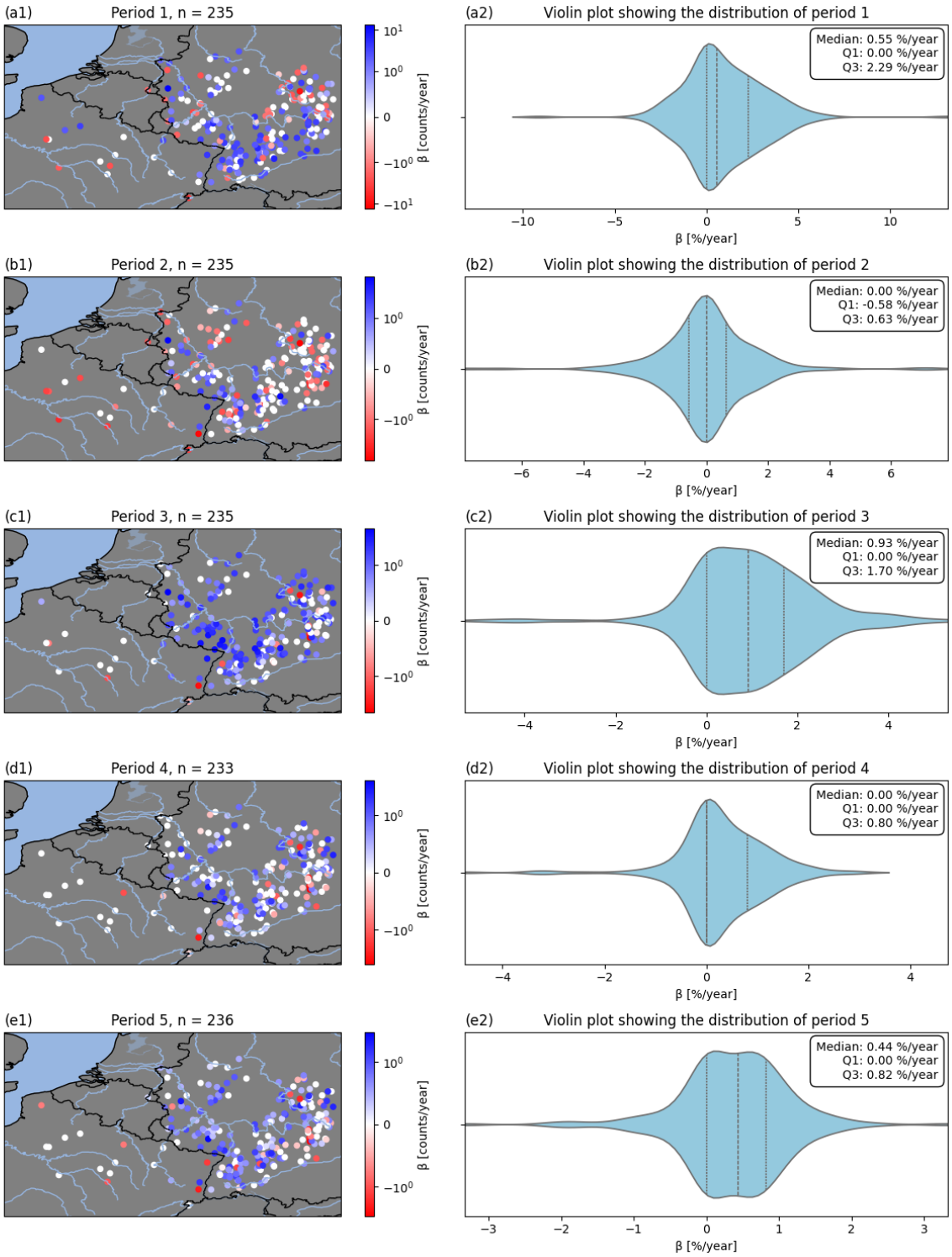


*Figure 21: Trend results for the LFPC, using only stream gauges with record length of at least 60 years. Scatterplot on the left shows the location of the trends and the violin plot on the right shows the distribution of trends over the entire study area. Blue circles represent positive trends and red circles represent negative trends. Period 1: 2000-2019, period 2: 1990-2019, period 3: 1980-2019, period 4: 1970-2019, period 5: 1960-2019.*

These graphs show the trends in the LFPC, using only the gauges which are available for the fifth period. These graphs are meant to the show the impact of the selected temporal range on the trend analysis.

The results of the first period clearly show that the trends are mostly positive across all of the gauges. The percentage of positive trends is 52.3 % and the percentage of negative trends is 19.1 %. The shape of the violin plot also shows that a large part of the stream gauges display no trend. Trends range from -9.12 %/year to 13.16 %/year, with a median value of 0.55 %/year.

The results of the second period show a clear shift in the distribution in the trends. There is no dominant pattern across the stream gauges, which is also shown by the shape of the violin plot. The percentage of positive trends is 28.9 % and the percentage of negative trends is 30.2 %. This indicates that the majority of trends is exactly zero. The relative trend values have become smaller, ranging from -8.26 %/year to 8.77 %/year with a median value of 0.00 %/year.

The results of the trend period show the most pronounced pattern across all stream gauges. The majority of stream gauges show positive trends, with a few stations in between displaying no trend. The percentage of positive trends 67.7 % and the percentage of negative trends is 6.8 %. The shape of the violin plot also shows this distribution, along with the fact that the relative values of trends have stayed similar. The outliers have decreased slightly most of the values have a similar order of magnitude compared to the previous period. The trends range from -7.22 %/year to 5.71 %/year with a median value of 0.93 %/year.

The results of the fourth period show an increase in gauges displaying no trends and a decrease in positive trends. The percentage of positive trends is 46.8 % and the percentage of negative trends is 13.3 %. The violin plot shows that the number of gauges displaying positive trends is higher than the number of gauges displaying negative trends, which is in line with the results of the previous period. The relative values of the trends have decreased slightly compared to those of the third period. The trends range from -5.36 %/year to 4.40 %/year with a median value of 0.00 %/year.

The results of the fifth period are similar to those of the third period, both the map and violin plot. The trends across all gauges are mostly positive, with the percentage of positive trends being 61.4 % and the percentage of negative trends being 13.6 %. This indicates that the number of stations which show no trend has decreased compared to the previous period. The relative trends have become smaller, ranging from -3.32 %/year to 3.28 %/year.

## 5.7 High flow pulse count

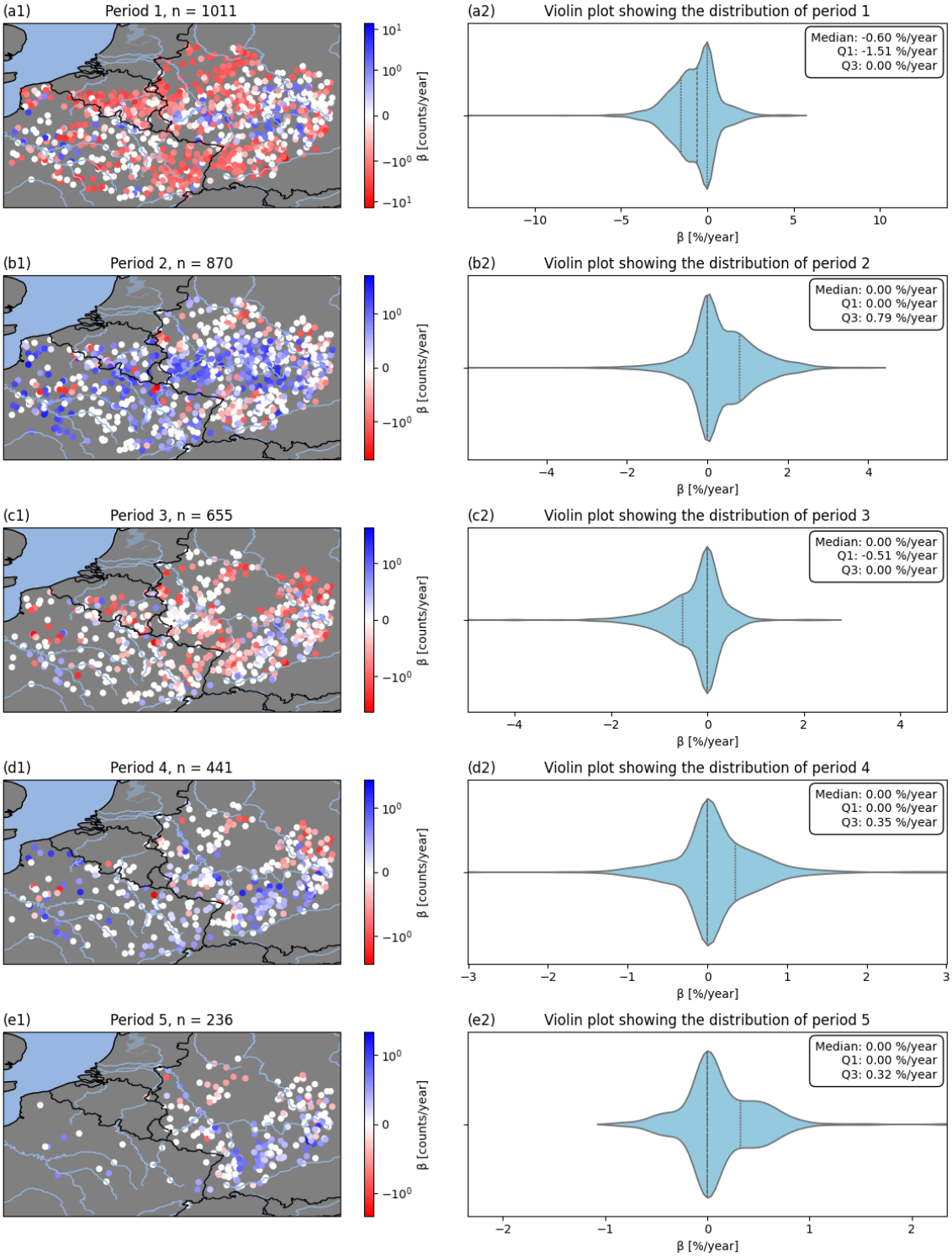


*Figure 22: Trend results for the HFPC. Scatterplot on the left shows the location of the trends and the violin plot on the right shows the distribution of trends over the entire study area. Blue circles represent positive trends and red circles represent negative trends. Period 1: 2000-2019, period 2: 1990-2019, period 3: 1980-2019, period 4: 1970-2019, period 5: 1960-2019.*

These figures show the results from the trend analysis on the HFPC signature. Trends are originally determined in counts per year. In order to make these trends less abstract, they are plotted as the percent change in mean HFPC per year. So for the first period, the mean of the HFPC signature over 20 years is taken and the trends are plotted relative to this value. Negative trends, which are shown by the red circles, represent decreasing counts (i.e. less occurrences). Positive trends, which are shown by the blue circles, represent increasing counts (i.e. more occurrences). White circles represent stream gauges for which the analysis found a trend of zero.

The results of the first period show clear spatial patterns in the trends for the HFPC. Across the entire study are there are mostly negative trends. This is mainly visible in the more central parts of the study area. The southwestern and eastern parts of the study area also show a large amount of stream gauges with no trend. The percentage of positive trends is 11.7 % and the percentage of negative trends is 55.8 %. The trends are distributed quite closely together, with the exception of one large outlier in the negative direction. Trends range from -13.89 %/year to 5.01 %/year with a median value of -0.60 %/year.

The results of the second period are almost opposite compared to the results of the first period. Across the entire study area, there are now mostly gauges with no trends or positive trends. The positive trends dominate in the central parts of the study area, with the outer parts showing mostly gauges with no trend. The percentage of positive trends is 46.0 % and the percentage of negative trends is 12.3 %. The shift in distribution is also clearly visible when comparing the shape of the violin plots. The violin plot of the second period looks like a mirrored version of the violin plot of the first period. The relative trend values have become significantly smaller, ranging from -5.97 %/year to 3.99 %/year with a median value of 0.00 %/year.

The results of the third period are less pronounced compared to those of the previous periods, but similarity can be seen with the first period rather than the second period. Most of the stream gauges display no trend, with negative trends appearing the most after that. The percentage of positive trends is 12.4 % and the percentage of negative trends is 38.5 %. The relative trend values have become slightly smaller, ranging from -4.97 %/year to 2.42 %/year with a median value of 0.00 %/year.

The results of the fourth period are, similar to the third period, less pronounced than the results of the first two periods. For this period, the similarity is found with the results of the second period. The percentage of positive trends is 34.0 % and the percentage of negative trends is 15.2 %. Again showing that most gauges show no trend in this period. The relative trend values have become slightly smaller in the negative direction and slightly larger in the positive direction. Trends range from -3.01 %/year to 2.95 %/year, with a median value of 0.00 %/year.

The results of the fifth period show mostly stream gauges with no trend, along with some positive trends. The percentage of positive trends is 35.2 % and the percentage of negative trends is 13.1 %. The shape of the violin plot is similar to those of period 2 and 4, with smaller relative trend values. Trends range from -0.83 %/year to 2.35 %/year with a median value of 0.00 %/year.

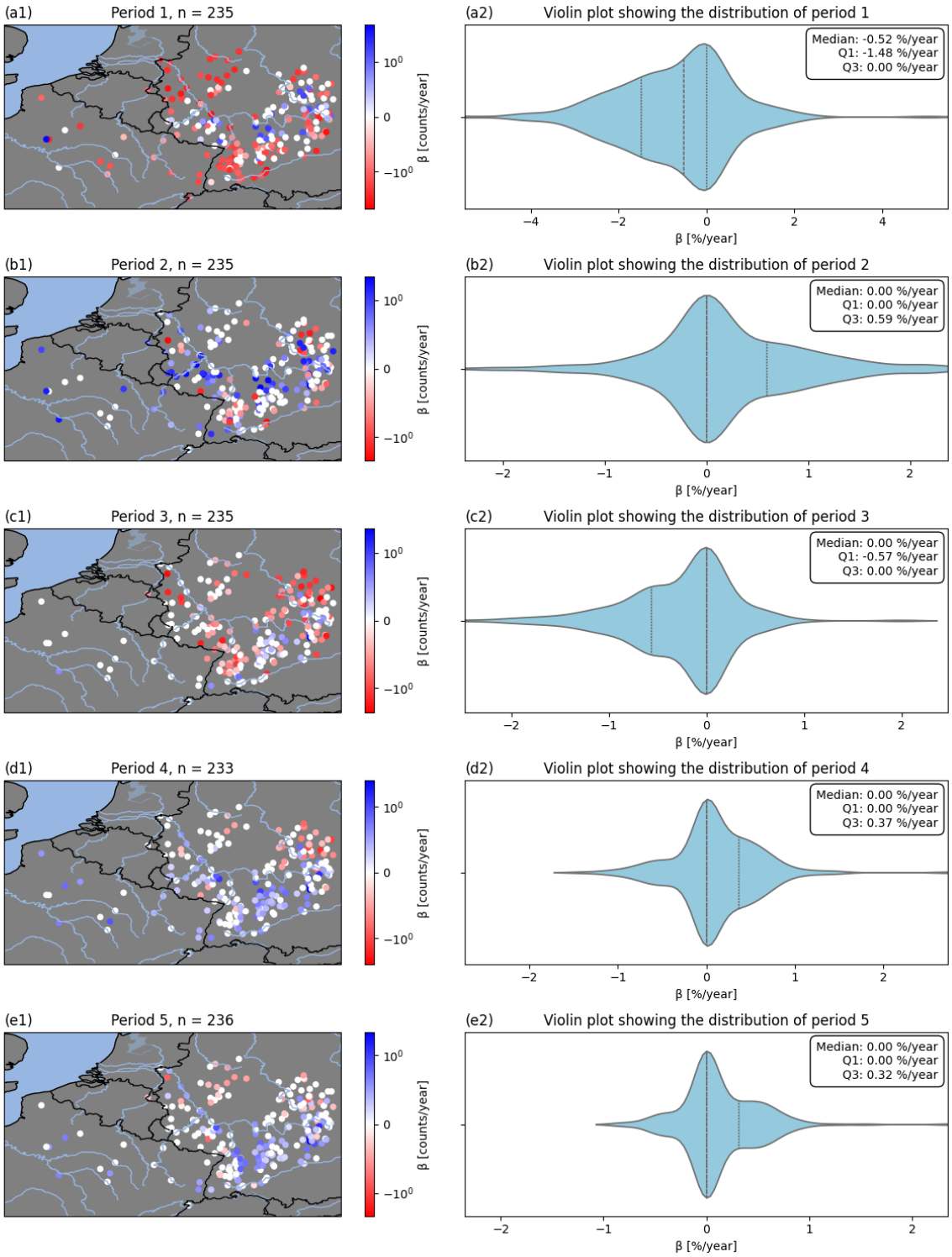


*Figure 23: Trend results for the HFPC, using only stream gauges with record length of at least 60 years. Scatterplot on the left shows the location of the trends and the violin plot on the right shows the distribution of trends over the entire study area. Blue circles represent positive trends and red circles represent negative trends. Period 1: 2000-2019, period 2: 1990-2019, period 3: 1980-2019, period 4: 1970-2019, period 5: 1960-2019.*

These graphs show the trends in the HFPC, using only the gauges which are available for the fifth period. These graphs are meant to the show the impact of the selected temporal range on the trend analysis.

Looking at the results of the first period, it is visible that most of these selected gauges show negative trends, with a significant number of gauges also displaying no trend. The percentage of positive trends is 13.6 % and the percentage of negative trends is 52.3 %. This pattern is similar to the pattern described in the previous section, containing all the stream gauges. The relative trends for the selected gauges range from -5.49 %/year to 5.01 %/year with a median value of -0.52 %/year.

A shift in pattern is seen similar to the one described in the previous section. For the second period, the gauges display mostly positive trends or no trend. The percentage of positive trends is 34.5 % and the percentage of negative trends is 15.7 %. This more even distribution is also shown by the shape of the violin plot. The relative trend values have decreased significantly for both directions. Trends range from -2.14 %/year to 2.37 %/year with a median value of 0.00 %/year.

The majority of positive trends which are visible in the results of the second period have disappeared in the results of the third period, showing mostly negative trends or no trend. The percentage of positive trends is 11.5 % and the percentage of negative trends is 42.1 %. This distribution is also shown by the violin plot, the shape of which is similar to the one of the first period. The relative trend values have stayed practically the same order of magnitude. Trends range from -2.47 %/year to 1.98 %/year with a median value of 0.00 %/year.

The results of the fourth period are more similar to the results of the second period rather than the third period. Most of the stream gauges show positive trends or no trend. The percentage of positive trends is 37.8 % and the percentage of negative trends is 15.0 %. For these selected gauges these are the first results that show a dominantly positive trend pattern. The relative trend values have become smaller in the negative direction and larger in the positive direction. Trends range from -1.41 %/year to 2.72 %/year with a median value of 0.00 %/year.

The results of the fifth period show an increase in stream gauges with no trend and a decrease in stream gauges with trends, in both directions. The percentage of positive trends is 35.2 % and the percentage of negative trends is 13.1 %. The shape of the violin plot is similar to the one of the fourth period, with a higher concentration of gauges at exactly zero, further supporting the shift towards no trend. The relative trend values have become smaller in both directions. The trends range from -0.83 %/year to 2.35 %/year with a median value of 0.00 %/year.

## 5.8 Low flow pulse duration

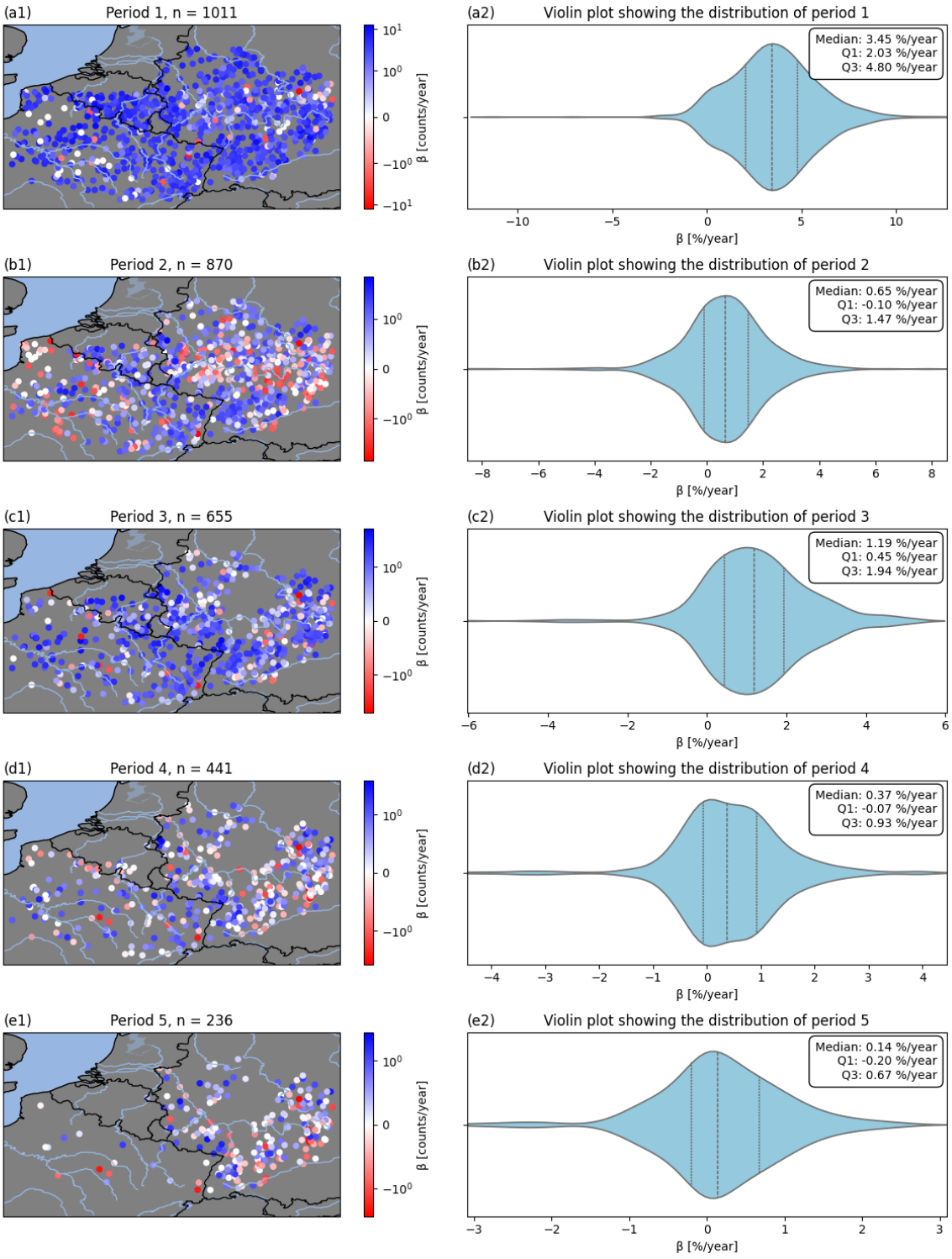


*Figure 24: Trend results for the LFPD. Scatterplot on the left shows the location of the trends and the violin plot on the right shows the distribution of trends over the entire study area. Blue circles represent positive trends and red circles represent negative trends. Period 1: 2000-2019, period 2: 1990-2019, period 3: 1980-2019, period 4: 1970-2019, period 5: 1960-2019.*

These figures show the results from the trend analysis on the LFPD signature. Trends are originally determined in days per year. In order to make these trends less abstract, they are plotted as the percent change in mean LFPD per year. So for the first period, the mean of the LFPD signature over 20 years is taken and the trends are plotted relative to this value. Negative trends, which are shown by the red circles, represent decreasing duration (i.e. shorter). Positive trends, which are shown by the blue circles, represent increasing duration (i.e. longer). White circles represent stream gauges for which the analysis found a trend of zero.

The results of the first period show almost exclusively positive trends across the entire study area, with a few gauges showing no trend. The percentage of positive trends is 93.9 % and the percentage of negative trends is 3.7 %. The shape of the violin plot further supports this finding. Apart from a large outlier on the negative side, almost no gauges show negative trends. The trends range from –11.36 %/year to 12.66 %/year with a median value of 3.45 %/year.

The results from the second period still show a majority of positive trends across the entire study area. However when looking at the map and violin plot, it becomes visible that there are significantly more gauges showing negative trends compared to the first period. The percentage of positive trends is 68.2 % and the percentage of negative trends is 27.8 %/year. The relative trend values have also become smaller in both directions. Trends range from -8.53 %/year to 7.83 %/year with a median value of 0.65 %/year.

The results of the third period again show a higher portion of positive trends compared to the second period. The percentage of positive trends is 86.9 % and the percentage of negative trends is 2.0 %. When examining both the map and violin plot, it becomes visible that, in relation to their respective ranges, the trends are smaller compared to those of the first period. The range of the relative trends has also become smaller. Trends range from -6.03 %/year to 5.25 %/year with a median value of 1.19 %/year.

The results of the fourth period show a shift towards smaller positive trends along with an increase in gauges showing negative trends or no trend. Whether this shift can be attributed to the elimination of gauges from period 3 to period 4 is difficult to say. This will be investigated in the next section. The percentage of positive trends is 64.4 % and the percentage of negative trends is 28.8 %. This shift comes with a general decrease in the range of the trend values, as well as a decrease of the positive trend values relative to this range. The trends range from -4.45 %/year to 4.05 %/year with a median value of 0.37 %/year.

The results of the fifth period show an almost even distribution between gauges showing positive trends, negative trends or no trend. This is most likely attributed to the elimination of gauges from period 4 to period 5 but this is further analysed in the next section. The percentage of positive trends is 55.5 % and the percentage of negative trends is 35.6 %. The range of the relative trend values has decreased in both the negative and positive direction. Trends range from -3.09 %/year to 2.56 %/year with a median value of 0.14 %/year.

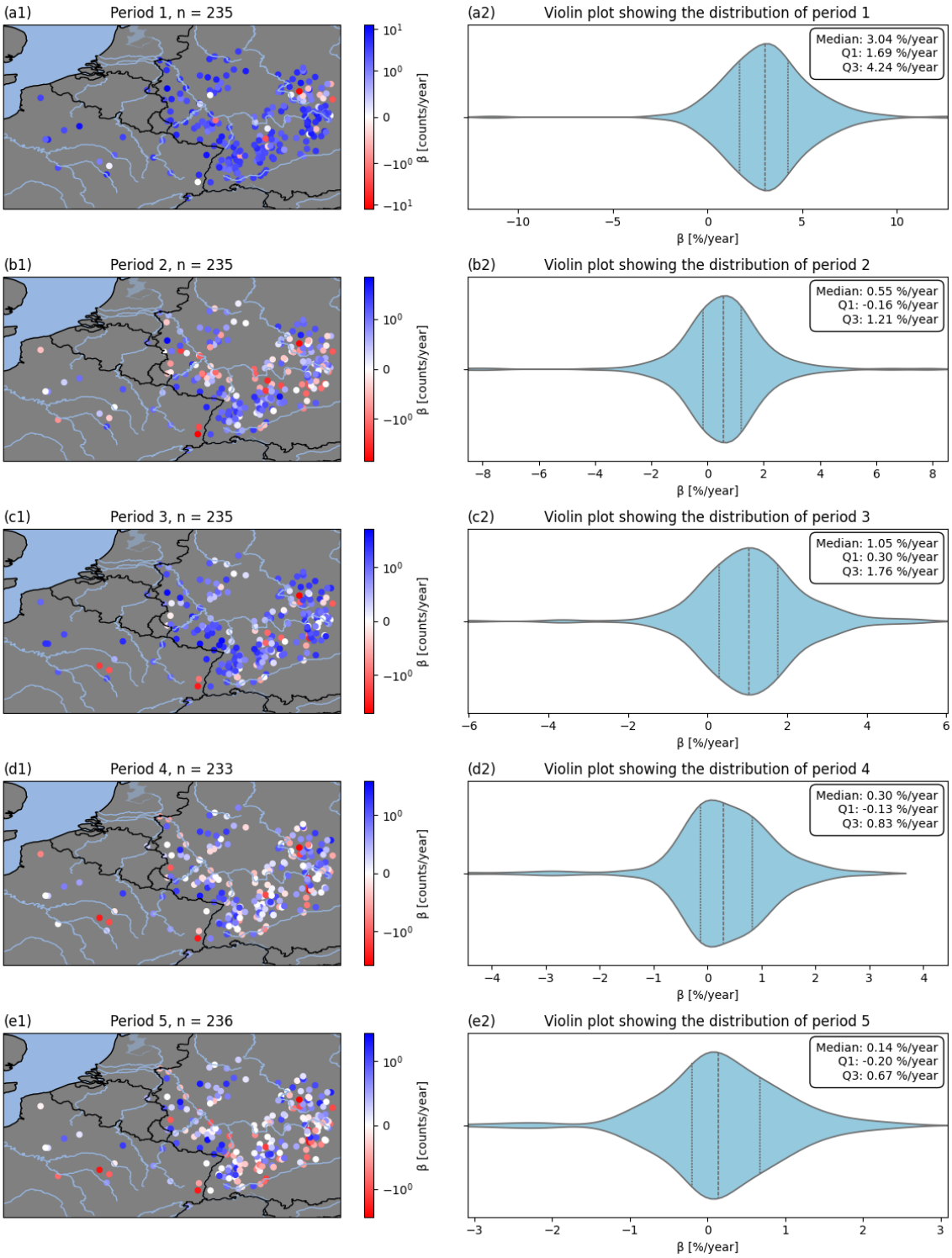


*Figure 25: Trend results for the LFPD, using only stream gauges with record length of at least 60 years. Scatterplot on the left shows the location of the trends and the violin plot on the right shows the distribution of trends over the entire study area. Blue circles represent positive trends and red circles represent negative trends. Period 1: 2000-2019, period 2: 1990-2019, period 3: 1980-2019, period 4: 1970-2019, period 5: 1960-2019.*

These graphs show the trends in the LFPD signature, using only the gauges which are available for the fifth period. These graphs are meant to the show the impact of the selected temporal range on the trend analysis.

The results of the first period show almost exclusively positive trends across all the selected gauges. The percentage of positive trends is 94.0 % and the percentage of negative trends is 5.1 %. This indicates that a large number of gauges have positive trends with a p-value below $\alpha = 0.10$. Except for one large outlier on the negative side, the trend values are concentrated close to the median value. Trends range from -11.36 %/year to 12.66 %/year with a median value of 3.04 %/year.

The results of the second period show an increase in gauges showing negative trends and no trends. In addition to this, there is a decrease in both the number of stations showing a positive trend and in the actual magnitude of this trend. The percentage of positive trends is 66.4 % and the percentage of negative trends is 29.4 %. As mentioned, the range of the relative trend values has become smaller in both directions. Trends range from -8.53 %/year to 7.83 %/year with a median value of 0.55 %/year.

The results of the third period are more similar to the results of the first period rather than the results of the second period. This becomes visible from both the map and the violin plot. The percentage of positive trends is 83.0 % and the percentage of negative trends is 13.6 %. The range of the relative trends has again become smaller in both directions. Trends range from -6.03 %/year to 5.25 %/year with a median value of 1.05 %/year.

The results of the fourth period have become significantly less pronounced than the results of the third period. There is both a more even distribution between positive and negative trends, as well as a decrease in the range of the relative trend values. The percentage of positive trends is 60.9 % and the percentage of negative trends is 30.9 %. The trends range from -4.45 %/year to 3.05 %/year with a median value of 0.30 %/year.

The results of the fifth period are similar to those of the fourth period, becoming even less pronounced and more evenly distributed between positive and negative trends. The percentage of positive trends is 55.5 % and the percentage of negative trends is 35.6 %. Trends range from -3.09 %/year to 2.56 %/year with a median value of 0.14 %/year.

## 5.9 High flow pulse duration

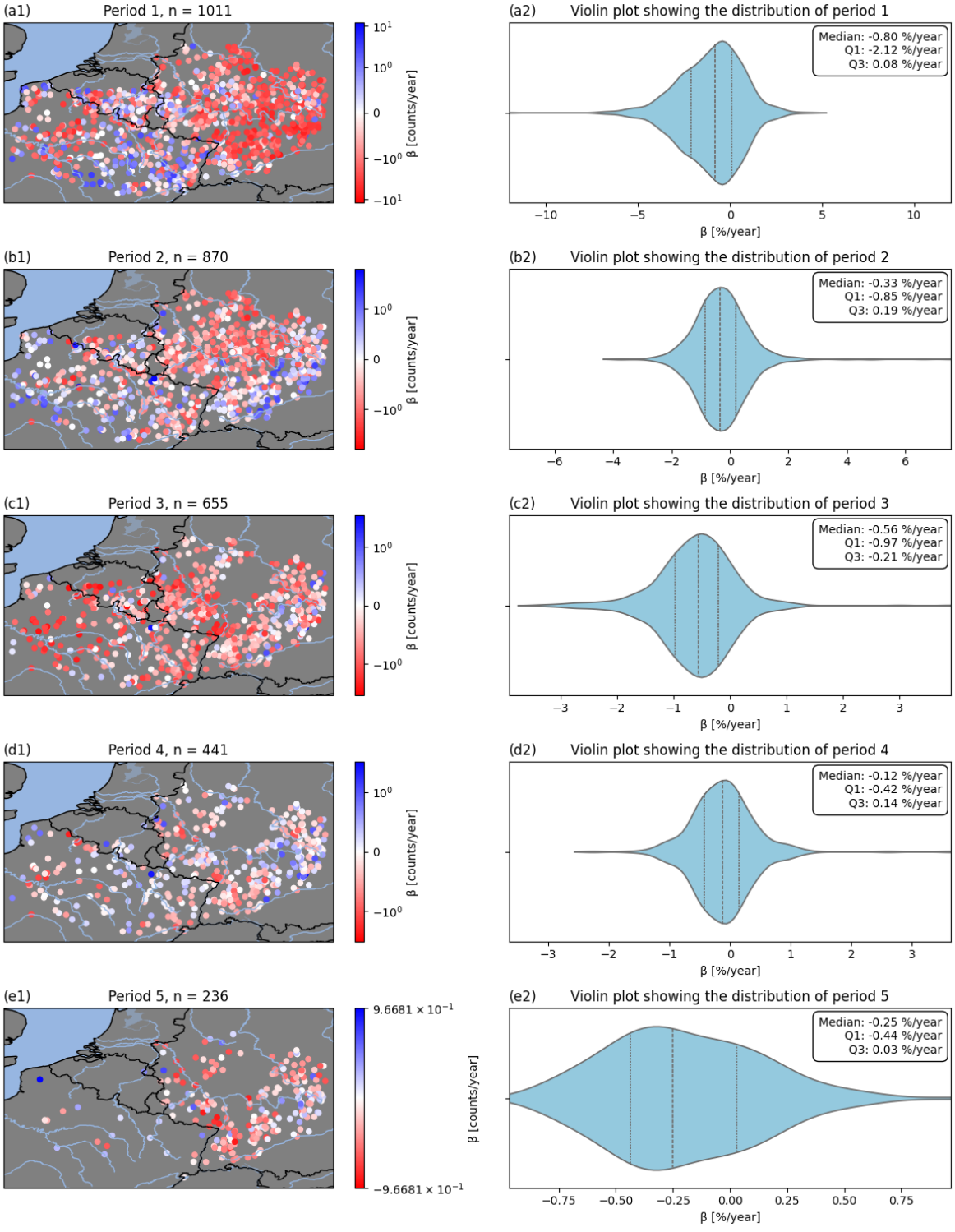


*Figure 26: Trend results for the HFPD. Scatterplot on the left shows the location of the trends and the violin plot on the right shows the distribution of trends over the entire study area. Blue circles represent positive trends and red circles represent negative trends. Period 1: 2000-2019, period 2: 1990-2019, period 3: 1980-2019, period 4: 1970-2019, period 5: 1960-2019.*

These figures show the results from the trend analysis on the HFPD signature. Trends are originally determined in days per year. In order to make these trends less abstract, they are plotted as the percent change in mean HFPD per year. So for the first period, the mean of the HFPD signature over 20 years is taken and the trends are plotted relative to this value. Negative trends, which are shown by the red circles, represent decreasing duration (i.e. shorter). Positive trends, which are shown by the blue circles, represent increasing duration (i.e. longer). White circles represent stream gauges for which the analysis found a trend of zero.

The results of the first period show mostly negative trends across the entire study area. There are some clusters of positive trends in the more southern and western parts of the study area. The percentage of positive trends is 26.7 % and the percentage of negative trends is 72.2 %. The violin plot show that the trend distribution is quite dispersed, along with one large outlier on the negative direction. The trends range from -12.00 %/year to 4.37 %/year with a median value of -0.80 %/year.

The results of the second pattern show nearly the same pattern as seen in the first period but less pronounced. The percentage of positive trends is 32.2 % and the percentage of negative trends is 65.7 %. The range of the relative trend values has decreased in the negative direction and increased in the positive direction. Trends range from -3.86 %/year to 7.55 %/year with a median value of -0.33 %/year.

The results of the third period show an increase in the portion of negative trends and a decrease in the range of the relative trend values compared to the previous periods. The percentage of positive trends is 13.7 % and the percentage of negative trends is 85.6 %. The trends range from -3.38 %/year to 3.91 %/year with a median value -0.56 %/year.

The results of the fourth period are significantly different than the results of the previous periods. The distribution, while still dominated by negative trends is much more even and less pronounced. The percentage of positive trends is 37.4 % and the percentage of negative trends is 60.5 %. The range of the relative trend values has decreased slightly in both directions. The trends range from -2.27 %/year to 3.64 %/year with a median value of -0.12 %/year.

The results of the fifth period are similar to those of the fourth period. Most stream gauges show a negative trend, but the distribution is much more even than for the first three periods. From the map plot it becomes visible that there is an increase in stream gauges that show no trend. The percentage of positive trends is 27.1% and the percentage of negative trends is 72.0 %. The range of the relative trend values has decreased significantly. Trends range from -0.87 %/year to 0.97 %/year with a median value of -0.25 %/year.

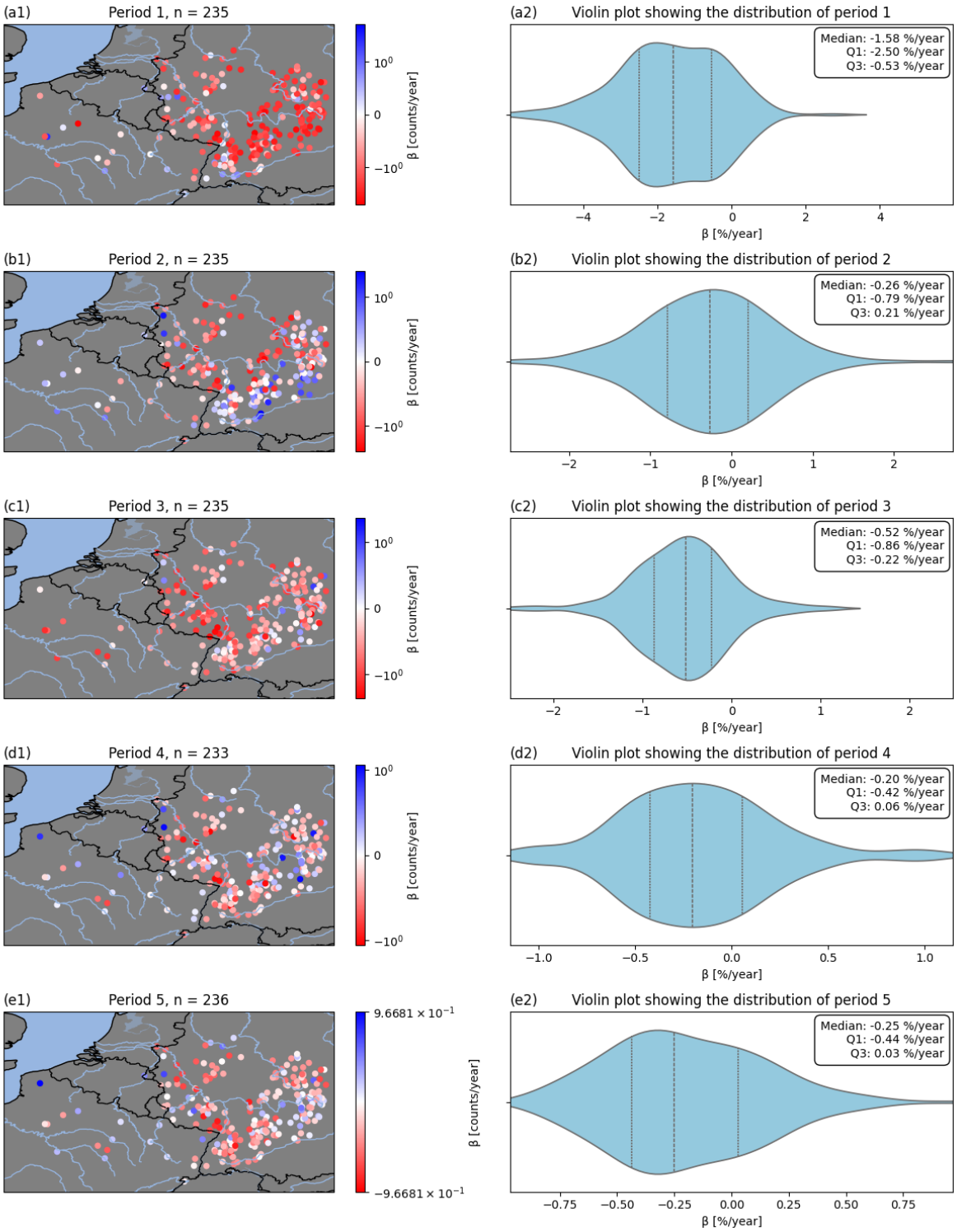


*Figure 27: Trend results for the LFPD, using only stream gauges with record length of at least 60 years. Scatterplot on the left shows the location of the trends and the violin plot on the right shows the distribution of trends over the entire study area. Blue circles represent positive trends and red circles represent negative trends. Period 1: 2000-2019, period 2: 1990-2019, period 3: 1980-2019, period 4: 1970-2019, period 5: 1960-2019.*

The results of the first period show almost exclusively negative trends across the selected stream gauges. The percentage of positive trends is 11.1 % and the percentage of negative trends is 88.9 %. The large outlier in the negative direction was not among the selected stream gauges so therefore the shape of the violin plot shows a more even distribution, especially in the negative direction. The trends range from -5.97 %/year to 2.70 %/year with a median value of -1.58 %/year.

The results of the second period show a more even distribution between negative and positive trends across the selected stream gauges. The percentage of positive trends is 34.5 % and the percentage of negative trends is 64.3 %. The range of the relative trend values has decreased slightly in both directions. The trends range from -2.67 %/year to 2.73 %/year with a median value of -0.26 %/year.

The results of the third period are again more similar to those of the first period rather than the second period. Showing a high percentage of negative trends across the selected stream gauges. The percentage of positive trends is 11.1 % and the percentage of negative trends is 88.9 %. In both directions the range of the relative trend values has decreased. The trends range from -2.48 %/year to 1.08 %/year with a median value of -0.52 %/year.

The results of the fourth period then is more similar to the results of the second period rather than those of the third period. Looking at the violin plot, a more even distribution between positive and negative trends is visible, while still being dominated by negative trends. The percentage of positive trends is 30.5 % and the percentage of negative trends is 68.7 %. The range of the trends has decreased in the negative direction and remained almost identical in the positive direction. The trends range from -1.15 %/year to 1.06 %/year with a median value of -0.20 %/year.

The results of the fifth period are similar to those of the fourth period. Most stream gauges show a negative trend, but the distribution is much more even than for the first three periods. From the map plot it becomes visible that there is an increase in stream gauges that show no trend. The percentage of positive trends is 27.1 % and the percentage of negative trends is 72.0 %. The range of the relative trend values has decreased significantly. Trends range from -0.87 %/year to 0.97 %/year with a median value of -0.25 %/year.

## 5.10 Temporal sensitivity analysis

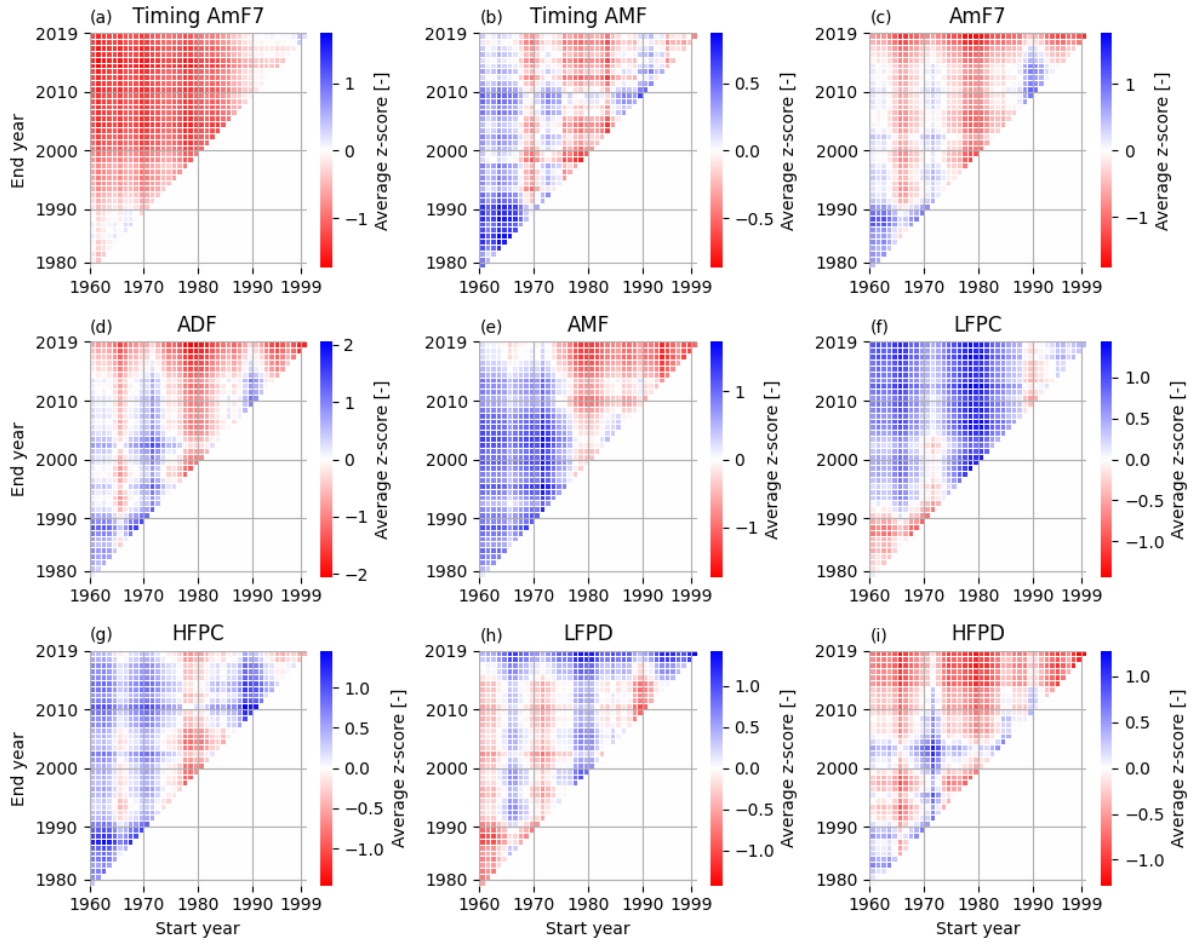


*Figure 28: Multi-temporal trend analysis for each signature. Mann-Kendall test applied and average Z-score shown for each possible combination of start year (x-axis) and end year (y-axis). Red representing negative trends and blue representing positive trends. Only gauges with at least 60 years of data are used (n = 235)*

Figure 28 shows the heatmaps that contain the average Z-scores for each possible combination of start-and-end year. The multi-temporal trend analysis is performed on the 235 stream gauges which contain at least 60 years of data. This selection corresponds to the stream gauges shown in Figure 9(e), which are almost exclusively located in Germany. The average Z-score across all gauges is calculated and represented by the colour of the cell. Each cell represents the combination of the start year on the x-axis and the end year on the y-axis. Red cells represent negative trends and blue cells represent positive trends. These heatmaps are described per signature.

The heatmap of the AmF7 timing shows a clear pattern. For nearly all combinations of start and end years, the average Z value is negative. The two exceptions to this being trends with a start year after 1990 of and end year before 1990. In these clusters, the negative trends are significantly less pronounced and for a handful of combinations, the trends are positive.

The heatmap of the AMF timing shows a more complex pattern compared to the AmF7 timing. Trend results are dependent on the choice of start year, regardless of the end year. The trend from 1999 – 2019, which coincided with period 1, is positive. Trends with a start year around 1990 are positive. Starting years between 1973 – 1985 show negative trends. Then positive trends around start year 1972 and negative trends around start year 1970. Trends with a start year prior to 1969 are negative. ‘Horizontal clusters’ are less clear but can be seen around end year 2000 (towards negative) and 2010 (towards positive).

In the AmF7 magnitude, all trends with an end year before 1990 are positive. Overall, the later the end year, the more negative the trend. There are two vertical clusters of positive trends around the start years of roughly 1962, 1972 and 1990. These positive trends all become less pronounced, and eventually negative as the end year becomes later. Irrespective of start year, all trends that end in 2019 are negative. The trends in the ADF magnitude are almost identical to the trends in the AmF7 magnitude, with the positive 'vertical' clusters being slightly larger.

The AMF magnitude trends are different slightly different than its counterparts. A much clearer pattern is seen in the heatmap. All trends with a start year prior to roughly 1975 are positive and all trends with a start year after 1975 are all negative. Additionally, a pattern is visible for each start year. The later the end year (i.e. the longer the period) the more negative the trend becomes. For the starting years prior to 1975 this means the positive trends become less pronounced and for the start years after 1975 this means the negative trends become more pronounced.

Trends in LFPC, with an end year after 1990, irrespective of start year, are almost exclusively positive. The exception to this is trends with a start year around 1990, which display slight negative trends for each end year. A similar pattern is seen around start years of roughly 1972, however these combinations show mostly less pronounced trends in the positive direction. Trends with a start year of 2019 are almost all positive, with the exception at the start years around 1990.

The trends in the HFPC show a more complex pattern than the trends in the LFPC. Almost all trends with a start year before 1975 show positive trends. As the end year becomes later, and thus the periods become longer, the positive trends become slightly less pronounced. Trends with a start year roughly around 1980 are negative for most end year. Then a large positive cluster is seen around start year 1990. These trends gradually become less pronounced as the start year becomes later (i.e. shorter periods).

Regardless of the start year, trends in the LFPD are positive for the end years of 2015 - 2019. Trends with an end year prior to 2015 show an alternating pattern based on the start year. Trends with a starting year between 1960 – 1965 are negative for end years prior to 2015. Then the starting years 1965 – 1970 display almost exclusively positive trends for end years prior to 2015. This pattern continues to the start year of 1995 – 1999.

The trends in the HFPD are opposite to the ones in LFPD. Regardless of the start year, the trends are almost exclusively negative for the end years of 2010 – 2019. Trends with an end year prior to 2010 show an opposing alternating pattern between positive and negative compared to the LFPD. However, in the HFPD, the positive trends are slightly less pronounced and the negative trends are more dominant.

# 6. Discussion

The three research objectives of this study are defined as:

- Analyse spatial patterns and temporal trends in river flows, considering the entire streamflow regime.
    - Create a proper set of hydrological signatures to characterize the streamflow regime.
    - Identify decadal-scale variability in streamflow trends across the streamflow regime.

To achieve these objectives, the methodology described in Chapter 4 of this report is applied to hydrological signatures described in section 4.4. This section discusses the implications of the results from these trend analyses. This discussion is meant to help achieve the research objectives and support the answers to the research questions. It is important to remember that no hypotheses and/or expectations are stated. The research is purely focused on showing the changes in the streamflow regime and temporal variability herein. Each signature will be discussed separately and afterwards some general insights and implications are discussed. Finally, answers to the research questions are given.

## 6.1 Timing signatures

When looking at the first period of the AMF timings trend results, a clear spatial pattern is discernible. Across the entire study area there exist mostly negative trends, with almost 70% of the gauges displaying a negative trend. This dominance is especially visible in the central and eastern regions of the study area. The exception to this are the more southern regions of the study area, where the distribution is more even. This implies that overall, the AMF event is occurring earlier in the year.

Interestingly, the pattern completely changes when moving to the second period. There are mostly positive trends visible, with small areas in the eastern part of the study area still showing negative trends. 65% of all gauges display a positive trend. Considering that positive trends indicate later AMF timings in the year, this sudden shift in direction can be the result of very early AMF timings for a period during the decade of 1990-2000.

This sensitivity is further demonstrated by the results of periods 3, 4 and 5. Periods 3 and 4 show similar trends to the first period (i.e. mostly negative trends) and the fifth period showing similar trends to the third period (i.e. mostly positive trends). The spatial pattern remains consistent over the time periods, although it becomes less pronounced. However, making a spatial comparison is challenging, given the considerable number of eliminated stream gauges in each period. These significant differences in the trend distribution imply that the AMF timing trend analysis is sensitive to the selection of time period.

The results with only gauges that contain at least 60 years of data show the temporal sensitivity in the AMF timing. 70 % of the gauges display a negative trend in the first period. This dominance of negative trends is consistent with the trends in period 3 and 4, but in period 2 and 5 almost 60 % of the gauges display a positive trend. This interdecadal variability is also displayed in the heatmap of the AMF timing, where this oscillating pattern is also visible. Interestingly, the pattern is quite consistent over the end years of the analysis. This implies that the AMF timing trends are more sensitive to the choice of start year than the choice of end year.

The results of the first period for the AmF7 timings show that across almost the entire study area, positive trends are dominant with 64 % of the gauges displaying a positive trend. A small area in the Northeastern part is showing more negative trends. This implies that for the first period, the AmF7 event generally occurs later in the year.

The results of the second period are still similar to the results of the first period but the trend distribution is now much more even. From period 3 and onwards, a shift in the trend patterns becomes clearly visible. From period 3 and onwards, the trends across the gauges are mostly negative. The percentage of negative trends increases gradually with each period, with 90% negative trends in period 5.

The results for gauges with at least 60 years of data also show this pattern of mainly positive trends transitioning to mainly negative trends. The percentage of negative trends in the first period is 34%, which gradually increases to a percentage of 90% in period 5. This pattern is also shown in the heatmap of the AmF7 timing. The heatmap shows a consistent pattern among most combinations of start and end year, with the exception of the short-term trends with start or end year 1990. This implies that the AmF7 timing is less sensitive to the choice of the time period than the AMF timing.

Similar to the AMF timing, the estimated trend slopes become smaller as the time period increases. On comparing the trend ranges from the AMF timing and the AmF7 timing, it is observed that the trend values for the AmF7 timing are higher for each period. This suggests that the shift in timing for the minimum flow event is greater than the shift in timing for the maximum flow event. This raises the question of whether this is expected? The AMF and AmF7 events are polar opposites, indicating the timing of high and low flow respectively. A key difference between the two signatures is the fact that the AmF7 occurs over seven consecutive days and the AMF event occurs on a single day. This makes the AMF event more susceptible to 'random' extreme events and the AmF7 event more predictable. This means that trends in the timing of the AmF7 event will be more pronounced than for the AMF event.

## 6.2 Magnitude signatures

The spatial pattern that is found in the trends of the magnitude of the AmF7 event is opposite to the one of the AmF7 timing trends. For the first period, the entire study displays 91% negative trends. This means that the magnitude of the AmF7 event has decreased over the period 2000-2019 for almost all of the stream gauges. The second period displays more positive trends, with 37 % of the trends displaying positive trends.

The higher number of positive trends is not visible in period 3, that displays 89 % negative trends. The fourth and fifth period show slightly more positive trends, but the majority of the trends remain negative. Whether this is due to the elimination of stream gauges with a negative trend is investigated using only the stream gauges with at least 60 years for each period.

The results for gauges with at least 60 years display the same pattern across the periods. The majority of the stream gauges display a negative trend for each period. With period 2 having the lowest percentage of negative trends at 66 % and period 1 the highest at 91 %. This implies that the AmF7 trends are relatively robust to the choice of time period. However, when looking at the heatmap of the AmF7 trends, it is seen that this statement is not entirely true. This heatmap shows that for the end year of 2019, the AmF7 trend is not sensitive to the choice of time period. However, this is not consistent with earlier end years. From end years prior to 2015, the trends show interdecadal fluctuations between negative and positive, with positive vertical clusters around the start year of 1990, 1970 and 1960. This illustrates the sensitivity to the selection of both start and end year for this signature.

For each period, the spatial patterns in the ADF trends are very similar to the spatial patterns in the AmF7 trends, with the ADF showing even higher percentages of negative trends in each period. In addition to this, the trends are less pronounced in the ADF than in the AmF7. This is to be expected, since the ADF is based on the average flow and the AmF7 is based on the low flow. Low flow is an extreme event, therefore trends will be more pronounced than for the average conditions.

As with the AmF7 trends, the gauges with at least 60 years of data confirm the temporal pattern in the ADF trends. The heatmap of the ADF trends shows an identical pattern to the heatmap of the AmF7 trends. All of this implies that the low flow magnitude and the medium flow magnitude are varying in tandem to each other.

The AMF magnitude trends, are similar to the AmF7 and ADF trends in the first three periods, with the percentage of negative trends being 90% for the third period. However, in the fourth and fifth period the percentage of positive trends increases significantly, which is not seen for the AmF7 and the ADF. The fifth period even shows more positive trends than negative trends, with a percentage of 56%.

This pattern can also be seen from the gauges with at least 60 years of data, as well as the heatmap with all possible combinations. A clear pattern is visible from the heatmap, showing positive trends for combinations with a start year prior to 1975. This implies that the short-term negative trends in the AMF are not consistent with the long-term trends, which are generally positive.

These similarities across the magnitude signatures imply a high degree of consistency in magnitude trends across the three stages of flow. This implies that the shape of the streamflow magnitude distribution does not change, it merely shifts towards higher or lower values. The accordance in trend direction for the three magnitude signatures is determined across the stream gauges is determined for each period and shown in Table 2.

| | AmF7 - ADF | ADF - AMF | AmF7 - AMF | All agree |
|---|---|---|---|---|
| Period 1 | n = 875 (86.5%) | n = 820 (81.1%) | n = 758 (75.0%) | n = 723 (71.5%) |
| Period 2 | n = 613 (70.5%) | n = 654 (75.2%) | n = 549 (63.1%) | n = 474 (54.5%) |
| Period 3 | n = 589 (89.9%) | n = 582 (88.9%) | n = 532 (81.2%) | n = 524 (80.0%) |
| Period 4 | n = 345 (78.2%) | n = 266 (60.3%) | n = 226 (51.2%) | n = 199 (45.1%) |
| Period 5 | n = 175 (74.2%) | n = 141 (59.7%) | n = 124 (52.5%) | n = 103 (43.6%) |

*Table 2: Number of stream gauges that have the same direction in the magnitude signatures.*

In the first three periods, or until 1980, the accordance in trend direction is relatively high. For the period 1980-2019 80% of the stream gauges show similar trend directions in the magnitude signatures. This means that the shape of the magnitude distribution is not changing, but the distribution is moving as a whole towards wetter or drier conditions. This implies that the streamflow magnitude is not intensifying.

However, the degree of accordance in trend direction greatly decreases in periods 4 and 5. For the period 1960-2019 just 40% of the stream gauges show similar trend directions in the magnitude signatures. In contrast to the shorter periods, this means that the shape of the distribution is changing, which implies that the streamflow magnitude is intensifying. This sudden 'shift' in accordance also becomes visible from the sensitivity heatmaps. There is more similarity between magnitude signatures with a start year after 1980 than periods with a start year before 1980.

Across all of the periods, the smallest trends are found in the ADF, followed by the AmF7. The AMF trends are the largest absolute trend values. This is to be expected. The average flow is expected to display the smallest trends because it is not an extreme event. The difference in absolute trend values between the AmF7 and AMF magnitude is explained simply by the fact that the magnitude of high flow is obviously higher than the magnitude of low flow. Furthermore, the trend values of these signatures could be plotted as a percentage of the mean to analyse which trends are relatively more pronounced.

In period 4 of the AMF trends a large outlier in the positive direction appears, which is absent in the preceding periods. Initially, this anomaly may appear to be a data error or a mistake in the trend analysis. To address this issue, the data is plotted alongside the estimated trend line for each period in Figure29:

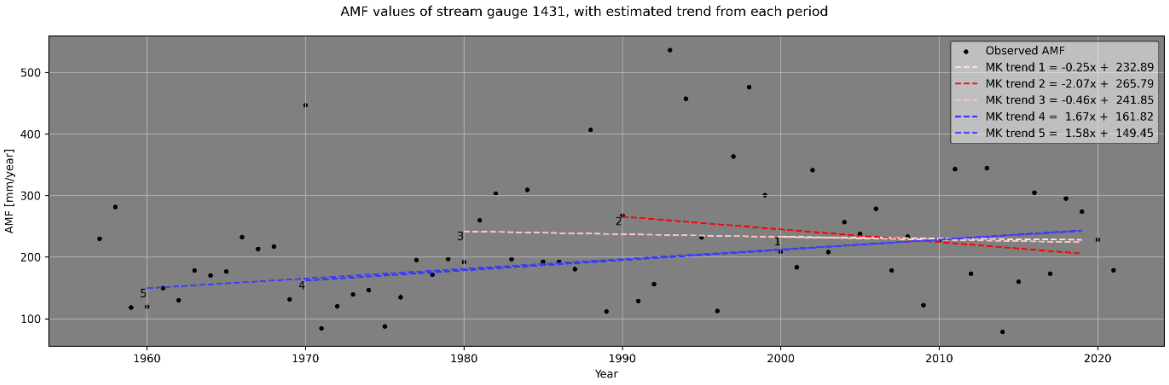


*Figure 29: AMF series of stream gauge 1431, with the estimated trend from each period*

Figure 29 demonstrates significant fluctuations in both trend direction and magnitude. The largest positive trend is given by a slope of 1.67 mm/year and the largest negative slope is given by a slope of -2.07 mm/year. These differences show how sensitive a trend analysis can be to the choice of the time period and that estimated trends have to be interpreted carefully. This observation is revisited in a later section of this chapter.

## 6.3 Frequency signatures

Before discussing the results in the signatures based on low and high flow pulses, it is crucial to restate how these signatures are determined. This is done because they are slightly more abstract than the other signatures and therefore require extra attention. As explained in section 4.5, the low and high flow pulses are determined based on the first and third quartile of the streamflow data. This means that the upper and lower threshold are set at the streamflow magnitude where 25% of the data is above and beneath it respectively. This means that this threshold cannot be determined annually since this would result in an identical number of pulse counts each year. Therefore, it was decided to determine these threshold values over the entire length of each individual timeseries and then determine each signature annually. The consideration was whether to determine this threshold for each of the five periods respectively, but ultimately the choice was made for the entire length of the time series. This because it more accurately reflects the physical low-and-high flow conditions at each stream gauge. Finally, the magnitude signatures are normalized by dividing the streamflow with the contributing catchment area. In order to normalize the pulse signatures, the estimated trend is divided by the mean value and plotted as a percentage of the mean value per year. This eliminates some of the abstractness of the trends. This approach can result in trend values that appear implausible. This will be discussed in more detail shortly.

In the first period, LFPC trends are positive in 46% gauges across the entire study area. Furthermore, there is a large number of stream gauges (31%) that display a trend of exactly zero, or rather no trend. This implies that many stream gauges do not display a (statistically significant) trend, or this trend is not detected using the methodology of this research. This is a recurring phenomenon in the pulse count signatures and will be discussed later in this section. Looking closer at the map plot, it becomes visible that stream gauges are somewhat clustered based on the direction of their trend. This implies that the changes in low flow pulses are consistent in the region that they are located in.

Period 2 shows mainly gauges with negative trends or no trends. This implies that for the period of 1990-2000, many stream gauges will have high annual LFPC values. The clusters which were mentioned are harder to detect for this period than for the first period, this is most likely attributed to the increase in stream gauges with no trend. The third period shows mostly positive trends, with a percentage of 68%. The results of the fourth and fifth periods display mostly positive trends, similar to the third period.

The gauges with at least 60 years of data show a similar temporal pattern across the periods. With the first period showing 52% positive trends, the second period being evenly distributed and period 3, 4 and 5 mostly positive trends. This pattern is also clear from the heatmap, which shows a relatively consistent pattern across all combinations. With the exception of two negative clusters around combinations 1960 – 1990 and start year 1990, all of the trends in LFPC are positive.

The results of the first period of the HFPC show a more distinct spatial pattern compared to the LFPC. Firstly, the majority (56%) of the trends is negative, which is opposite to the LFPC signature. This is logical since the HFPC and LFPC are exact opposites of each other. The negative trends have clustered in both the southern and the northern part of the study area. In the eastern part of the study area there is a majority of stream gauges that display no trend. This further supports the finding of spatial clustering of pulse count from the LFPC signature. The clusters are both more pronounced and larger in the HFPC when compared to the LFPC.

The majority of the stream gauges within period 2 display either a positive trend (46%) or no trend (42%). This is parallel to the results of the LFPC in the second period, which further supports the contrast

between the two signatures. This parallel temporal pattern further continues in period 3, where the majority of trends in the HFPC is either zero or negative. Trends in the HFPC are generally less pronounced than the trends in the LFPC. In both of the last two periods, 50% of gauges show a trend of exactly zero. Interestingly, there are more gauges displaying a positive trend in these final two periods, 35% for both periods. This implies that for the long-term trends, the LFPC and HFPC move in the same direction.

The gauges with at least 60 years of data also show this fluctuating pattern in the HFPC trends. This pattern also becomes visible from the heatmap of the HFPC trends. The heatmap also shows that the trends in HFPC are relatively robust to the choice of end year, but sensitive to the choice of start year of the analysis.

As mentioned previously, the trends in the pulse count signatures might seem implausible. The trend range in the LFPC over the first period translates to -180 % and 260 % of the mean value. These trends are shown in the Figure 30 and 31 respectively:

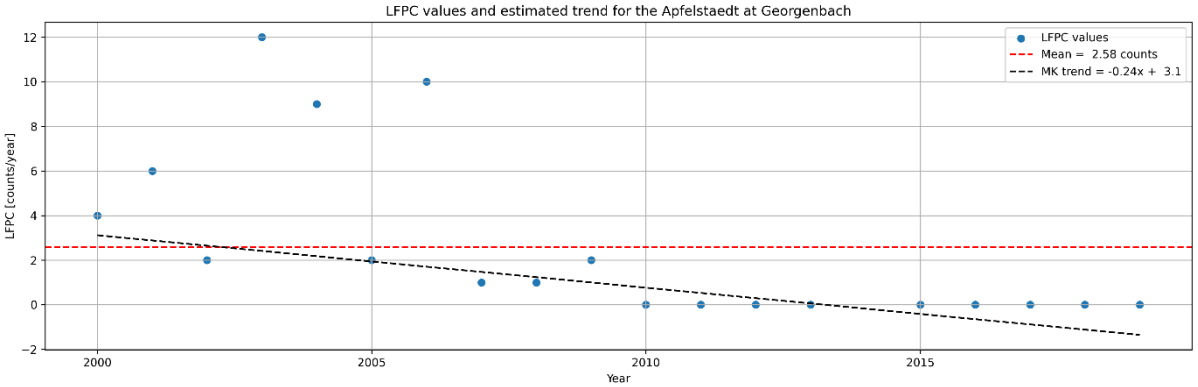


*Figure 30: LFPC values and estimated trend for the Apfelstaedt at Georgenbach*

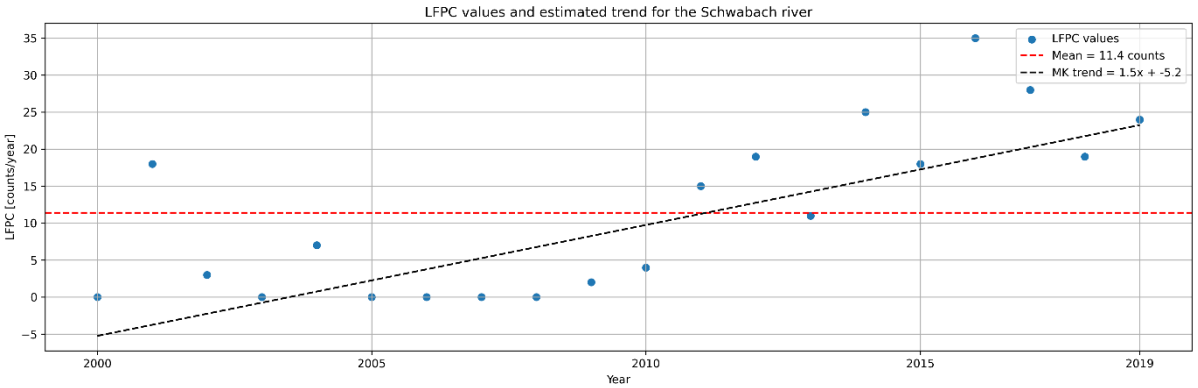


*Figure 31: LFPC values and estimated trend for the Schwabach river*

From Figures 30 and 31 it becomes clear that these high relative trend slopes are in fact possible. Both of these stream gauges have multiple years in which the LFPC value is zero and this causes the mean value to be low. When these values of zero are located at the beginning or end of the period this will result in a positive or negative trend respectively. This trend will then be relatively high compared to the mean value.

Secondly, the most obvious finding of the results in the pulse count signatures is the large number of stream gauges where the trend is estimated to be exactly zero. This number is significantly different than all of the other signatures. This implies that, for these two signatures specifically, there are many stream gauges which do not have a (significant) trend across the multiple time periods. However, it can also

imply that trends in the frequency of low and high flow frequency are hard to find using these signatures. This would be because of the interaction between the signatures and the Theil-Sen slope estimator. This interaction is best described with the help of the Figure 32

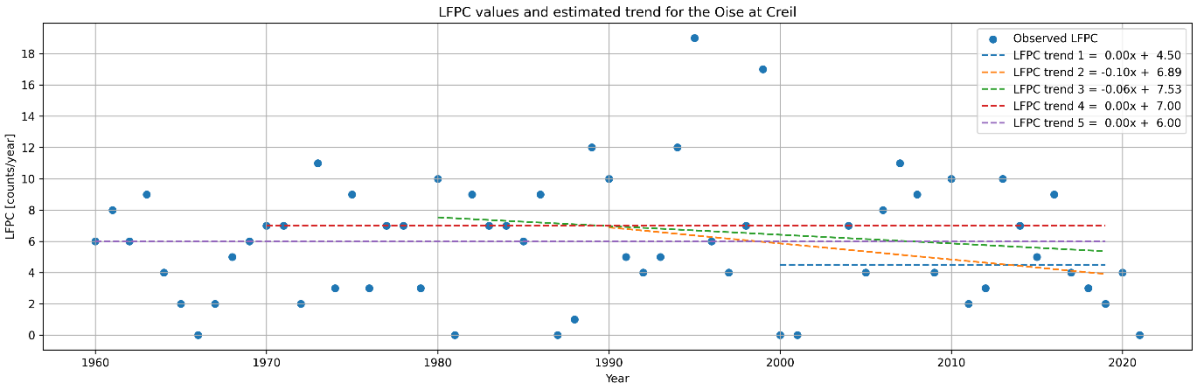


*Figure 32: LFPC values and estimated trends for the Oise at Creil*

Figure 32 shows the observed values for the LFPC and estimated trends for a single stream gauge. Many of the trends are estimated to be exactly zero. The values of the LFPC and HFPC are whole integers. This means that the value of 2 years can be exactly the same. This mean that the slope between a pair can be exactly zero for multiple pairs. Since the estimated trend slope is defined as the median of the slopes between all possible pairs, the possibility exists that this median value is exactly zero. Thus resulting in many stream gauges that display a trend of exactly zero.

Overall, the temporal patterns visible for the LFPC and HFPC are parallel to each other, which means that negative trends in the low flow signature generally mean positive trends in the high flow signature. This supports the arguments made previously for a more general shift of the streamflow magnitude distribution rather than a change of shape in the distribution. Alternatively, the changes in pulse count signatures can also mean changes in the variability of streamflow. An increase in HFPC does not necessarily mean an increase in the streamflow magnitude, it can also imply that the streamflow has become ‘flashier’. In order to correctly assess what these changes imply for the overall streamflow developments the results of the duration signatures have to be discussed first.

However, as with the magnitude signatures, there seems to be a sudden shift in trend accordance around the start year 1980. Trend accordance in the frequency signatures is given by parallel trends. For example, an increase in the number of low flow pulses would be in accordance with a decrease in the number of high flow pulses. Looking at Figure 28(f) and 28(g) a clear difference is seen between periods starting before and after 1980.

Periods starting after 1980 have mostly parallel trends, which means that the trends are in accordance with each other. This implies that the streamflow frequency distribution is not intensifying. However, periods starting before 1980 show a different combination, showing mostly positive trends in both the LFPC and HFPC, which means more low flow periods and more high flow periods. This implies an intensifying of the streamflow frequency distribution.

## 6.4 Duration signatures

94% of stream gauges show a positive trend in LFPD for the first period. This dominance is consistent over the five periods, with the percentage of positive trends gradually decreasing to 56% in the fifth period. Mostly positive trends in the LFPD imply that overall, the low flow periods have become longer over the time period. In combination with the trends in the LFPC, which were also mostly positive across most periods, this would indicate that the low flow pulses occur more often in the year and also last

longer. This combination suggests an increase in the overall number of days of low streamflow for most gauges.

The gauges with at least 60 years confirm this pattern of mostly positive trends over all periods. However, the heatmap shows a much more complex and heterogeneous pattern over all combinations. The top of the heatmap, which corresponds to an end year of 2019, indeed shows that the trends are mostly positive for all start years of the analysis. However, this finding is inconsistent for start years prior to 2015. For those combinations, the trend value is dependent to the choice of start year. An almost cyclical pattern is found. This implies that the LFPD values in the years of 2015-2019 are so large compared to past years, that the trends are more robust to the choice of start year.

The HFPD trends in period 1 show almost exclusively negative trends in the eastern part of the study area and a small area in the central / southern part of the study area shows a cluster of positive trends. Around 70% of the gauges in the first period show a negative trend. Similar to the pulse count signatures, the trend direction of the HFPD is opposite to the LFPD. In addition to this, the trends are much less pronounced in their relative values. The majority of stream gauges showing negative trends remains consistent over all periods.

This temporal pattern is even more pronounced in the gauges with at least 60 years of data. However, the same inconsistency that was found in the LFPD heatmap is also found in the HFPD heatmap, albeit less pronounced. Regardless of the start year, all trends with an end year between 2015 – 2019 show a negative trend. This implies that the HFPD values in the years of 2015-2019 are so small compared to past years, that the trends are more robust to the choice of start year. The earlier end year show an alternating pattern similar to that of the LFPD, with the opposite direction. This pattern is less discernible than in the LFPD. This is most likely a result of the aforementioned sensitivity of high flows to 'random' extreme events.

The parallel found in the trends of the pulse count signatures is also found in the pulse duration signatures. This implies that for most of the stream gauges, the duration of the high flow pulses has decreased and the duration of the low flow pulses has decreased. Overall, the trends in the LFPD are more pronounced than the trends in the HFPD. An increase in LFPD and a decrease in HFPD means that the low flow pulses have become longer and the high flow pulses shorter. This implies that the low flow conditions have become steadier and the high flow conditions have become flashier.

## 6.5 Overall insights and implications

There are a number of insights that are consistent across all the trend analyses in the present study. In general, the estimated trend slopes decrease over time, i.e. the estimated trend slopes become smaller when analysed over longer time period. This phenomenon can be explained by a number of factors related to both the properties of the dataset and the nature of the hydrological processes. Firstly, the daily streamflow data on which the trend analysis is performed can be highly variable due to a number of factors. When the data is analysed over a longer period, these short-term variations tend to average out, resulting in smaller trend values. This goes hand in hand with the fact that shorter time periods are more susceptible to the influence of random variability. This increased variability can lead to larger apparent trends. Furthermore, hydrological systems are affected by natural climate variability patterns, which will be discussed later in this section. These patterns operate on different time scales and can potentially influence the trend analyses over time.

The second major insight is found in the sensitivity heatmaps of the signatures of all signatures. Across all signatures except the AmF7 timing, it is clearly visible that there are more 'vertical trend clusters' rather than 'horizontal trend clusters. This show that the trend analysis is more sensitive to the choice of the start year of the period rather than the choice of the end year. This implies that in the period 1960-2000 there have been more clusters of dry or wet years than in the more recent years. However, there is one horizontal cluster which is found across multiple signatures, being the horizontal cluster around the

most recent end years. In four signatures, the AmF7, the ADF, the LFPD and the HFPD, a similar pattern is found across all combinations. Firstly, all of these combinations display a fluctuating pattern between positive and negative trends based on the start years of the analysis. Additionally, this pattern remains consistent for all end years prior to the most recent years (2015 – 2019). For these end years, the trend is homogeneous for all start years of the analysis. The similar pattern in this combination of signatures, along with the homogeneity, implies that the most recent years have shown significantly dry years.

To further indicate these sensitivity patterns in the choice of both start and end year, timeseries of two hydrological signatures are plotted, along with the corresponding Z-statistic, for a single stream gauge. These plots are shown in Figure 33 and 34

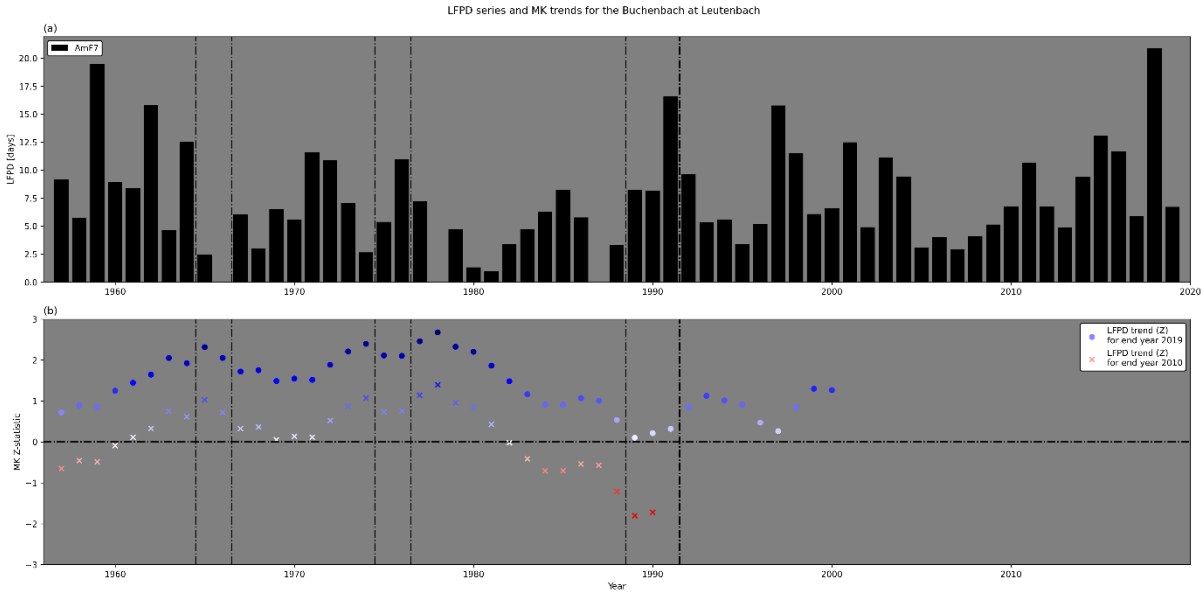


*Figure 33: LFPD series and MK trends for the Buchenbach at Leutenbach. Upper plot (a) shows the observed values of the LFPD and the bottom (b) graph shows the Z-statistic of the MK trend with end years 2019 and 2010.*

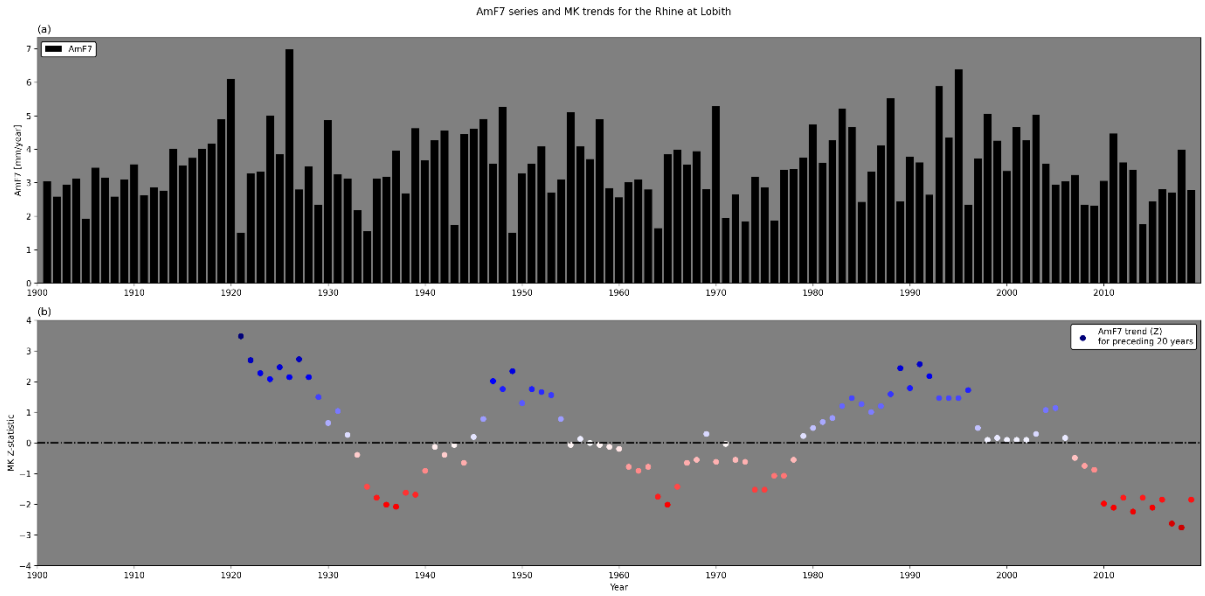


*Figure 34: AmF7 series and MK trends for the Rhine at Lobith. Upper plot (a) shows the observed values of the AmF7 and the bottom (b) graph shows the Z-statistic of the MK trend with record length of 20 years.*

Figure 33 shows the LFPD signatures of the river Buchenbach at Leutenbach and two series of MK trend results. Trend values are determined at multiple start years but have an identical end year. The end years are 2019 and 2010 for the two series respectively. From Figure 28, it is seen that the Z-values are positive for all combinations with end year 2019. This is also seen in Figure 33(b), where all Z-values are positive for the series with end year 2019. However, for the periods with end year 2010 the Z-values are significantly smaller for each start year, and even negative for the most recent years. Interestingly, the shape of the trend series are similar to each other.

Figure 34 shows the observed AmF7 series for the Rhine at Lobith and a MK series consisting of periods with a record length of 20 years. Each circle in the MK series represents the trend of the preceding 20-year period (e.g. circle at 1940 represents the period 1920-1940). This graph shows that, for a single stream gauge, the temporal variability in signatures is still visible. There also seems to be a somewhat quasi-cyclical pattern in the trend results. How this cyclical pattern can be investigated further will be discussed shortly in a following section.

Change is detected in every aspect of the streamflow regime. In one way or another, all of the signatures display some sort of change across the periods. However, these changes do not necessarily imply that there has been a long-term trend in the characteristics of the streamflow regime. These changes have already been discussed extensively in this chapter. An overall assessment of how the river flow characteristics have changed is impossible to make. This is because there is no combination that is consistent across all the analyses, both in spatial-and-temporal patterns. These spatial patterns and differences in temporal trends are distinctive for their respective signature. However, a good degree of coherency is found between the signatures of annual low, average and high flow on the short-term. This implies that these aspects of the streamflow regime are broadly varying in the same manner. Therefore, this study suggests that there is little evidence for the divergence between low- and-high flow extremes (i.e. wet getting wetter and dry getting drier). These findings are in line with the findings by (Hannaford et al., 2013)

Achieving the second research objective and answering the corresponding research questions is not as straightforward as initially thought. The most important aspects of the streamflow as stated by (Poff et al., 1997) are generally accepted across hydrological studies. However, as stated by (Gao et al., 2009; McMillan, 2020; McMillan et al., 2017) there are a great number of hydrological processes and corresponding hydrological signatures. It is vital for a hydrological trend analysis study to clearly state the research objectives and to accurately select hydrological signatures for the respective objective. All hydrological signatures are initially created for a specific purpose and therefore not a single one of them is redundant. Overall, the most commonly used signatures are the ones which are the least abstract and the most straightforward to interpret. A proper set of hydrological signatures to characterize the streamflow regime has been created in this study. However, hydrological signatures should always be chosen based on specific objectives of a hydrological study. (McMillan et al., 2017) provides five guidelines for selecting hydrological signatures. Additionally, (Olden & Poff, 2003) can be used to investigate possible redundancy between signatures.

The temporal sensitivity analysis indicates, for each signature respectively, how consistent the trends are for all combinations of start-and-end years. There is just one signature which displays a homogeneous pattern in the heatmap. This signature is the AmF7 timing, which shows almost only negative trends. All of the other heatmaps show a certain degree of heterogeneity, which visually shows the high degrees of variability in the signatures. The aforementioned similarity in the patterns of AmF7, ADF, LFPD and HFPD implies that the short-term trends with more recent end years are relatively consistent with the long-term trends. However, this consistency of short-term trends with long-term trends is not visible for analyses with end years prior to 2015. This means that the years 2015 – 2019 are significantly dry, that all of the trend analyses will show consistency when ending in these years. For sake of explanation, this is called a ‘horizontal cluster’, as it appears horizontally on the heatmap. One interesting finding is that there appear to be significantly fewer horizontal clusters than vertical clusters.

Vertical clusters are found around start years that also show consistency in short-term and long-term trends. Notable vertical clusters are found around 1970, 1980, and 1990.

An interesting method to investigate this is by using the Fast Fourier Transform (FFT). In short, this method involves analysing a signal's frequency components by transforming it from the time domain to the frequency domain. The Fast Fourier Transform efficiently computes these frequency components, providing valuable insights into the underlying patterns and characteristics of the signal. The power density spectrum can then be computed to investigate the relative power of a certain frequency in the signal (i.e. how much of the signal's variance can be explained by that frequency). To visualize this, this is performed on the AMF series of a single stream gauge. Figure 35 shows the results of this FFT.

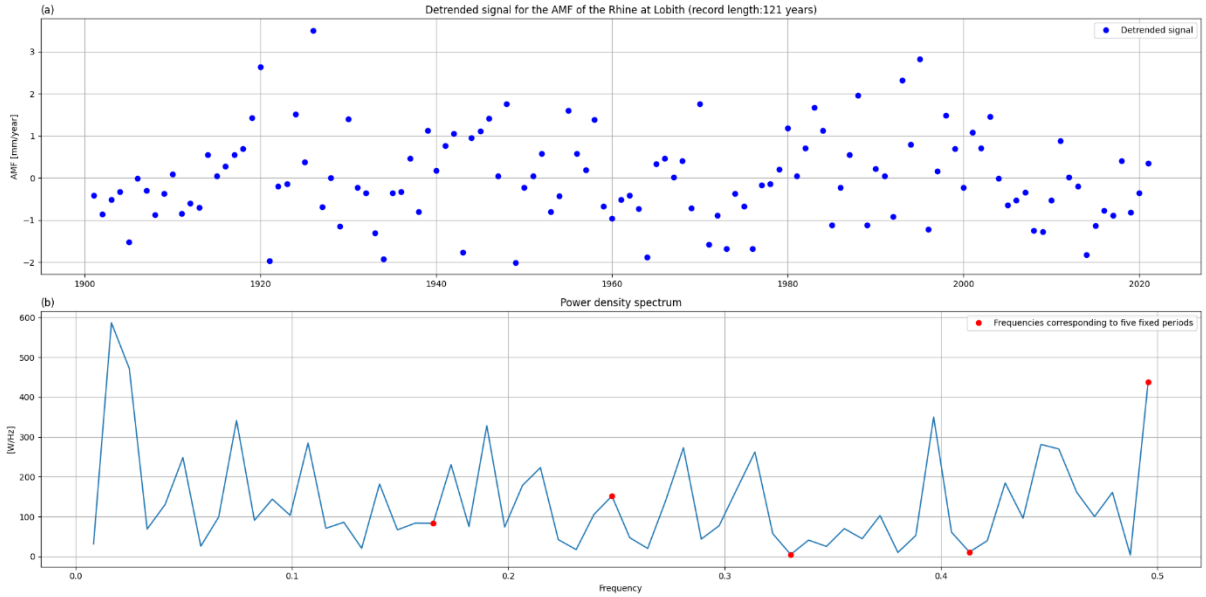


*Figure 35: FFT for the AMF of a single stream gauge. Top graph shows the detrended signal and the bottom graph the power density spectrum. Red dots in the graph correspond to the frequencies of the five fixed periods.*

Of all the fixed periods, the 60-year period has the highest value on the power density spectrum, which implies that it explains the most variance in the signal. This somewhat agrees with the results from the temporal sensitivity analysis. The top left of the heatmap shows that for the 60-year period, an average Z score of around zero is found, which aligns with a period of 60 years. The FFT method is worth mentioning, as it can provide even more detailed insights into the temporal patterns in hydrological signatures. However, in this research it is performed very exploratory. Gaining useful insights from the FFT method on a large dataset requires a lot of additional work, which was considered outside the scope of this research.

The largest overall implication that this study provides is the large amount of temporal variability in hydrological trend analyses. This study elucidates the importance of carefully interpreting analysed trends, which is most likely due to the large number of factors influencing the trend analysis. Trends will be different across different time periods. The importance of different driving mechanisms has to be considered when interpreting different changes in the streamflow regime (Berghuijs & Slater, 2023; Mediero et al., 2015). When analysing climate driven trends, the choice should be made to assemble a dataset of near-natural streamflow records (Stahl et al., 2010). There are many different factors that influence streamflow developments and many considerations that must be considered. This analysis forms a reference point against which the results of existing and future studies can be assessed.

# 7. Conclusion

The results of this study demonstrate a considerable amount of temporal variability in trends across most signatures. Fixed periods are crucial for trend analyses, as they provide an appropriate visualization and quantification of trends on a geographical sense. However, these fixed periods represent just one cell in the temporal sensitivity analysis. The considerable variation seen in the figure of the temporal sensitivity analysis suggests that an extrapolation of both short-and-long-term trends is not justified in most cases. An extrapolation, into the past of the future can easily lead to wrong interpretations or false trend patterns. This study has shown how interdecadal variability has influenced short-term trends and their consistency with long-term trends in western Europe. This is true for more recent short-term trends, but also short-term trends from the past. In many signatures, the direction and strength of trends are dependent on the choice of start year, end year or both.

In the more recent years of the dataset, there has been a higher degree of consistency across short-and-long-term trends. Whether this homogeneity will continue to exist in the future is a mystery. As mentioned, an extrapolation of these trends, both in the past or the future is not justified. Additionally, this homogeneity exists in a multitude of signatures. This indicates that the signatures chosen in this study are relatively coherent with each other and properly describe the changes of the entire streamflow regime as a whole. There will always be specific applications for each signature and the streamflow is influenced by too many factors and phenomena to develop in a truly homogenous manner.

The high amount of temporal variability and inconsistency across trends shown by this research elucidates the necessity of contextualising short-term trends. The multi-temporal approach used in this study is recommended for use in future hydrological trend analysis studies. The signatures provided in this study serve as a good baseline to broadly assess the changes in the streamflow regime across a larger area. The results in this study can be used for future studies which intend to delve deeper into more specific parts of the streamflow regime to indicate how the streamflow has broadly developed and how these changes are highly variable in both the spatial and temporal scale. Future research should expand on this research by attempting to explain the driving mechanisms of the temporal variability and thereby developing more sophisticated and innovative methods of trend detection that consider temporal variability and its driving mechanisms.

One obstacle is that long records are sparse and often less desirable for trend analysis due to inhomogeneities caused by anthropogenic influence. Unfortunately, there is just one true solution for this obstacle, which is patience. With time, the number of stream gauges that have a long record length will increase and the spatial coverage with it. Ideally, a dataset of near natural catchments should be used for the analysis, both on short-term and long-term trends. Where these are unavailable, other methods, such as reconstruction methods from precipitation or model simulations can be used.

# 8. Bibliography


Abbott, B. W., Bishop, K., Zarnetske, J. P., Minaudo, C., Chapin, F. S., Krause, S., Hannah, D. M., Conner, L., Ellison, D., Godsey, S. E., Plont, S., Marçais, J., Kolbe, T., Huebner, A., Frei, R. J., Hampton, T., Gu, S., Buhman, M., Sara Sayedi, S., … Pinay, G. (2019). Human domination of the global water cycle absent from depictions and perceptions. *Nature Geoscience*, *12*(7), 533–540. https://doi.org/10.1038/s41561-019-0374-y

Allan, R. P., Barlow, M., Byrne, M. P., Cherchi, A., Douville, H., Fowler, H. J., Gan, T. Y., Pendergrass, A. G., Rosenfeld, D., Swann, A. L. S., Wilcox, L. J., & Zolina, O. (2020). Advances in understanding large-scale responses of the water cycle to climate change. *Annals of the New York Academy of Sciences*, *1472*(1), 49–75. https://doi.org/10.1111/nyas.14337

Anderson, M. G., & McDonnell, J. J. (Eds.). (2005). *Encyclopedia of Hydrological Sciences*. Wiley. https://doi.org/10.1002/0470848944

Barker, L. J., Hannaford, J., Chiverton, A., & Svensson, C. (2016). From meteorological to hydrological drought using standardised indicators. *Hydrology and Earth System Sciences*, *20*(6), 2483–2505. https://doi.org/10.5194/hess-20-2483-2016

Bayliss, A. C., & Jones, R. C. (1993). *Peaks-over-threshold flood database: Summary statistics and seasonality*.

Berghuijs, W. R., Harrigan, S., Molnar, P., Slater, L. J., & Kirchner, J. W. (2019). The Relative Importance of Different Flood-Generating Mechanisms Across Europe. *Water Resources Research*, *55*(6), 4582–4593. https://doi.org/10.1029/2019WR024841

Berghuijs, W. R., Hartmann, A., & Woods, R. A. (2016). Streamflow sensitivity to water storage changes across Europe. *Geophysical Research Letters*, *43*(5), 1980–1987. https://doi.org/10.1002/2016GL067927

Berghuijs, W. R., & Slater, L. J. (2023). Groundwater shapes North American river floods. *Environmental Research Letters*, *18*(3), 034043. https://doi.org/10.1088/1748-9326/acbecc

Berghuijs, W. R., Woods, R. A., Hutton, C. J., & Sivapalan, M. (2016). Dominant flood generating mechanisms across the United States. *Geophysical Research Letters*, *43*(9), 4382–4390. https://doi.org/10.1002/2016GL068070

Bertola, M., Viglione, A., Lun, D., Hall, J., & Blöschl, G. (2020). Flood trends in Europe: are changes in small and big floods different? *Hydrology and Earth System Sciences*, *24*(4), 1805–1822. https://doi.org/10.5194/hess-24-1805-2020

Blöschl, G., Hall, J., Parajka, J., Perdigão, R. A. P., Merz, B., Arheimer, B., Aronica, G. T., Bilibashi, A., Bonacci, O., Borga, M., Čanjevac, I., Castellarin, A., Chirico, G. B., Claps, P., Fiala, K., Frolova, N., Gorbachova, L., Gül, A., Hannaford, J., … Živković, N. (2017). Changing climate shifts timing of European floods. *Science*, *357*(6351), 588–590. https://doi.org/10.1126/science.aan2506

Blöschl, G., Hall, J., Viglione, A., Perdigão, R. A. P., Parajka, J., Merz, B., Lun, D., Arheimer, B., Aronica, G. T., Bilibashi, A., Boháč, M., Bonacci, O., Borga, M., Čanjevac, I., Castellarin, A., Chirico, G. B., Claps, P., Frolova, N., Ganora, D., … Živković, N. (2019). Changing climate both increases and decreases European river floods. *Nature*, *573*(7772), 108–111. https://doi.org/10.1038/s41586-019-1495-6

Blöschl, G., Kiss, A., Viglione, A., Barriendos, M., Böhm, O., Brázdil, R., Coeur, D., Demarée, G., Llasat, M. C., Macdonald, N., Retsö, D., Roald, L., Schmocker-Fackel, P., Amorim, I., Bělínová, M., Benito, G., Bertolin, C., Camuffo, D., Cornel, D., … Wetter, O. (2020). Current European flood-rich period exceptional compared with past 500 years. *Nature*, *583*(7817), 560–566. https://doi.org/10.1038/s41586-020-2478-3

Briffa, K. R., Jones, P. D., & Hulme, M. (1994). Summer moisture variability across Europe, 1892–1991: An analysis based on the palmer drought severity index. *International Journal of Climatology*, *14*(5), 475–506. https://doi.org/10.1002/joc.3370140502

Buckley, B. M., Anchukaitis, K. J., Penny, D., Fletcher, R., Cook, E. R., Sano, M., Nam, L. C., Wichienkeeo, A., Minh, T. T., & Hong, T. M. (2010). Climate as a contributing factor in the demise of Angkor, Cambodia. *Proceedings of the National Academy of Sciences*, *107*(15), 6748–6752. https://doi.org/10.1073/pnas.0910827107

Clausen, B., & Biggs, B. J. F. (2000). Flow variables for ecological studies in temperate streams: groupings based on covariance. *Journal of Hydrology*, *237*(3–4), 184–197. https://doi.org/10.1016/S0022-1694(00)00306-1

Collins, M. J. (2019). River flood seasonality in the Northeast United States: Characterization and trends. *Hydrological Processes*, *33*(5), 687–698. https://doi.org/10.1002/hyp.13355

Collins, M. J., Hodgkins, G. A., Archfield, S. A., & Hirsch, R. M. (2022). The Occurrence of Large Floods in the United States in the Modern Hydroclimate Regime: Seasonality, Trends, and Large-Scale Climate Associations. *Water Resources Research*, *58*(2). https://doi.org/10.1029/2021WR030480

Cornes, R. C., van der Schrier, G., van den Besselaar, E. J. M., & Jones, P. D. (2018). An Ensemble Version of the E-OBS Temperature and Precipitation Data Sets. *Journal of Geophysical Research: Atmospheres*, *123*(17), 9391–9409. https://doi.org/10.1029/2017JD028200

Cunnane, C. (1973). A particular comparison of annual maxima and partial duration series methods of flood frequency prediction. *Journal of Hydrology*, *18*(3–4), 257–271. https://doi.org/10.1016/0022-1694(73)90051-6

'Desai, B., 'Maskrey, A., 'Peduzzi, P., 'De Bono, A., & 'Herold, C. (2015). *Making Development Sustainable: The Future of Disaster Risk Management, Global Assessment Report on Disaster Risk Reduction*.

Dracup, J. A., Lee, K. S., & Paulson, E. G. (1980). On the definition of droughts. *Water Resources Research*, *16*(2), 297–302. https://doi.org/10.1029/WR016i002p00297

Field, C. B. (2012). *Managing the risks of extreme events and disasters to advance climate change adaptation: special report of the intergovernmental panel on climate change*. Cambridge University Press.

Frei, A., Kunkel, K. E., & Matonse, A. (2015). The Seasonal Nature of Extreme Hydrological Events in the Northeastern United States. *Journal of Hydrometeorology*, *16*(5), 2065–2085. https://doi.org/10.1175/JHM-D-14-0237.1

Gao, Y., Merz, C., Lischeid, G., & Schneider, M. (2018). A review on missing hydrological data processing. *Environmental Earth Sciences*, *77*(2), 47. https://doi.org/10.1007/s12665-018-7228-6

Gao, Y., Vogel, R. M., Kroll, C. N., Poff, N. L., & Olden, J. D. (2009). Development of representative indicators of hydrologic alteration. *Journal of Hydrology*, *374*(1–2), 136–147. https://doi.org/10.1016/j.jhydrol.2009.06.009

García, S., Ramírez-Gallego, S., Luengo, J., Benítez, J. M., & Herrera, F. (2016). Big data preprocessing: methods and prospects. *Big Data Analytics*, *1*(1), 9. https://doi.org/10.1186/s41044-016-0014-0

Gellens, D., & Roulin, E. (1998). Streamflow response of Belgian catchments to IPCC climate change scenarios. *Journal of Hydrology*, *210*(1–4), 242–258. https://doi.org/10.1016/S0022-1694(98)00192-9

Glaser, R., Riemann, D., Schönbein, J., Barriendos, M., Brázdil, R., Bertolin, C., Camuffo, D., Deutsch, M., Dobrovolný, P., van Engelen, A., Enzi, S., Halíčková, M., Koenig, S. J., Kotyza, O., Limanówka, D., Macková, J., Sghedoni, M., Martin, B., & Himmelsbach, I. (2010). The variability of European floods since AD 1500. *Climatic Change*, *101*(1–2), 235–256. https://doi.org/10.1007/s10584-010-9816-7

Hall, J., Arheimer, B., Aronica, G. T., Bilibashi, A., Boháč, M., Bonacci, O., Borga, M., Burlando, P., Castellarin, A., Chirico, G. B., Claps, P., Fiala, K., Gaál, L., Gorbachova, L., Gül, A., Hannaford, J., Kiss, A., Kjeldsen, T., Kohnová, S., … Blöschl, G. (2015). A European Flood Database: facilitating comprehensive flood research beyond administrative boundaries. *Proceedings of the International Association of Hydrological Sciences*, *370*, 89–95. https://doi.org/10.5194/piahs-370-89-2015

Han, J., Pei, J., & Tong, H. (2022). *Data mining: concepts and techniques*. Morgan Kaufmann.

Hannaford, J., Buys, G., Stahl, K., & Tallaksen, L. M. (2013). The influence of decadal-scale variability on trends in long European streamflow records. *Hydrology and Earth System Sciences*, *17*(7), 2717–2733. https://doi.org/10.5194/hess-17-2717-2013

Haug, G. H., Günther, D., Peterson, L. C., Sigman, D. M., Hughen, K. A., & Aeschlimann, B. (2003). Climate and the Collapse of Maya Civilization. *Science*, *299*(5613), 1731–1735. https://doi.org/10.1126/science.1080444

Hawkins, E., & Sutton, R. (2011). The potential to narrow uncertainty in projections of regional precipitation change. *Climate Dynamics*, *37*(1–2), 407–418. https://doi.org/10.1007/s00382-010-0810-6

Hintze, J. L., & Nelson, R. D. (1998). Violin Plots: A Box Plot-Density Trace Synergism. *The American Statistician*, *52*(2), 181–184. https://doi.org/10.1080/00031305.1998.10480559

Hisdal, H., Stahl, K., Tallaksen, L. M., & Demuth, S. (2001). Have streamflow droughts in Europe become more severe or frequent? *International Journal of Climatology*, *21*(3), 317–333. https://doi.org/10.1002/joc.619

Hussain, Md., & Mahmud, I. (2019). pyMannKendall: a python package for non parametric Mann Kendall family of trend tests. *Journal of Open Source Software*, *4*(39), 1556. https://doi.org/10.21105/joss.01556

Ide, T. (2018). Climate War in the Middle East? Drought, the Syrian Civil War and the State of Climate-Conflict Research. *Current Climate Change Reports*, *4*(4), 347–354. https://doi.org/10.1007/s40641-018-0115-0

Intergovernmental Panel on Climate Change (Ed.). (2014). *Climate Change 2013 – The Physical Science Basis*. Cambridge University Press. https://doi.org/10.1017/CBO9781107415324

Jolliffe, I. T., & Cadima, J. (2016). Principal component analysis: a review and recent developments. *Philosophical Transactions of the Royal Society A: Mathematical, Physical and Engineering Sciences*, *374*(2065), 20150202. https://doi.org/10.1098/rsta.2015.0202

KENDALL, M. G. (1938). A NEW MEASURE OF RANK CORRELATION. *Biometrika*, *30*(1–2), 81–93. https://doi.org/10.1093/biomet/30.1-2.81

KOUTSOYIANNIS, D. (2003). Climate change, the Hurst phenomenon, and hydrological statistics. *Hydrological Sciences Journal*, *48*(1), 3–24. https://doi.org/10.1623/hysj.48.1.3.43481

Kudyba, S. (2014). *Big Data, Mining, and Analytics*. Auerbach Publications. https://doi.org/10.1201/b16666

Kundzewicz, Z. W., Kanae, S., Seneviratne, S. I., Handmer, J., Nicholls, N., Peduzzi, P., Mechler, R., Bouwer, L. M., Arnell, N., Mach, K., Muir-Wood, R., Brakenridge, G. R., Kron, W., Benito, G., Honda, Y., Takahashi, K., & Sherstyukov, B. (2014). Flood risk and climate change: global and regional perspectives. *Hydrological Sciences Journal*, *59*(1), 1–28. https://doi.org/10.1080/02626667.2013.857411

Kundzewicz, Z. W., & Robson, A. J. (2004). Change detection in hydrological records—a review of the methodology / Revue méthodologique de la détection de changements dans les chroniques hydrologiques. *Hydrological Sciences Journal*, *49*(1), 7–19. https://doi.org/10.1623/hysj.49.1.7.53993

Kunkel, K. E., Andsager, K., & Easterling, D. R. (1999). Long-Term Trends in Extreme Precipitation Events over the Conterminous United States and Canada. *Journal of Climate*, *12*(8), 2515–2527. https://doi.org/10.1175/1520-0442(1999)012<2515:LTTIEP>2.0.CO;2

Liu, J., Yang, H., Gosling, S. N., Kummu, M., Flörke, M., Pfister, S., Hanasaki, N., Wada, Y., Zhang, X., Zheng, C., Alcamo, J., & Oki, T. (2017). Water scarcity assessments in the past, present, and future. *Earth's Future*, *5*(6), 545–559. https://doi.org/10.1002/2016EF000518

Madsen, H., Rasmussen, P. F., & Rosbjerg, D. (1997). Comparison of annual maximum series and partial duration series methods for modeling extreme hydrologic events: 1. At-site modeling. *Water Resources Research*, *33*(4), 747–757. https://doi.org/10.1029/96WR03848

Mangini, W., Viglione, A., Hall, J., Hundecha, Y., Ceola, S., Montanari, A., Rogger, M., Salinas, J. L., Borzì, I., & Parajka, J. (2018). Detection of trends in magnitude and frequency of flood peaks across Europe. *Hydrological Sciences Journal*, *63*(4), 493–512. https://doi.org/10.1080/02626667.2018.1444766

Mann, H. B. (1945). Nonparametric Tests Against Trend. *Econometrica*, *13*(3), 245. https://doi.org/10.2307/1907187

Mardia, K. V. (1975). Statistics of Directional Data. *Journal of the Royal Statistical Society: Series B (Methodological)*, *37*(3), 349–371. https://doi.org/10.1111/j.2517-6161.1975.tb01550.x

Marsh, T. J., & Monkhouse, R. A. (1993). Drought in the United Kingdom, 1988-92. *Weather*, *48*(1), 15–22. https://doi.org/10.1002/j.1477-8696.1993.tb07217.x

McMillan, H. (2020). Linking hydrologic signatures to hydrologic processes: A review. *Hydrological Processes*, *34*(6), 1393–1409. https://doi.org/10.1002/hyp.13632

McMillan, H., Westerberg, I., & Branger, F. (2017). Five guidelines for selecting hydrological signatures. *Hydrological Processes*, *31*(26), 4757–4761. https://doi.org/10.1002/hyp.11300

Mediero, L., Kjeldsen, T. R., Macdonald, N., Kohnova, S., Merz, B., Vorogushyn, S., Wilson, D., Alburquerque, T., Blöschl, G., Bogdanowicz, E., Castellarin, A., Hall, J., Kobold, M., Kriauciuniene, J., Lang, M., Madsen, H., Onuşluel Gül, G., Perdigão, R. A. P., Roald, L. A., … Þórarinsson, Ó. (2015). Identification of coherent flood regions across Europe by using the

longest streamflow records. *Journal of Hydrology*, *528*, 341–360. https://doi.org/10.1016/j.jhydrol.2015.06.016

Milly, P. C. D., Betancourt, J., Falkenmark, M., Hirsch, R. M., Kundzewicz, Z. W., Lettenmaier, D. P., & Stouffer, R. J. (2008). Stationarity Is Dead: Whither Water Management? *Science*, *319*(5863), 573–574. https://doi.org/10.1126/science.1151915

Mishra, A. K., & Singh, V. P. (2010). A review of drought concepts. *Journal of Hydrology*, *391*(1–2), 202–216. https://doi.org/10.1016/j.jhydrol.2010.07.012

Montanari, A., & Koutsoyiannis, D. (2014). Modeling and mitigating natural hazards: Stationarity is immortal! *Water Resources Research*, *50*(12), 9748–9756. https://doi.org/10.1002/2014WR016092

Morgenthaler, S. (2009). Exploratory data analysis. *Wiley Interdisciplinary Reviews: Computational Statistics*, *1*(1), 33–44. https://doi.org/10.1002/wics.2

Oki, T., & Kanae, S. (2006). Global Hydrological Cycles and World Water Resources. *Science*, *313*(5790), 1068–1072. https://doi.org/10.1126/science.1128845

Olden, J. D., & Poff, N. L. (2003). Redundancy and the choice of hydrologic indices for characterizing streamflow regimes. *River Research and Applications*, *19*(2), 101–121. https://doi.org/10.1002/rra.700

Palmer, W. C. (1965). *Meteorological drought* (Vol. 30). US Department of Commerce, Weather Bureau.

Peña-Angulo, D., Vicente-Serrano, S. M., Domínguez-Castro, F., Lorenzo-Lacruz, J., Murphy, C., Hannaford, J., Allan, R. P., Tramblay, Y., Reig-Gracia, F., & El Kenawy, A. (2022). The Complex and Spatially Diverse Patterns of Hydrological Droughts Across Europe. *Water Resources Research*, *58*(4). https://doi.org/10.1029/2022WR031976

Pendergrass, A. G., Knutti, R., Lehner, F., Deser, C., & Sanderson, B. M. (2017). Precipitation variability increases in a warmer climate. *Scientific Reports*, *7*(1), 17966. https://doi.org/10.1038/s41598-017-17966-y

Petrow, T., & Merz, B. (2009). Trends in flood magnitude, frequency and seasonality in Germany in the period 1951–2002. *Journal of Hydrology*, *371*(1–4), 129–141. https://doi.org/10.1016/j.jhydrol.2009.03.024

POFF, N. (1996). A hydrogeography of unregulated streams in the United States and an examination of scale-dependence in some hydrological descriptors. *Freshwater Biology*, *36*(1), 71–79. https://doi.org/10.1046/j.1365-2427.1996.00073.x

Poff, N. L., Allan, J. D., Bain, M. B., Karr, J. R., Prestegaard, K. L., Richter, B. D., Sparks, R. E., & Stromberg, J. C. (1997). The Natural Flow Regime. *BioScience*, *47*(11), 769–784. https://doi.org/10.2307/1313099

Poff, N. L., & Ward, J. V. (1989). Implications of Streamflow Variability and Predictability for Lotic Community Structure: A Regional Analysis of Streamflow Patterns. *Canadian Journal of Fisheries and Aquatic Sciences*, *46*(10), 1805–1818. https://doi.org/10.1139/f89-228

Richter, B. D., Baumgartner, J. V., Braun, D. P., & Powell, J. (1998). A spatial assessment of hydrologic alteration within a river network. *Regulated Rivers: Research & Management*, *14*(4), 329–340.

Richter, B. D., Baumgartner, J. V., Powell, J., & Braun, D. P. (1996). A Method for Assessing Hydrologic Alteration within Ecosystems. *Conservation Biology*, *10*(4), 1163–1174. https://doi.org/10.1046/j.1523-1739.1996.10041163.x

Rousseeuw, P. J., & Leroy, A. M. (1987). *Robust Regression and Outlier Detection*. Wiley. https://doi.org/10.1002/0471725382

Schafer, J. L., & Graham, J. W. (2002). Missing data: Our view of the state of the art. *Psychological Methods*, *7*(2), 147–177. https://doi.org/10.1037/1082-989X.7.2.147

Sen, P. K. (1968). Estimates of the Regression Coefficient Based on Kendall's Tau. *Journal of the American Statistical Association*, *63*(324), 1379–1389. https://doi.org/10.1080/01621459.1968.10480934

Sheffield, J., Wood, E. F., & Roderick, M. L. (2012). Little change in global drought over the past 60 years. *Nature*, *491*(7424), 435–438. https://doi.org/10.1038/nature11575

Stahl, K., Hisdal, H., Hannaford, J., Tallaksen, L. M., van Lanen, H. A. J., Sauquet, E., Demuth, S., Fendekova, M., & Jódar, J. (2010). Streamflow trends in Europe: evidence from a dataset of near-natural catchments. *Hydrology and Earth System Sciences*, *14*(12), 2367–2382. https://doi.org/10.5194/hess-14-2367-2010

Steirou, E., Gerlitz, L., Apel, H., & Merz, B. (2017). Links between large-scale circulation patterns and streamflow in Central Europe: A review. *Journal of Hydrology*, *549*, 484–500. https://doi.org/10.1016/j.jhydrol.2017.04.003

Stewart, B. (2015). Measuring what we manage – the importance of hydrological data to water resources management. *Proceedings of the International Association of Hydrological Sciences*, *366*, 80–85. https://doi.org/10.5194/piahs-366-80-2015

Thompson, D. W. J., Barnes, E. A., Deser, C., Foust, W. E., & Phillips, A. S. (2015). Quantifying the Role of Internal Climate Variability in Future Climate Trends. *Journal of Climate*, *28*(16), 6443–6456. https://doi.org/10.1175/JCLI-D-14-00830.1

Tselepidaki, I., Zarifis, B., & Asimakopoulos, D. N. (1992). Low precipitation over Greece during 1989?1990. *Theoretical and Applied Climatology*, *46*(2–3), 115–121. https://doi.org/10.1007/BF00866091

Tukey, J. W. (1962). The Future of Data Analysis. *The Annals of Mathematical Statistics*, *33*(1), 1–67. http://www.jstor.org.tudelft.idm.oclc.org/stable/2237638

Van Loon, A. F., & Laaha, G. (2015). Hydrological drought severity explained by climate and catchment characteristics. *Journal of Hydrology*, *526*, 3–14. https://doi.org/10.1016/j.jhydrol.2014.10.059

von Uexkull, N., Croicu, M., Fjelde, H., & Buhaug, H. (2016). Civil conflict sensitivity to growing-season drought. *Proceedings of the National Academy of Sciences*, *113*(44), 12391–12396. https://doi.org/10.1073/pnas.1607542113

Vorogushyn, S., & Merz, B. (2013). Flood trends along the Rhine: the role of river training. *Hydrology and Earth System Sciences*, *17*(10), 3871–3884. https://doi.org/10.5194/hess-17-3871-2013

Walker, K. F., Sheldon, F., & Puckridge, J. T. (1995). A perspective on dryland river ecosystems. *Regulated Rivers: Research & Management*, *11*(1), 85–104. https://doi.org/10.1002/rrr.3450110108

Wilhite, D. A., & Glantz, M. H. (1985). Understanding: the Drought Phenomenon: The Role of Definitions. *Water International*, *10*(3), 111–120. https://doi.org/10.1080/02508068508686328

Wilhite, D. A., & Pulwarty, R. S. (2017). *Drought and Water Crises* (D. Wilhite & R. S. Pulwarty, Eds.). CRC Press. https://doi.org/10.1201/b22009

Wilkinson, M. D., Dumontier, M., Aalbersberg, Ij. J., Appleton, G., Axton, M., Baak, A., Blomberg, N., Boiten, J.-W., da Silva Santos, L. B., Bourne, P. E., Bouwman, J., Brookes, A. J., Clark, T., Crosas, M., Dillo, I., Dumon, O., Edmunds, S., Evelo, C. T., Finkers, R., … Mons, B. (2016). The FAIR Guiding Principles for scientific data management and stewardship. *Scientific Data*, *3*(1), 160018. https://doi.org/10.1038/sdata.2016.18

Winsemius, H. C., Aerts, J. C. J. H., van Beek, L. P. H., Bierkens, M. F. P., Bouwman, A., Jongman, B., Kwadijk, J. C. J., Ligtvoet, W., Lucas, P. L., van Vuuren, D. P., & Ward, P. J. (2016). Global drivers of future river flood risk. *Nature Climate Change*, *6*(4), 381–385. https://doi.org/10.1038/nclimate2893

Wolman, M. G., & Miller, J. P. (1960). Magnitude and Frequency of Forces in Geomorphic Processes. *The Journal of Geology*, *68*(1), 54–74. https://doi.org/10.1086/626637

# A

# Data-and-trend analysis code

```python
import numpy as np
import pandas as pd
import os
import glob
import datetime
from tqdm import tqdm
import pickle

"A Python function called process_dataframes is written.  This function takes 4 input parameters: The directory, the prefix, the suffix and an empty dictionary."
def process_dataframes(directory, prefix, suffix, dictionary):
    for file_path in tqdm(glob.glob(os.path.join(directory, prefix + '*' + suffix))):
        # Extract the identifier from the file name
        identifier = os.path.basename(file_path)[len(prefix):-len(suffix)]

        # Read the Excel file into a pandas DataFrame
        df = pd.read_excel(file_path)

        # DATAFRAME PROCESSING...
        # Check if the date is written in serial date values
        if isinstance(df['Date'][0], np.int64):
            # Convert serial date values to datetime values
            serial_dates = df['Date']
            actual_dates = []
            for serial_date in serial_dates:
                actual_date = datetime.datetime(1900, 1, 1) + datetime.timedelta(days=
                    serial_date - 2)
                actual_dates.append(actual_date)
            df['Date'] = actual_dates
        df.dropna(axis=0, inplace=True)

        # Remove years with less than 300 days of data
        df_grouped = df.groupby(df['Date'].dt.year)['Mean daily flow']
        entries_per_year = df_grouped.count()
        threshold = 300
        mask = entries_per_year < threshold
        years_to_remove = entries_per_year[mask].index
        df = df[~df['Date'].dt.year.isin(years_to_remove)]

        dictionary[identifier] = df

    return dictionary


# Set directory
directory = r'C:\Users\dstou\Documents\Civiel\Master\MscThesis\Programming\Data'

# Dutch data
prefix = 'N_'
suffix = '_Q_daily.xlsx'
```

```
Ndataframes = process_dataframes(directory, prefix, suffix, {})

# French data
prefix = 'F_'
suffix = '_Q_daily.xlsx'
Fdataframes = process_dataframes(directory, prefix, suffix, {})

# Luxembourg data
prefix = 'L_'
suffix = '_Q_daily.xlsx'
Ldataframes = process_dataframes(directory, prefix, suffix, {})

# Germany data
prefix = 'G_'
suffix = '_Q_daily.xlsx'
Gdataframes = process_dataframes(directory, prefix, suffix, {})

# Belgium data
prefix = 'B_'
suffix = '_Q_daily.xlsx'
Bdataframes = process_dataframes(directory, prefix, suffix, {})

#Write dataframes into local files
with open(r'C:\Users\dstou\Documents\Civiel\Master\MscThesis\Programming\Data\
    PROCESSABLE_DATA\Fdataframes.pkl','wb') as file:
    pickle.dump(Fdataframes, file)

with open(r'C:\Users\dstou\Documents\Civiel\Master\MscThesis\Programming\Data\
    PROCESSABLE_DATA\Bdataframes.pkl','wb') as file:
    pickle.dump(Bdataframes, file)

with open(r'C:\Users\dstou\Documents\Civiel\Master\MscThesis\Programming\Data\
    PROCESSABLE_DATA\Gdataframes.pkl','wb') as file:
    pickle.dump(Gdataframes, file)

with open(r'C:\Users\dstou\Documents\Civiel\Master\MscThesis\Programming\Data\
    PROCESSABLE_DATA\Ndataframes.pkl','wb') as file:
    pickle.dump(Ndataframes, file)

with open(r'C:\Users\dstou\Documents\Civiel\Master\MscThesis\Programming\Data\
    PROCESSABLE_DATA\Ldataframes.pkl','wb') as file:
    pickle.dump(Ldataframes, file)
```

*Dataframe_preprocessing.py*

```
    import pickle
import matplotlib.pyplot as plt
from Dataframes import *
from tqdm import tqdm
import numpy as np

def Define_record_length(df):
    max = df.groupby(df['Date'].dt.year)['Mean daily flow'].max()
    years = max.index
    yearlist = years.values
    start_year = years[0]
    end_year = years[-1]
    record_length = len(years)

    return start_year, end_year, record_length, yearlist

lengthslist = []
startlist = []
endlist = []
yearslist = []

for identifier in tqdm(Bdataframes):
    df = Bdataframes[identifier]
    dfw = df.copy()
    start_year, end_year, record_length, years = Define_record_length(dfw)
```

```
    lengthslist.append((record_length))
    startlist.append(start_year)
    endlist.append(end_year)
    for year in (years):
        yearslist.append((year))

for identifier in tqdm(Fdataframes):
    df = Fdataframes[identifier]
    dfw = df.copy()
    start_year, end_year, record_length, years = Define_record_length(dfw)
    lengthslist.append((record_length))
    startlist.append(start_year)
    endlist.append(end_year)
    for year in (years):
        yearslist.append((year))

for identifier in tqdm(Gdataframes):
    df = Gdataframes[identifier]
    dfw = df.copy()
    start_year, end_year, record_length, years = Define_record_length(dfw)
    lengthslist.append((record_length))
    startlist.append(start_year)
    endlist.append(end_year)
    for year in (years):
        yearslist.append((year))

for identifier in tqdm(Ldataframes):
    df = Ldataframes[identifier]
    dfw = df.copy()
    start_year, end_year, record_length, years = Define_record_length(dfw)
    lengthslist.append((record_length))
    startlist.append(start_year)
    endlist.append(end_year)
    for year in (years):
        yearslist.append((year))

for identifier in tqdm(Ndataframes):
    df = Ndataframes[identifier]
    dfw = df.copy()
    start_year, end_year, record_length, years = Define_record_length(dfw)
    lengthslist.append((record_length))
    startlist.append(start_year)
    endlist.append(end_year)
    for year in (years):
        yearslist.append((year))

# Create a figure with three subplots
fig, axes = plt.subplots(1, 3, figsize=(15, 5))

# Create the histogram of the available years
count_years, bin_years, pat = axes[0].hist(yearslist, bins = (max(yearslist) - min(yearslist)
     + 1), range = [min(yearslist), max(yearslist)], edgecolor = 'black')
maxbin_years = int(np.round(bin_years[count_years.argmax()]))
pdf_years = count_years / sum(count_years)
cdf_years = np.cumsum(pdf_years)

axes[0].set_ylabel('# of entries')
axes[0].set_xlabel('Year')
axes[0].set_title('Histogram of data availability per year')

ax_cdf_years = axes[0].twinx()
ax_cdf_years.plot(bin_years[1:], cdf_years, color = 'red')
ax_cdf_years.set_ylim([0,1])

# Create the histogram of the record lengths
count_lengths, bin_lengths, pat = axes[1].hist(lengthslist, bins = (max(lengthslist) - min(
    lengthslist) + 1), range = [min(lengthslist), max(lengthslist)], edgecolor = 'black')
maxbin_lengths = int(np.round(bin_lengths[count_lengths.argmax()]))
pdf_lengths = count_lengths / sum(count_lengths)
cdf_lengths = np.cumsum(pdf_lengths)

```

```
axes[1].set_xlabel('Record length [year]')
axes[1].set_title('Histogram of the record lengths')

ax_cdf_lengths = axes[1].twinx()
ax_cdf_lengths.plot(bin_lengths[1:], cdf_lengths, color = 'red')
ax_cdf_lengths.set_ylim([0,1])

# Create a histogram of the starting years
count_start, bin_start, pat = axes[2].hist(startlist, bins = (max(startlist) - min(startlist) + 1), range = [min(startlist), max(startlist)], edgecolor = 'black')
maxbin_start = int(np.round(bin_start[count_start.argmax()]))
pdf_start = count_start / sum(count_start)
cdf_start = np.cumsum(pdf_start)

axes[2].set_xlabel('Year')
axes[2].set_title('Histogram of the first years of the timeseries')

ax_cdf_start = axes[2].twinx()
ax_cdf_start.plot(bin_start[1:], cdf_start, color = 'red')
ax_cdf_start.set_ylabel('CDF')
ax_cdf_start.set_ylim([0,1])


plt.tight_layout()
plt.savefig(r'C:\Users\dstou\Documents\Civiel\Master\MscThesis\Programming\PyCharm\Results\Figures\timeseries_histograms.png')
plt.show()
```

*Timeseries_information.py*

```
    """Function to determine the annual average streamflow, returns the corresponding years to be used as index values"""


def Annual_averages(df):

    # Create a copy of the input dataframe, so it is not altered
    dfw = df.copy()

    # Group the streamflow column by year and determine the mean value for each year
    annual_averages = dfw.groupby(dfw['Date'].dt.year)['Mean daily flow'].mean()  # Compute the mean value for each year
    annual_averages = annual_averages.rename('Average annual flow [m3/s]')
    years = annual_averages.index
    return annual_averages, years
```

*Annual_averages.py*

```
    """Function created to determine both the magnitude and timing of Annual maximum flow"""
def Annual_maximum_flows(df):
    # Create a copy of the input dataframe, so it is not altered
    dfw = df.copy()

    # Group the streamflow column by year and determine the maximum value for each year
    Annual_maxima = dfw.groupby(dfw['Date'].dt.year)['Mean daily flow'].max()
    Annual_maxima = Annual_maxima.rename('Annual maximum flow')

    # Group the streamflow by year and determine where the maximum value occurs each year
    dfw['Year'] = dfw['Date'].dt.year
    dfw_grouped = dfw.groupby(dfw['Date'].dt.year)
    max_flow_dates = dfw_grouped.apply(lambda x: x.loc[x['Mean daily flow'].idxmax()]['Date']) #Returns timestamp of maximum streamflow occurence
    day_of_year = max_flow_dates.dt.dayofyear  #Convert the timestamp to Julian date
    return Annual_maxima, day_of_year
```

*Annual_maximum_flow.py*

```
    import numpy as np
import pandas as pd
```

```

"Function created to determine both the magnitude and timing of Annual 7-day minimum flow"
def Annual_7day_minimum(df):
    # Create a copy of the input dataframe, so it is not altered
    dfw = df.copy()
    dfw = dfw.reset_index(drop=True)  # Reset the index values in order for the loop to work. The index values have not been reset in pre-processing

    # Create a new column which calculate the difference in dates between two consecutive rows.
    dfw['Date'] = pd.to_datetime(dfw['Date'])
    dfw['Difference in dates'] = dfw['Date'].diff().dt.days

    # Create a new column which contains the total 7-day streamflow
    Streamflow_7days = np.empty(len(dfw))
    Streamflow_7days.fill(99999999)  # Fill the array with 99999, values which can not be calculated will still have this value. This does not affect the analysis any further
    Streamflow = dfw['Mean daily flow']
    Date_differences = dfw['Difference in dates']
    for i in range(len(Streamflow_7days) - 6):
        if all(Date_differences[i : i + 7] == 1):  # Check whether the 7 values which are to be used are all consecutive days. Otherwise the value would be incorrect
            Streamflow_7days[i + 3] = Streamflow[i] + Streamflow[i + 1] + Streamflow[i + 2] + Streamflow[i + 3] + Streamflow[i + 4] + Streamflow[i + 5] + Streamflow[i + 6] #Fill the

    # Write a new column in the dataframe, group the column by year and determine the minimum value per year
    dfw['7-day streamflow total'] = Streamflow_7days
    Annual_minima = dfw.groupby(dfw['Date'].dt.year)['7-day streamflow total'].min()
    Annual_minima = Annual_minima.rename('Annual minimum 7-day flow')

    # Group the streamflow by year and determine where the minimum value occurs each year
    dfw['Year'] = dfw['Date'].dt.year
    dfw_grouped = dfw.groupby(dfw['Date'].dt.year)
    min_flow_dates = dfw_grouped.apply(lambda x: x.loc[x['7-day streamflow total'].idxmin()]['Date'])
    day_of_year = min_flow_dates.dt.dayofyear  # Convert the timestamp to Julian date
    return Annual_minima, day_of_year
```

*Annual_minimum_7day_flow.py*

```
    import pandas as pd

def Low_pulse_statistics(df):
    # Create a copy of the input dataframe, so it is not altered
    global day
    dfw = df.copy()

    # Create lists to save the output data
    countlist = []
    durationlist = []

    # Determine the threshold value, and group the streamflow by year
    threshold = dfw['Mean daily flow'].quantile(q = 0.25)
    dfw['Date'] = pd.to_datetime(dfw['Date'])
    dfw['Year'] = dfw['Date'].dt.year
    grouped_dfw = dfw.groupby('Year')

    # Loop through the streamflow data for each year
    for year, data in grouped_dfw:
        streamflow_data = data['Mean daily flow']

        exceed_count = 0  # Set the exceed count to 0
        duration_sum = 0  # Set the duration sum to 0
        period_start = None  # Create a variable called period_start which will be used to calculate the duration of each pulse
        prev_exceed = False  # Create a boolean to check whether a period has started or not

        # Loop through the daily streamflow data
```

```
        for day, streamflow in streamflow_data.items():
            if streamflow < threshold:  # Check whether the streamflow value drops below the threshold
                if not prev_exceed:  # Check whether a period has already started
                    period_start = day
                prev_exceed = True  # Start the period
            else:
                if prev_exceed:  # Check if a period has ended
                    duration = (day - period_start)  # Determine period duration
                    duration_sum += duration
                    exceed_count += 1  # Add 1 to the pulse count
                    period_start = None  # Reset period_start
                prev_exceed = False  # Stop the period

        # Check if there is a period ongoing until the end of the data
        if prev_exceed:
            duration = (day - period_start)
            duration_sum += duration
            exceed_count += 1

        average_duration = duration_sum / exceed_count if exceed_count > 0 else 0  # Determine the mean duration of the period

        countlist.append(exceed_count)
        durationlist.append(average_duration)
    return countlist, durationlist
```

*Low_flow_pulses.py*

```
    import pandas as pd

def High_pulse_statistics(df):
    # Create a copy of the input dataframe, so it is not altered
    global day
    dfw = df.copy()

    # Create lists to save the output data
    countlist = []
    durationlist = []

    # Determine the threshold value, and group the streamflow by year
    threshold = dfw['Mean daily flow'].quantile(q = 0.75)
    dfw['Date'] = pd.to_datetime(dfw['Date'])
    dfw['Year'] = dfw['Date'].dt.year
    grouped_dfw = dfw.groupby('Year')

    # Loop through the streamflow data for each year
    for year, data in grouped_dfw:
        streamflow_data = data['Mean daily flow']

        exceed_count = 0  # Set the exceed count to 0
        duration_sum = 0  # Set the duration sum to 0
        period_start = None  #C reate a variable called period_start which will be used to calculate the duration of each pulse
        prev_exceed = False  # Create a boolean to check whether a period has started or not

        # Loop through the daily streamflow data
        for day, streamflow in streamflow_data.items():
            if streamflow > threshold:  # Check whether the streamflow value exceeds the threshold
                if not prev_exceed:  # Check whether a period has already started
                    period_start = day
                prev_exceed = True  # Start the period
            else:
                if prev_exceed:  # Check if a period has ended
                    duration = (day - period_start)  # Determine period duration
                    duration_sum += duration
                    exceed_count += 1  # Add 1 to the pulse count
                    period_start = None  # Reset period_start
                prev_exceed = False  # Stop the period
```

```

        # Check if there is a period ongoing until the end of the data
        if prev_exceed:
            duration = (day - period_start)
            duration_sum += duration
            exceed_count += 1

        average_duration = duration_sum / exceed_count if exceed_count > 0 else 0  # Determine the mean duration of the period

        countlist.append(exceed_count)
        durationlist.append(average_duration)
    return countlist, durationlist
```

*High_flow_pulses.py*

```
    import pickle
from tqdm import tqdm
from Annual_averages import *
from Annual_maximum_flow import *
from Annual_minimum_7day_flow import *
from High_flow_pulses import *
from Low_flow_pulses import *

N_areas = pd.read_excel(r'C:\Users\dstou\Documents\Civiel\Master\MscThesis\Programming\PyCharm\Catchment_characteristics\N_Discharge_Gauges.xlsx', index_col = 'ID', usecols = [0,3]).sort_index()['Catchment Area [km2]']
L_areas = pd.read_excel(r'C:\Users\dstou\Documents\Civiel\Master\MscThesis\Programming\PyCharm\Catchment_characteristics\L_Discharge_Gauges.xlsx', index_col = 'ID', usecols = [0,3]).sort_index()['Catchment Area [km2]']
B_areas = pd.read_excel(r'C:\Users\dstou\Documents\Civiel\Master\MscThesis\Programming\PyCharm\Catchment_characteristics\B_Discharge_Gauges.xlsx', index_col = 'ID', usecols = [0,3]).sort_index()['Catchment Area [km2]']
G_areas = pd.read_excel(r'C:\Users\dstou\Documents\Civiel\Master\MscThesis\Programming\PyCharm\Catchment_characteristics\G_Discharge_Gauges.xlsx', index_col = 'ID', usecols = [0,3]).sort_index()['Catchment Area [km2]']
F_areas = pd.read_excel(r'C:\Users\dstou\Documents\Civiel\Master\MscThesis\Programming\PyCharm\Catchment_characteristics\F_Discharge_Gauges.xlsx', index_col = 'ID', usecols = [0,3]).sort_index()['Catchment Area [km2]']


with open(r'C:\Users\dstou\Documents\Civiel\Master\MscThesis\Programming\Data\PROCESSABLE_DATA\Fdataframes.pkl', 'rb') as file:
    Fdataframes = pickle.load(file)
with open(r'C:\Users\dstou\Documents\Civiel\Master\MscThesis\Programming\Data\PROCESSABLE_DATA\Bdataframes.pkl', 'rb') as file:
    Bdataframes = pickle.load(file)
with open(r'C:\Users\dstou\Documents\Civiel\Master\MscThesis\Programming\Data\PROCESSABLE_DATA\Gdataframes.pkl', 'rb') as file:
    Gdataframes = pickle.load(file)
with open(r'C:\Users\dstou\Documents\Civiel\Master\MscThesis\Programming\Data\PROCESSABLE_DATA\Ndataframes.pkl', 'rb') as file:
    Ndataframes = pickle.load(file)
with open(r'C:\Users\dstou\Documents\Civiel\Master\MscThesis\Programming\Data\PROCESSABLE_DATA\Ldataframes.pkl', 'rb') as file:
    Ldataframes = pickle.load(file)

"Function written to calculate all the signatures at once" \
"Input = Dictionary with the raw dataframes (grouped by country)" \
"Output = Dictionary containing the dataframes with all of the signatures determined annually"
def Calculate_all_signatures(dict,areas):
    signatures = {} # Create a dictionary like the pre-processed unanalysed dataframe dictionary
    # Loop through the input dictionary
    for identifier, area_value in zip(dict.keys(), tqdm(areas)):
        if not pd.isna(area_value):  # Check if the area_value is not NaN
            df = dict[identifier]
            Annual_maxima, Maxima_dates = Annual_maximum_flows(df)  # Calculate Annual maxima and julian dates
```

```
            Annual_minima, Julian_dates_minima = Annual_7day_minimum(df)  # Calculate Annual 7-day minima and Julian dates
            averages, years = Annual_averages(df)  # Calculate annual averages and the corresponding year (to be used as indices)
            High_flow_counts, High_flow_duration = High_pulse_statistics(df)  # Calculate high flow pulse counts and mean durations
            Low_flow_counts, Low_flow_duration = Low_pulse_statistics(df)  # Calculate low flow pulse counts and mean durations

            averages = (averages / 1000 / area_value) * 86400  # Normalize Qavg by dividing it by the catchment area. Then convert to mm
            Annual_maxima = (Annual_maxima / 1000 / area_value) * 86400  # Normalize AMF by dividing it by the catchment area. Then convert to
            Annual_minima = (Annual_minima / 1000 / area_value) * 86400  # Normalize AmF7 by dividing it by the catchment area. Then convert to mm

            # Create dataframe, using the years as index values. Append all signatures
            dfS = pd.DataFrame(data=averages, index=years)
            dfS['Annual maximum flow [mm]'] = Annual_maxima
            dfS['Julian date of AMF [-]'] = Maxima_dates
            dfS['Annual minimum 7-day flow [mm]'] = Annual_minima
            dfS['Julian date of AmF7 [-]'] = Julian_dates_minima
            dfS['High flow pulse count [count/year]'] = High_flow_counts
            dfS['High flow pulse duration [days]'] = High_flow_duration
            dfS['Low flow pulse count [count/year]'] = Low_flow_counts
            dfS['Low flow pulse duration [days]'] = Low_flow_duration

            # Write the dataframe in the dictionary using the identifier as the key
            signatures[identifier] = dfS
    return signatures

Bdataframes_signatures = Calculate_all_signatures(Bdataframes, B_areas)
Gdataframes_signatures = Calculate_all_signatures(Gdataframes, G_areas)
Ndataframes_signatures = Calculate_all_signatures(Ndataframes, N_areas)
Ldataframes_signatures = Calculate_all_signatures(Ldataframes, L_areas)
Fdataframes_signatures = Calculate_all_signatures(Fdataframes, F_areas)


# Write dataframes into local files
with open(r'C:\Users\dstou\Documents\Civiel\Master\MscThesis\Programming\Data\PROCESSABLE_DATA\Fdataframes_signatures0.pkl','wb') as file:
    pickle.dump(Fdataframes_signatures, file)

with open(r'C:\Users\dstou\Documents\Civiel\Master\MscThesis\Programming\Data\PROCESSABLE_DATA\Bdataframes_signatures0.pkl','wb') as file:
    pickle.dump(Bdataframes_signatures, file)

with open(r'C:\Users\dstou\Documents\Civiel\Master\MscThesis\Programming\Data\PROCESSABLE_DATA\Gdataframes_signatures0.pkl','wb') as file:
    pickle.dump(Gdataframes_signatures, file)

with open(r'C:\Users\dstou\Documents\Civiel\Master\MscThesis\Programming\Data\PROCESSABLE_DATA\Ndataframes_signatures0.pkl','wb') as file:
    pickle.dump(Ndataframes_signatures, file)

with open(r'C:\Users\dstou\Documents\Civiel\Master\MscThesis\Programming\Data\PROCESSABLE_DATA\Ldataframes_signatures0.pkl','wb') as file:
    pickle.dump(Ldataframes_signatures, file)
```

*Calculate_signatures.py*

```
    from pymannkendall import original_test
import numpy as np
""" All trends slopes, except for the timing signatures, are calculated by using the original_test from the pymannkendall package"""


def MannKenndallAMF(dict):
    slopelist = []
    plist = []
```

```
    taulist = []
    slist = []
    meanlist = []

    for identifier in dict:
        df = dict[identifier]
        result = original_test(df['Annual maximum flow [mm]'], alpha=0.10)
        slopelist.append(result[7])
        meanlist.append(np.mean(df['Annual maximum flow [mm]']))
        plist.append(result[2])
        taulist.append(result[4])
        slist.append(result[5])
    return slopelist, plist, taulist, slist, meanlist

def MannKenndallADF(dict):
    slopelist = []
    plist = []
    taulist = []
    slist = []
    meanlist = []

    for identifier in dict:
        df = dict[identifier]
        result = original_test(df['Average annual flow [m3/s]'], alpha=0.10)
        slopelist.append(result[7])
        meanlist.append(np.mean(df['Average annual flow [m3/s]']))
        plist.append(result[2])
        taulist.append(result[4])
        slist.append(result[5])
    return slopelist, plist, taulist, slist, meanlist

def MannKenndallAmF7(dict):
    slopelist = []
    plist = []
    taulist = []
    slist = []
    meanlist = []

    for identifier in dict:
        df = dict[identifier]
        result = original_test(df['Annual minimum 7-day flow [mm]'], alpha=0.10)
        slopelist.append(result[7])
        meanlist.append(np.mean(df['Annual minimum 7-day flow [mm]']))
        plist.append(result[2])
        taulist.append(result[4])
        slist.append(result[5])
    return slopelist, plist, taulist, slist, meanlist

def MannKenndallHFPD(dict):
    slopelist = []
    plist = []
    taulist = []
    slist = []
    meanlist = []

    for identifier in dict:
        df = dict[identifier]
        result = original_test(df['High flow pulse duration [days]'], alpha=0.10)
        slopelist.append(result[7])
        meanlist.append(np.mean(df['High flow pulse duration [days]']))
        plist.append(result[2])
        taulist.append(result[4])
        slist.append(result[5])
    return slopelist, plist, taulist, slist, meanlist

def MannKenndallHFPC(dict):
    slopelist = []
    plist = []
    taulist = []
    slist = []
    meanlist = []
```

```
80
81      for identifier in dict:
82          df = dict[identifier]
83          result = original_test(df['High flow pulse count [count/year]'], alpha=0.10)
84          slopelist.append(result[7])
85          meanlist.append(np.mean(df['High flow pulse count [count/year]']))
86          plist.append(result[2])
87          taulist.append(result[4])
88          slist.append(result[5])
89      return slopelist, plist, taulist, slist, meanlist
90
91  def MannKenndallLFPD(dict):
92      slopelist = []
93      plist = []
94      taulist = []
95      slist = []
96      meanlist = []
97
98      for identifier in dict:
99          df = dict[identifier]
100         result = original_test(df['Low flow pulse duration [days]'], alpha=0.10)
101         slopelist.append(result[7])
102         meanlist.append(np.mean(df['Low flow pulse duration [days]']))
103         plist.append(result[2])
104         taulist.append(result[4])
105         slist.append(result[5])
106     return slopelist, plist, taulist, slist, meanlist
107
108 def MannKenndallLFPC(dict):
109     slopelist = []
110     plist = []
111     taulist = []
112     slist = []
113     meanlist = []
114
115     for identifier in dict:
116         df = dict[identifier]
117         result = original_test(df['Low flow pulse count [count/year]'], alpha=0.10)
118         slopelist.append(result[7])
119         meanlist.append(np.mean(df['Low flow pulse count [count/year]']))
120         plist.append(result[2])
121         taulist.append(result[4])
122         slist.append(result[5])
123     return slopelist, plist, taulist, slist, meanlist
```

*MannKendall.py*

```
1       import numpy as np
2   from tqdm import *
3   from pymannkendall import original_test
4   "Function written to determine the circular statistics of the timing signatures"
5   "Input: Julian dates and the days in the corresponding years"
6   "Output: Average date of occurrence(D), concentration around the average date(R), the angular
        values (theta) and the Theil slope estimator"
7
8
9   def determine_circular_statisticsAMF(dict):
10      betalist = []
11      plist = []
12
13      for identifier in tqdm(dict):
14          df = dict[identifier]
15          timing = df['Julian date of AMF [-]']
16          "Determine the number of days in each year"
17          years = timing.index
18
19          m = 365.25  # Average number of days in a year
20
21
22          "Calculate the estimated trend in timing using Theil-Sen slope estimator"
```

```
        theil_combinations = []  # Create an empty list to store all the combinations in
        for i in timing.index:
            for j in timing.index:  # Double for loop to capture all the possible pairs of years
                if j != i:  # if statement to skip pairs where the years are identical, to avoid errors
                    if timing[j] - timing[i] >= m / 2:
                        k = -m
                    elif timing[j] - timing[i] <= -m / 2:
                        k = m
                    else:
                        k = 0  # k makes the adjustment for the circular nature of the dates
                    combination = ((timing[j] - timing[i] + k) / (j - i))  # Calculate the difference in timing between a pair of years
                    theil_combinations.append(combination)  # Append the difference in timing to the list
        beta= np.median(theil_combinations)  # Calculate the slope estimator by taking the median of all the combinations

        trend_MK = original_test(timing, alpha=0.10)
        p = trend_MK[2]

        betalist.append(beta)
        plist.append(p)

    return betalist, plist

def determine_circular_statisticsAmF7(dict):
    betalist = []
    plist = []

    for identifier in tqdm(dict):
        df = dict[identifier]
        timing = df['Julian date of AmF7 [-]']
        "Determine the number of days in each year"
        years = timing.index

        m = 365.25  # Average number of days in a year


        "Calculate the estimated trend in timing using Theil-Sen slope estimator"
        theil_combinations = []  # Create an empty list to store all the combinations in
        for i in timing.index:
            for j in timing.index:  # Double for loop to capture all the possible pairs of years
                if j != i:  # if statement to skip pairs where the years are identical, to avoid errors
                    if timing[j] - timing[i] >= m / 2:
                        k = -m
                    elif timing[j] - timing[i] <= -m / 2:
                        k = m
                    else:
                        k = 0  # k makes the adjustment for the circular nature of the dates
                    combination = ((timing[j] - timing[i] + k) / (j - i))  # Calculate the difference in timing between a pair of years
                    theil_combinations.append(combination)  # Append the difference in timing to the list
        beta= np.median(theil_combinations)  # Calculate the slope estimator by taking the median of all the combinations

        trend_MK = original_test(timing, alpha=0.10)
        p = trend_MK[2]

        betalist.append(beta)
        plist.append(p)

    return betalist, plist


def calculate_Z_circular(data):
    # Convert the pandas Series to a NumPy array
```

```
    data_array = data.to_numpy()

    n = len(data_array)
    m = 365.25
    S = 0
    for i in range(n - 1):
        for j in range(i + 1, n):
            if data_array[j] - data_array[i] >= m / 2:
                k = -m
            elif data_array[j] - data_array[i] <= -m / 2:
                k = m
            else:
                k = 0  # k makes the adjustment for the circular nature of the dates
            S += np.sign(data_array[j] - data_array[i] + k)

    var_S = (n * (n - 1) * ((2 * n) + 5)) / 18

    if var_S == 0:
        Z = 0
    else:
        if S == 0:
            Z = 0
        elif S < 0:
            Z = (S - 1) / np.sqrt(var_S)
        elif S > 0:
            Z = (S + 1) / np.sqrt(var_S)

    return Z
```

*Circular_statistics.py*

```
    from Filter_timeseries_dates import filter_timeseries_by_year
from Signatures_and_catchments import *
import numpy as np
import pandas as pd
from tqdm import *
from Circular_statistics import calculate_Z_circular

"Function written to create a heatmap based on the combination of start and end years" \
"Only uses gauges available for the fifth period"

filtered_signatures_B = filter_timeseries_by_year(B_signatures, B_id, 1960, 2019)[0]
filtered_signatures_F = filter_timeseries_by_year(F_signatures, F_id, 1960, 2019)[0]
filtered_signatures_G = filter_timeseries_by_year(G_signatures, G_id, 1960, 2019)[0]
filtered_signatures_L = filter_timeseries_by_year(L_signatures, L_id, 1960, 2019)[0]
filtered_signatures_N = filter_timeseries_by_year(N_signatures, N_id, 1960, 2019)[0]

# Create an empty dictionary to store the combined result
combined_signatures = {}

# Update the combined dictionary with individual dictionaries
combined_signatures.update(filtered_signatures_B)
combined_signatures.update(filtered_signatures_F)
combined_signatures.update(filtered_signatures_G)
combined_signatures.update(filtered_signatures_L)
combined_signatures.update(filtered_signatures_N)


def calculate_heatmap_dataframe_timing(signature):
    # Define the index and column values
    end_years = list(range(1980, 2020))  # Reversed end years (2020 to 1980)
    start_years = list(range(1960, 2000))

    # Create an empty DataFrame with specified index and columns
    heatmap_data = pd.DataFrame(index=end_years[::-1], columns=start_years)

    for start_year in tqdm(start_years):
        for i in range(40):
            end_year = min(2019, (start_year + 20 + i))
            zlist = []
```

```
            for identifier in combined_signatures:
                df = combined_signatures[identifier]
                filtered_df = df[(df.index >= start_year) & (df.index <= end_year)]
                sig = filtered_df[signature]
                z = calculate_Z_circular(sig)
                zlist.append(z)
                if end_year == 2020:
                    break
            average_z = np.average(zlist)
            heatmap_data.at[end_year, start_year] = average_z

    # Replace NaN values with 0
    heatmap_data_filled = heatmap_data.fillna(0)
    return heatmap_data_filled


timing_names = ['Julian date of AmF7 [-]', 'Julian date of AMF [-]']
heatmap_dict = {}

for name in timing_names:
    heatmap_df = calculate_heatmap_dataframe_timing(name)
    heatmap_dict[name] = heatmap_df
```

*heatmap_Z_timing.py*

```
    from Filter_timeseries_dates import filter_timeseries_by_year
from Signatures_and_catchments import *
import numpy as np
import pandas as pd
from tqdm import *
from pymannkendall import original_test
from Circular_statistics import calculate_Z_circular

"Function written to create a heatmap based on the combination of start and end years" \
"Only uses gauges available for the fifth period"

filtered_signatures_B = filter_timeseries_by_year(B_signatures, B_id, 1960, 2019)[0]
filtered_signatures_F = filter_timeseries_by_year(F_signatures, F_id, 1960, 2019)[0]
filtered_signatures_G = filter_timeseries_by_year(G_signatures, G_id, 1960, 2019)[0]
filtered_signatures_L = filter_timeseries_by_year(L_signatures, L_id, 1960, 2019)[0]
filtered_signatures_N = filter_timeseries_by_year(N_signatures, N_id, 1960, 2019)[0]

# Create an empty dictionary to store the combined result
combined_signatures = {}

# Update the combined dictionary with individual dictionaries
combined_signatures.update(filtered_signatures_B)
combined_signatures.update(filtered_signatures_F)
combined_signatures.update(filtered_signatures_G)
combined_signatures.update(filtered_signatures_L)
combined_signatures.update(filtered_signatures_N)

def calculate_heatmap_dataframe(signature):
    # Define the index and column values
    end_years = list(range(1980, 2020))  # Reversed end years (2020 to 1980)
    start_years = list(range(1960, 2000))

    # Create an empty DataFrame with specified index and columns
    heatmap_data = pd.DataFrame(index=end_years[::-1], columns=start_years)

    for start_year in tqdm(start_years):
        for i in range(40):
            end_year = min(2019, (start_year + 20 + i))
            zlist = []
            for identifier in combined_signatures:
                df = combined_signatures[identifier]
                filtered_df = df[(df.index >= start_year) & (df.index <= end_year)]
                sig = filtered_df[signature]
                z = original_test(sig, alpha=0.10)[3]
                zlist.append(z)
```

```
                if end_year == 2020:
                    break
            average_z = np.average(zlist)
            heatmap_data.at[end_year, start_year] = average_z

    # Replace NaN values with 0
    heatmap_data_filled = heatmap_data.fillna(0)
    return heatmap_data_filled

def calculate_heatmap_dataframe_timing(signature):
    # Define the index and column values
    end_years = list(range(1980, 2020))  # Reversed end years (2020 to 1980)
    start_years = list(range(1960, 2000))

    # Create an empty DataFrame with specified index and columns
    heatmap_data = pd.DataFrame(index=end_years[::-1], columns=start_years)

    for start_year in tqdm(start_years):
        for i in range(40):
            end_year = min(2019, (start_year + 20 + i))
            zlist = []
            for identifier in combined_signatures:
                df = combined_signatures[identifier]
                filtered_df = df[(df.index >= start_year) & (df.index <= end_year)]
                sig = filtered_df[signature]
                z = calculate_Z_circular(sig)
                zlist.append(z)
                if end_year == 2020:
                    break
            average_z = np.average(zlist)
            heatmap_data.at[end_year, start_year] = average_z

    # Replace NaN values with 0
    heatmap_data_filled = heatmap_data.fillna(0)
    return heatmap_data_filled

timing_names = ['Julian date of AmF7 [-]', 'Julian date of AMF [-]']
names = ['Annual minimum 7-day flow [mm]', 'Average annual flow [m3/s]', 'Annual maximum flow
     [mm]', 'Low flow pulse count [count/year]', 'High flow pulse count [count/year]', 'Low
    flow pulse duration [days]', 'High flow pulse duration [days]']
heatmap_dict ={}

for name in timing_names:
    heatmap_df = calculate_heatmap_dataframe_timing(name)
    heatmap_dict[name] = heatmap_df
for name in names:
    heatmap_df = calculate_heatmap_dataframe(name)
    heatmap_dict[name] = heatmap_df

with open(r'C:\Users\dstou\Documents\Civiel\Master\MscThesis\Programming\PyCharm\Results\
    Heatmaps\Heatmaps_z_average','wb') as file:
    pickle.dump(heatmap_dict, file)
```

*Sensitivity_heatmap.py*

```
    def filter_timeseries_by_year(dict, IDframe, start_year, end_year):
    filtered_dictionary = {}  # Create a new empty dictionary
    ID = IDframe
    for identifier, idframe in zip(dict, ID.iterrows()):
        df = dict[identifier]
        years = df.index
        idx, row = idframe

        # Check if both start_year and end_year are present in the years list
        if (start_year in years) and (end_year in years):
            # Filter the dataframe to keep only data between start_year and end_year
            filtered_df = df[(df.index >= start_year) & (df.index <= end_year)]

            # Update the filtered dictionary and saved_entries list
            filtered_dictionary[identifier] = filtered_df
```

```
        else:
            ID = ID.drop(idx)
    return filtered_dictionary, ID
```

*Filter_timeseries_dates.py*

```
    from Circular_statistics import determine_circular_statisticsAMF
from Circular_statistics import determine_circular_statisticsAmF7
from Filter_timeseries_dates import filter_timeseries_by_year
from MannKenndall import *
from Signatures_and_catchments import *

"Function to perform the full-scale trend analysis on all of the selected signatures"
"Input: Catchment dataframes, Signatures dictionary, first and final year of the desired period"
"Output: Catchment dataframe containing the desired trend parameters for the selected signatures"

def full_scale_trend_analysis(signatures_dictionary, catchments_dataframe, start_year, end_year):

    'First begin with filtering both the signatures dictionary and catchments dataframe to ensure they are the same length'
    filtered_signatures, catchments_filtered = filter_timeseries_by_year(signatures_dictionary, catchments_dataframe, start_year, end_year)

    results = catchments_filtered.copy()

    results['beta_AMF_timing'], results['p_AMF_timing'] = determine_circular_statisticsAMF(filtered_signatures)
    results['beta_AmF7_timing'], results['p_AmF7_timing'] = determine_circular_statisticsAmF7(filtered_signatures)

    results['beta AMF'], results['p AMF'], results['tau AMF'], results['s AMF'], results['mean AMF'] = MannKenndallAMF(filtered_signatures)
    results['beta ADF'], results['p ADF'], results['tau ADF'], results['s ADF'], results['mean ADF'] = MannKenndallADF(filtered_signatures)
    results['beta AmF7'], results['p AmF7'], results['tau AmF7'], results['s AmF7'], results['mean AmF7'] = MannKenndallAmF7(filtered_signatures)
    results['beta HFPC'], results['p HFPC'], results['tau HFPC'], results['s HFPC'], results['mean HFPC'] = MannKenndallHFPC(filtered_signatures)
    results['beta HFPD'], results['p HFPD'], results['tau HFPD'], results['s HFPD'], results['mean HFPD'] = MannKenndallHFPD(filtered_signatures)
    results['beta LFPC'], results['p LFPC'], results['tau LFPC'], results['s LFPC'], results['mean LFPC'] = MannKenndallLFPC(filtered_signatures)
    results['beta LFPD'], results['p LFPD'], results['tau LFPD'], results['s LFPD'], results['mean LFPD'] = MannKenndallLFPD(filtered_signatures)

    return results

# Running of the results over period 1
results_B = full_scale_trend_analysis(B_signatures, B_id, 2000, 2019)
results_N = full_scale_trend_analysis(N_signatures, N_id, 2000, 2019)
results_G = full_scale_trend_analysis(G_signatures, G_id, 2000, 2019)
results_F = full_scale_trend_analysis(F_signatures, F_id, 2000, 2019)
results_L = full_scale_trend_analysis(L_signatures, L_id, 2000, 2019)

results_G = results_G.drop([309, 470])

results_L.to_excel(r'C:\Users\dstou\Documents\Civiel\Master\MscThesis\Programming\PyCharm\Results\Trend_Analysis\Period1\L_results.xlsx', index = False)
results_B.to_excel(r'C:\Users\dstou\Documents\Civiel\Master\MscThesis\Programming\PyCharm\Results\Trend_Analysis\Period1\B_results.xlsx', index = False)
results_G.to_excel(r'C:\Users\dstou\Documents\Civiel\Master\MscThesis\Programming\PyCharm\Results\Trend_Analysis\Period1\G_results.xlsx', index = False)
results_F.to_excel(r'C:\Users\dstou\Documents\Civiel\Master\MscThesis\Programming\PyCharm\Results\Trend_Analysis\Period1\F_results.xlsx', index = False)
results_N.to_excel(r'C:\Users\dstou\Documents\Civiel\Master\MscThesis\Programming\PyCharm\Results\Trend_Analysis\Period1\N_results.xlsx', index = False)

```

```
full_results = pd.concat([results_L, results_F, results_G, results_N, results_B])
full_results.to_excel(r'C:\Users\dstou\Documents\Civiel\Master\MscThesis\Programming\PyCharm\
    Results\Trend_Analysis\Period1\full_results.xlsx', index = False)

# Running of the results over period 2
results_B = full_scale_trend_analysis(B_signatures, B_id, 1990, 2019)
results_N = full_scale_trend_analysis(N_signatures, N_id, 1990, 2019)
results_G = full_scale_trend_analysis(G_signatures, G_id, 1990, 2019)
results_F = full_scale_trend_analysis(F_signatures, F_id, 1990, 2019)
results_L = full_scale_trend_analysis(L_signatures, L_id, 1990, 2019)

results_G = results_G.drop([309, 470])

results_L.to_excel(r'C:\Users\dstou\Documents\Civiel\Master\MscThesis\Programming\PyCharm\
    Results\Trend_Analysis\Period2\L_results.xlsx', index = False)
results_B.to_excel(r'C:\Users\dstou\Documents\Civiel\Master\MscThesis\Programming\PyCharm\
    Results\Trend_Analysis\Period2\B_results.xlsx', index = False)
results_G.to_excel(r'C:\Users\dstou\Documents\Civiel\Master\MscThesis\Programming\PyCharm\
    Results\Trend_Analysis\Period2\G_results.xlsx', index = False)
results_F.to_excel(r'C:\Users\dstou\Documents\Civiel\Master\MscThesis\Programming\PyCharm\
    Results\Trend_Analysis\Period2\F_results.xlsx', index = False)
results_N.to_excel(r'C:\Users\dstou\Documents\Civiel\Master\MscThesis\Programming\PyCharm\
    Results\Trend_Analysis\Period2\N_results.xlsx', index = False)

full_results = pd.concat([results_L, results_F, results_G, results_N, results_B])
full_results.to_excel(r'C:\Users\dstou\Documents\Civiel\Master\MscThesis\Programming\PyCharm\
    Results\Trend_Analysis\Period2\full_results.xlsx', index = False)

# Running of the results over period 3
results_B = full_scale_trend_analysis(B_signatures, B_id, 1980, 2019)
results_N = full_scale_trend_analysis(N_signatures, N_id, 1980, 2019)
results_G = full_scale_trend_analysis(G_signatures, G_id, 1980, 2019)
results_F = full_scale_trend_analysis(F_signatures, F_id, 1980, 2019)
results_L = full_scale_trend_analysis(L_signatures, L_id, 1980, 2019)

results_G = results_G.drop([470])

results_L.to_excel(r'C:\Users\dstou\Documents\Civiel\Master\MscThesis\Programming\PyCharm\
    Results\Trend_Analysis\Period3\L_results.xlsx', index = False)
results_B.to_excel(r'C:\Users\dstou\Documents\Civiel\Master\MscThesis\Programming\PyCharm\
    Results\Trend_Analysis\Period3\B_results.xlsx', index = False)
results_G.to_excel(r'C:\Users\dstou\Documents\Civiel\Master\MscThesis\Programming\PyCharm\
    Results\Trend_Analysis\Period3\G_results.xlsx', index = False)
results_F.to_excel(r'C:\Users\dstou\Documents\Civiel\Master\MscThesis\Programming\PyCharm\
    Results\Trend_Analysis\Period3\F_results.xlsx', index = False)
results_N.to_excel(r'C:\Users\dstou\Documents\Civiel\Master\MscThesis\Programming\PyCharm\
    Results\Trend_Analysis\Period3\N_results.xlsx', index = False)

full_results = pd.concat([results_L, results_F, results_G, results_N, results_B])
full_results.to_excel(r'C:\Users\dstou\Documents\Civiel\Master\MscThesis\Programming\PyCharm\
    Results\Trend_Analysis\Period3\full_results.xlsx', index = False)

# Running of the results over period 4
results_B = full_scale_trend_analysis(B_signatures, B_id, 1970, 2019)
results_N = full_scale_trend_analysis(N_signatures, N_id, 1970, 2019)
results_G = full_scale_trend_analysis(G_signatures, G_id, 1970, 2019)
results_F = full_scale_trend_analysis(F_signatures, F_id, 1970, 2019)
results_L = full_scale_trend_analysis(L_signatures, L_id, 1970, 2019)

results_G = results_G.drop([470])

results_L.to_excel(r'C:\Users\dstou\Documents\Civiel\Master\MscThesis\Programming\PyCharm\
    Results\Trend_Analysis\Period4\L_results.xlsx', index = False)
results_B.to_excel(r'C:\Users\dstou\Documents\Civiel\Master\MscThesis\Programming\PyCharm\
    Results\Trend_Analysis\Period4\B_results.xlsx', index = False)
results_G.to_excel(r'C:\Users\dstou\Documents\Civiel\Master\MscThesis\Programming\PyCharm\
    Results\Trend_Analysis\Period4\G_results.xlsx', index = False)
results_F.to_excel(r'C:\Users\dstou\Documents\Civiel\Master\MscThesis\Programming\PyCharm\
    Results\Trend_Analysis\Period4\F_results.xlsx', index = False)
results_N.to_excel(r'C:\Users\dstou\Documents\Civiel\Master\MscThesis\Programming\PyCharm\
    Results\Trend_Analysis\Period4\N_results.xlsx', index = False)
```

```
99
100 full_results = pd.concat([results_L, results_F, results_G, results_N, results_B])
101 full_results.to_excel(r'C:\Users\dstou\Documents\Civiel\Master\MscThesis\Programming\PyCharm\
        Results\Trend_Analysis\Period4\full_results.xlsx', index = False)
102
103 # Running of the results over period 5
104 results_B = full_scale_trend_analysis(B_signatures, B_id, 1960, 2019)
105 results_N = full_scale_trend_analysis(N_signatures, N_id, 1960, 2019)
106 results_G = full_scale_trend_analysis(G_signatures, G_id, 1960, 2019)
107 results_F = full_scale_trend_analysis(F_signatures, F_id, 1960, 2019)
108 results_L = full_scale_trend_analysis(L_signatures, L_id, 1960, 2019)
109
110 results_G = results_G.drop([470])
111
112 results_L.to_excel(r'C:\Users\dstou\Documents\Civiel\Master\MscThesis\Programming\PyCharm\
        Results\Trend_Analysis\Period5\L_results.xlsx', index = False)
113 results_B.to_excel(r'C:\Users\dstou\Documents\Civiel\Master\MscThesis\Programming\PyCharm\
        Results\Trend_Analysis\Period5\B_results.xlsx', index = False)
114 results_G.to_excel(r'C:\Users\dstou\Documents\Civiel\Master\MscThesis\Programming\PyCharm\
        Results\Trend_Analysis\Period5\G_results.xlsx', index = False)
115 results_F.to_excel(r'C:\Users\dstou\Documents\Civiel\Master\MscThesis\Programming\PyCharm\
        Results\Trend_Analysis\Period5\F_results.xlsx', index = False)
116 results_N.to_excel(r'C:\Users\dstou\Documents\Civiel\Master\MscThesis\Programming\PyCharm\
        Results\Trend_Analysis\Period5\N_results.xlsx', index = False)
117
118 full_results = pd.concat([results_L, results_F, results_G, results_N, results_B])
119 full_results.to_excel(r'C:\Users\dstou\Documents\Civiel\Master\MscThesis\Programming\PyCharm\
        Results\Trend_Analysis\Period5\full_results.xlsx', index = False)
```

*Trend_analysis.py*

# B

# Tables representing distribution of trends

| | Signature: AmF7 timing | Positive trend | Negative trend | No trend | All |
|---|---|---|---|---|---|
| Period 1 | Significant | n = 35 (3.5)% | n = 13 (1.3%) | n = 0 (0%) | n = 48 (4.7%) |
| | Not significant | n = 611 (60.4)% | n = 334 (33.0%) | n = 18 (1.8%) | n = 963 (95.3%) |
| | All | n = 646 (63.9)% | n = 347 (34.3%) | n = 18 (1.8%) | n = 1011 (100%) |
| Period 2 | Significant | n = 19 (2.2)% | n = 24 (2.8%) | n = 0 (0%) | n = 43 (4.9%) |
| | Not significant | n = 433 (49.8)% | n = 354 (40.7%) | n = 40 (4.6%) | n = 827 (95.1%) |
| | All | n = 452 (52.0)% | n = 378 (43.4%) | n = 40 (4.6%) | n = 870 (100%) |
| Period 3 | Significant | n = 8 (1.2)% | n = 132 (20.2%) | n = 0 (0%) | n = 140 (21.4%) |
| | Not significant | n = 113 (17.3)% | n = 380 (58.0%) | n = 22 (3.4%) | n = 515 (78.6%) |
| | All | n = 121 (18.5)% | n = 512 (78.2%) | n = 22 (3.4%) | n = 655 (100%) |
| Period 4 | Significant | n = 6 (1.4)% | n = 103 (23.4%) | n = 0 (0%) | n = 109 (24.7%) |
| | Not significant | n = 41 (9.3)% | n = 283 (64.2%) | n = 8 (1.8%) | n = 332 (75.3%) |
| | All | n = 47 (10.7)% | n = 386 (87.5%) | n = 8 (1.8%) | n = 441 (100%) |
| Period 5 | Significant | n = 4 (1.7)% | n = 38 (16.1%) | n = 0 (0%) | n = 42 (17.8%) |
| | Not significant | n = 17 (7.2)% | n = 174 (73.7%) | n = 3 (1.3%) | n = 194 (82.2%) |
| | All | n = 21 (8.9)% | n = 212 (89.8%) | n = 3 (1.3%) | n = 236 (100%) |

**Table B.1:** Distribution of the AmF7 timing trends

| | Signature: AMF timing | Positive trend | Negative trend | No trend | All |
|---|---|---|---|---|---|
| Period 1 | Significant | n = 32 (3.2)% | n = 21 (2.1%) | n = 0 (0%) | n = 53 (5.2%) |
| | Not significant | n = 366 (36.2)% | n = 578 (57.2%) | n = 14 (1.4%) | n = 958 (94.8%) |
| | All | n = 398 (39.4)% | n = 599 (59.2%) | n = 14 (1.4%) | n = 1011 (100%) |
| Period 2 | Significant | n = 24 (2.8)% | n = 15 (1.7%) | n = 0 (0%) | n = 39 (4.5%) |
| | Not significant | n = 544 (62.5)% | n = 260 (29.9%) | n = 27 (3.1%) | n = 831 (95.5%) |
| | All | n = 568 (65.3)% | n = 275 (31.6%) | n = 27 (3.1%) | n = 870 (100%) |
| Period 3 | Significant | n = 7 (1.1)% | n = 8 (1.2%) | n = 0 (0%) | n = 15 (2.3%) |
| | Not significant | n = 212 (32.4)% | n = 388 (59.2%) | n = 40 (6.1%) | n = 640 (97.7%) |
| | All | n = 219 (33.4)% | n = 396 (60.5%) | n = 40 (6.1%) | n = 655 (100%) |
| Period 4 | Significant | n = 10 (2.3)% | n = 8 (1.8%) | n = 0 (0%) | n = 18 (4.1%) |
| | Not significant | n = 140 (31.7)% | n = 253 (57.4%) | n = 30 (6.8%) | n = 423 (95.9%) |
| | All | n = 150 (34.0)% | n = 261 (59.2%) | n = 30 (6.8%) | n = 441 (100%) |
| Period 5 | Significant | n = 26 (11.0)% | n = 7 (3.0%) | n = 0 (0%) | n = 33 (14.0%) |
| | Not significant | n = 114 (48.3)% | n = 78 (33.1%) | n = 11 (4.7%) | n = 203 (86.0%) |
| | All | n = 140 (59.3)% | n = 85 (36.0%) | n = 11 (4.7%) | n = 236 (100%) |

**Table B.2:** Distribution of the AMF timing trends

| | Signature: AmF7 magnitude | Positive trend | Negative trend | No trend | All |
|---|---|---|---|---|---|
| Period 1 | Significant | n = 7 (0.7)% | n = 535 (52.9%) | n = 0 (0%) | n = 542 (53.6%) |
| | Not significant | n = 88 (8.7)% | n = 380 (37.6%) | n = 1 (0.1%) | n = 469 (46.4%) |
| | All | n = 95 (9.4)% | n = 915 (90.5%) | n = 1 (0.1%) | n = 1011 (100%) |
| Period 2 | Significant | n = 66 (7.6)% | n = 168 (19.3%) | n = 0 (0%) | n = 234 (26.9%) |
| | Not significant | n = 253 (29.1)% | n = 373 (42.9%) | n = 10 (1.1%) | n = 636 (73.1%) |
| | All | n = 319 (36.7)% | n = 541 (62.2%) | n = 10 (1.1%) | n = 870 (100%) |
| Period 3 | Significant | n = 14 (2.1)% | n = 361 (55.1%) | n = 0 (0%) | n = 375 (57.3%) |
| | Not significant | n = 64 (9.8)% | n = 216 (33.0%) | n = 0 (0.0%) | n = 280 (42.7%) |
| | All | n = 78 (11.9)% | n = 577 (88.1%) | n = 0 (0.0%) | n = 655 (100%) |
| Period 4 | Significant | n = 30 (6.8)% | n = 146 (33.1%) | n = 0 (0%) | n = 176 (39.9%) |
| | Not significant | n = 89 (20.2)% | n = 174 (39.5%) | n = 2 (0.5%) | n = 265 (60.1%) |
| | All | n = 119 (27.0)% | n = 320 (72.6%) | n = 2 (0.5%) | n = 441 (100%) |
| Period 5 | Significant | n = 18 (7.6)% | n = 65 (27.5%) | n = 0 (0%) | n = 83 (35.2%) |
| | Not significant | n = 56 (23.7)% | n = 96 (40.7%) | n = 1 (0.4%) | n = 153 (64.8%) |
| | All | n = 74 (31.4)% | n = 161 (68.2%) | n = 1 (0.4%) | n = 236 (100%) |

**Table B.3:** Distribution of the AmF7 magnitude trends

| | Signature: ADF magnitude | Positive trend | Negative trend | No trend | All |
|---|---|---|---|---|---|
| Period 1 | Significant | n = 0 (0.0)% | n = 314 (31.1%) | n = 0 (0%) | n = 314 (31.1%) |
| | Not significant | n = 70 (6.9)% | n = 627 (62.0%) | n = 0 (0.0%) | n = 697 (68.9%) |
| | All | n = 70 (6.9)% | n = 941 (93.1%) | n = 0 (0.0%) | n = 1011 (100%) |
| Period 2 | Significant | n = 16 (1.8)% | n = 112 (12.9%) | n = 0 (0%) | n = 128 (14.7%) |
| | Not significant | n = 250 (28.7)% | n = 492 (56.6%) | n = 0 (0.0%) | n = 742 (85.3%) |
| | All | n = 266 (30.6)% | n = 604 (69.4%) | n = 0 (0.0%) | n = 870 (100%) |
| Period 3 | Significant | n = 3 (0.5)% | n = 436 (66.6%) | n = 0 (0%) | n = 439 (67.0%) |
| | Not significant | n = 19 (2.9)% | n = 197 (30.1%) | n = 0 (0.0%) | n = 216 (33.0%) |
| | All | n = 22 (3.4)% | n = 633 (96.6%) | n = 0 (0.0%) | n = 655 (100%) |
| Period 4 | Significant | n = 11 (2.5)% | n = 60 (13.6%) | n = 0 (0%) | n = 71 (16.1%) |
| | Not significant | n = 89 (20.2)% | n = 281 (63.7%) | n = 0 (0.0%) | n = 370 (83.9%) |
| | All | n = 100 (22.7)% | n = 341 (77.3%) | n = 0 (0.0%) | n = 441 (100%) |
| Period 5 | Significant | n = 6 (2.5)% | n = 39 (16.5%) | n = 0 (0%) | n = 45 (19.1%) |
| | Not significant | n = 48 (20.3)% | n = 143 (60.6%) | n = 0 (0.0%) | n = 191 (80.9%) |
| | All | n = 54 (22.9)% | n = 182 (77.1%) | n = 0 (0.0%) | n = 236 (100%) |

**Table B.4:** Distribution of the ADF magnitude trends

| | Signature: AMF magnitude | Positive trend | Negative trend | No trend | All |
|---|---|---|---|---|---|
| Period 1 | Significant | n = 9 (0.9)% | n = 111 (11.0%) | n = 0 (0%) | n = 120 (11.9%) |
| | Not significant | n = 181 (17.9)% | n = 705 (69.7%) | n = 5 (0.5%) | n = 891 (88.1%) |
| | All | n = 190 (18.8)% | n = 816 (80.7%) | n = 5 (0.5%) | n = 1011 (100%) |
| Period 2 | Significant | n = 9 (1.0)% | n = 204 (23.4%) | n = 0 (0%) | n = 213 (24.5%) |
| | Not significant | n = 147 (16.9)% | n = 506 (58.2%) | n = 4 (0.5%) | n = 657 (75.5%) |
| | All | n = 156 (17.9)% | n = 710 (81.6%) | n = 4 (0.5%) | n = 870 (100%) |
| Period 3 | Significant | n = 8 (1.2)% | n = 271 (41.4%) | n = 0 (0%) | n = 279 (42.6%) |
| | Not significant | n = 54 (8.2)% | n = 319 (48.7%) | n = 3 (0.5%) | n = 376 (57.4%) |
| | All | n = 62 (9.5)% | n = 590 (90.1%) | n = 3 (0.5%) | n = 655 (100%) |
| Period 4 | Significant | n = 27 (6.1)% | n = 20 (4.5%) | n = 0 (0%) | n = 47 (10.7%) |
| | Not significant | n = 185 (42.0)% | n = 204 (46.3%) | n = 5 (1.1%) | n = 394 (89.3%) |
| | All | n = 212 (48.1)% | n = 224 (50.8%) | n = 5 (1.1%) | n = 441 (100%) |
| Period 5 | Significant | n = 32 (13.6)% | n = 11 (4.7%) | n = 0 (0%) | n = 43 (18.2%) |
| | Not significant | n = 99 (41.9)% | n = 92 (39.0%) | n = 2 (0.8%) | n = 193 (81.8%) |
| | All | n = 131 (55.5)% | n = 103 (43.6%) | n = 2 (0.8%) | n = 236 (100%) |

**Table B.5:** Distribution of the AMF magnitude trends

| | Signature: LFPC | Positive trend | Negative trend | No trend | All |
|---|---|---|---|---|---|
| Period 1 | Significant | n = 100 (9.9)% | n = 23 (2.3%) | n = 0 (0%) | n = 123 (12.2%) |
| | Not significant | n = 369 (36.5)% | n = 211 (20.9%) | n = 308 (30.5%) | n = 888 (87.8%) |
| | All | n = 469 (46.4)% | n = 234 (23.1%) | n = 308 (30.5%) | n = 1011 (100%) |
| Period 2 | Significant | n = 68 (7.8)% | n = 69 (7.9%) | n = 0 (0%) | n = 137 (15.7%) |
| | Not significant | n = 170 (19.5)% | n = 226 (26.0%) | n = 337 (38.7%) | n = 733 (84.3%) |
| | All | n = 238 (27.4)% | n = 295 (33.9%) | n = 337 (38.7%) | n = 870 (100%) |
| Period 3 | Significant | n = 284 (43.4)% | n = 16 (2.4%) | n = 0 (0%) | n = 300 (45.8%) |
| | Not significant | n = 158 (24.1)% | n = 30 (4.6%) | n = 167 (25.5%) | n = 355 (54.2%) |
| | All | n = 442 (67.5)% | n = 46 (7.0%) | n = 167 (25.5%) | n = 655 (100%) |
| Period 4 | Significant | n = 103 (23.4)% | n = 22 (5.0%) | n = 0 (0%) | n = 125 (28.3%) |
| | Not significant | n = 103 (23.4)% | n = 35 (7.9%) | n = 178 (40.4%) | n = 316 (71.7%) |
| | All | n = 206 (46.7)% | n = 57 (12.9%) | n = 178 (40.4%) | n = 441 (100%) |
| Period 5 | Significant | n = 82 (34.7)% | n = 15 (6.4%) | n = 0 (0%) | n = 97 (41.1%) |
| | Not significant | n = 63 (26.7)% | n = 17 (7.2%) | n = 59 (25.0%) | n = 139 (58.9%) |
| | All | n = 145 (61.4)% | n = 32 (13.6%) | n = 59 (25.0%) | n = 236 (100%) |

**Table B.6:** Distribution of the LFPC trends

| | Signature: HFPC | Positive trend | Negative trend | No trend | All |
|---|---|---|---|---|---|
| Period 1 | Significant | n = 10 (1.0)% | n = 101 (10.0%) | n = 0 (0%) | n = 111 (11.0%) |
| | Not significant | n = 108 (10.7)% | n = 463 (45.8%) | n = 329 (32.5%) | n = 900 (89.0%) |
| | All | n = 118 (11.7)% | n = 564 (55.8%) | n = 329 (32.5%) | n = 1011 (100%) |
| Period 2 | Significant | n = 105 (12.1)% | n = 15 (1.7%) | n = 0 (0%) | n = 120 (13.8%) |
| | Not significant | n = 295 (33.9)% | n = 92 (10.6%) | n = 363 (41.7%) | n = 750 (86.2%) |
| | All | n = 400 (46.0)% | n = 107 (12.3%) | n = 363 (41.7%) | n = 870 (100%) |
| Period 3 | Significant | n = 7 (1.1)% | n = 73 (11.1%) | n = 0 (0%) | n = 80 (12.2%) |
| | Not significant | n = 74 (11.3)% | n = 179 (27.3%) | n = 322 (49.2%) | n = 575 (87.8%) |
| | All | n = 81 (12.4)% | n = 252 (38.5%) | n = 322 (49.2%) | n = 655 (100%) |
| Period 4 | Significant | n = 65 (14.7)% | n = 29 (6.6%) | n = 0 (0%) | n = 94 (21.3%) |
| | Not significant | n = 85 (19.3)% | n = 38 (8.6%) | n = 224 (50.8%) | n = 347 (78.7%) |
| | All | n = 150 (34.0)% | n = 67 (15.2%) | n = 224 (50.8%) | n = 441 (100%) |
| Period 5 | Significant | n = 42 (17.8)% | n = 14 (5.9%) | n = 0 (0%) | n = 56 (23.7%) |
| | Not significant | n = 41 (17.4)% | n = 17 (7.2%) | n = 122 (51.7%) | n = 180 (76.3%) |
| | All | n = 83 (35.2)% | n = 31 (13.1%) | n = 122 (51.7%) | n = 236 (100%) |

**Table B.7:** Distribution of the HFPC trends

| | Signature: LFPD | Positive trend | Negative trend | No trend | All |
|---|---|---|---|---|---|
| Period 1 | Significant | n = 510 (50.4)% | n = 3 (0.3%) | n = 0 (0%) | n = 513 (50.7%) |
| | Not significant | n = 439 (43.4)% | n = 34 (3.4%) | n = 25 (2.5%) | n = 498 (49.3%) |
| | All | n = 949 (93.9)% | n = 37 (3.7%) | n = 25 (2.5%) | n = 1011 (100%) |
| Period 2 | Significant | n = 142 (16.3)% | n = 23 (2.6%) | n = 0 (0%) | n = 165 (19.0%) |
| | Not significant | n = 451 (51.8)% | n = 219 (25.2%) | n = 35 (4.0%) | n = 705 (81.0%) |
| | All | n = 593 (68.2)% | n = 242 (27.8%) | n = 35 (4.0%) | n = 870 (100%) |
| Period 3 | Significant | n = 293 (44.7)% | n = 13 (2.0%) | n = 0 (0%) | n = 306 (46.7%) |
| | Not significant | n = 276 (42.1)% | n = 57 (8.7%) | n = 16 (2.4%) | n = 349 (53.3%) |
| | All | n = 569 (86.9)% | n = 70 (10.7%) | n = 16 (2.4%) | n = 655 (100%) |
| Period 4 | Significant | n = 112 (25.4)% | n = 17 (3.9%) | n = 0 (0%) | n = 129 (29.3%) |
| | Not significant | n = 172 (39.0)% | n = 110 (24.9%) | n = 30 (6.8%) | n = 312 (70.7%) |
| | All | n = 284 (64.4)% | n = 127 (28.8%) | n = 30 (6.8%) | n = 441 (100%) |
| Period 5 | Significant | n = 58 (24.6)% | n = 22 (9.3%) | n = 0 (0%) | n = 80 (33.9%) |
| | Not significant | n = 73 (30.9)% | n = 62 (26.3%) | n = 21 (8.9%) | n = 156 (66.1%) |
| | All | n = 131 (55.5)% | n = 84 (35.6%) | n = 21 (8.9%) | n = 236 (100%) |

**Table B.8:** Distribution of the LFPD trends

| | Signature: HFPD | Positive trend | Negative trend | No trend | All |
|---|---|---|---|---|---|
| Period 1 | Significant | n = 11 (1.1)% | n = 157 (15.5%) | n = 0 (0%) | n = 168 (16.6%) |
| | Not significant | n = 259 (25.6)% | n = 573 (56.7%) | n = 11 (1.1%) | n = 843 (83.4%) |
| | All | n = 270 (26.7)% | n = 730 (72.2%) | n = 11 (1.1%) | n = 1011 (100%) |
| Period 2 | Significant | n = 22 (2.5)% | n = 96 (11.0%) | n = 0 (0%) | n = 118 (13.6%) |
| | Not significant | n = 258 (29.7)% | n = 476 (54.7%) | n = 18 (2.1%) | n = 752 (86.4%) |
| | All | n = 280 (32.2)% | n = 572 (65.7%) | n = 18 (2.1%) | n = 870 (100%) |
| Period 3 | Significant | n = 10 (1.5)% | n = 215 (32.8%) | n = 0 (0%) | n = 225 (34.4%) |
| | Not significant | n = 80 (12.2)% | n = 346 (52.8%) | n = 4 (0.6%) | n = 430 (65.6%) |
| | All | n = 90 (13.7)% | n = 561 (85.6%) | n = 4 (0.6%) | n = 655 (100%) |
| Period 4 | Significant | n = 20 (4.5)% | n = 56 (12.7%) | n = 0 (0%) | n = 76 (17.2%) |
| | Not significant | n = 145 (32.9)% | n = 211 (47.8%) | n = 9 (2.0%) | n = 365 (82.8%) |
| | All | n = 165 (37.4)% | n = 267 (60.5%) | n = 9 (2.0%) | n = 441 (100%) |
| Period 5 | Significant | n = 6 (2.5)% | n = 45 (19.1%) | n = 0 (0%) | n = 51 (21.6%) |
| | Not significant | n = 58 (24.6)% | n = 125 (53.0%) | n = 2 (0.8%) | n = 185 (78.4%) |
| | All | n = 64 (27.1)% | n = 170 (72.0%) | n = 2 (0.8%) | n = 236 (100%) |

**Table B.9:** Distribution of the HFPD trends

| | Signature: AmF7 timing | Positive trend | Negative trend | No trend | All |
|---|---|---|---|---|---|
| Period 1 | Significant | n = 4 (1.7)% | n = 1 (0.4%) | n = 0 (0%) | n = 5 (2.1%) |
| | Not significant | n = 149 (63.4)% | n = 78 (33.2%) | n = 3 (1.3%) | n = 230 (97.9%) |
| | All | n = 153 (65.1)% | n = 79 (33.6%) | n = 3 (1.3%) | n = 235 (100%) |
| Period 2 | Significant | n = 1 (0.4)% | n = 7 (3.0%) | n = 0 (0%) | n = 8 (3.4%) |
| | Not significant | n = 115 (48.9)% | n = 102 (43.4%) | n = 10 (4.3%) | n = 227 (96.6%) |
| | All | n = 116 (49.4)% | n = 109 (46.4%) | n = 10 (4.3%) | n = 235 (100%) |
| Period 3 | Significant | n = 0 (0.0)% | n = 58 (24.7%) | n = 0 (0%) | n = 58 (24.7%) |
| | Not significant | n = 28 (11.9)% | n = 144 (61.3%) | n = 5 (2.1%) | n = 177 (75.3%) |
| | All | n = 28 (11.9)% | n = 202 (86.0%) | n = 5 (2.1%) | n = 235 (100%) |
| Period 4 | Significant | n = 2 (0.9)% | n = 59 (25.3%) | n = 0 (0%) | n = 61 (26.2%) |
| | Not significant | n = 16 (6.9)% | n = 153 (65.7%) | n = 3 (1.3%) | n = 172 (73.8%) |
| | All | n = 18 (7.7)% | n = 212 (91.0%) | n = 3 (1.3%) | n = 233 (100%) |
| Period 5 | Significant | n = 4 (1.7)% | n = 38 (16.1%) | n = 0 (0%) | n = 42 (17.8%) |
| | Not significant | n = 17 (7.2)% | n = 174 (73.7%) | n = 3 (1.3%) | n = 194 (82.2%) |
| | All | n = 21 (8.9)% | n = 212 (89.8%) | n = 3 (1.3%) | n = 236 (100%) |

**Table B.10:** Distribution of the AmF7 timing trends, using only gauges that have a record length of at least 60 years

| | Signature: AMF timing | Positive trend | Negative trend | No trend | All |
|---|---|---|---|---|---|
| Period 1 | Significant | n = 4 (1.7)% | n = 2 (0.9%) | n = 0 (0%) | n = 6 (2.6%) |
| | Not significant | n = 67 (28.5)% | n = 160 (68.1%) | n = 2 (0.9%) | n = 229 (97.4%) |
| | All | n = 71 (30.2)% | n = 162 (68.9%) | n = 2 (0.9%) | n = 235 (100%) |
| Period 2 | Significant | n = 4 (1.7)% | n = 9 (3.8%) | n = 0 (0%) | n = 13 (5.5%) |
| | Not significant | n = 131 (55.7)% | n = 81 (34.5%) | n = 10 (4.3%) | n = 222 (94.5%) |
| | All | n = 135 (57.4)% | n = 90 (38.3%) | n = 10 (4.3%) | n = 235 (100%) |
| Period 3 | Significant | n = 2 (0.9)% | n = 3 (1.3%) | n = 0 (0%) | n = 5 (2.1%) |
| | Not significant | n = 76 (32.3)% | n = 137 (58.3%) | n = 17 (7.2%) | n = 230 (97.9%) |
| | All | n = 78 (33.2)% | n = 140 (59.6%) | n = 17 (7.2%) | n = 235 (100%) |
| Period 4 | Significant | n = 5 (2.1)% | n = 5 (2.1%) | n = 0 (0%) | n = 10 (4.3%) |
| | Not significant | n = 82 (35.2)% | n = 125 (53.6%) | n = 16 (6.9%) | n = 223 (95.7%) |
| | All | n = 87 (37.3)% | n = 130 (55.8%) | n = 16 (6.9%) | n = 233 (100%) |
| Period 5 | Significant | n = 26 (11.0)% | n = 7 (3.0%) | n = 0 (0%) | n = 33 (14.0%) |
| | Not significant | n = 114 (48.3)% | n = 78 (33.1%) | n = 11 (4.7%) | n = 203 (86.0%) |
| | All | n = 140 (59.3)% | n = 85 (36.0%) | n = 11 (4.7%) | n = 236 (100%) |

**Table B.11:** Distribution of the AMF timing trends, using only gauges that have a record length of at least 60 years

| | Signature: AmF7 magnitude | Positive trend | Negative trend | No trend | All |
|---|---|---|---|---|---|
| Period 1 | Significant | n = 2 (0.9)% | n = 126 (53.6%) | n = 0 (0%) | n = 128 (54.5%) |
| | Not significant | n = 19 (8.1)% | n = 88 (37.4%) | n = 0 (0.0%) | n = 107 (45.5%) |
| | All | n = 21 (8.9)% | n = 214 (91.1%) | n = 0 (0.0%) | n = 235 (100%) |
| Period 2 | Significant | n = 21 (8.9)% | n = 47 (20.0%) | n = 0 (0%) | n = 68 (28.9%) |
| | Not significant | n = 59 (25.1)% | n = 107 (45.5%) | n = 1 (0.4%) | n = 167 (71.1%) |
| | All | n = 80 (34.0)% | n = 154 (65.5%) | n = 1 (0.4%) | n = 235 (100%) |
| Period 3 | Significant | n = 8 (3.4)% | n = 128 (54.5%) | n = 0 (0%) | n = 136 (57.9%) |
| | Not significant | n = 20 (8.5)% | n = 79 (33.6%) | n = 0 (0.0%) | n = 99 (42.1%) |
| | All | n = 28 (11.9)% | n = 207 (88.1%) | n = 0 (0.0%) | n = 235 (100%) |
| Period 4 | Significant | n = 15 (6.4)% | n = 70 (30.0%) | n = 0 (0%) | n = 85 (36.5%) |
| | Not significant | n = 46 (19.7)% | n = 101 (43.3%) | n = 1 (0.4%) | n = 148 (63.5%) |
| | All | n = 61 (26.2)% | n = 171 (73.4%) | n = 1 (0.4%) | n = 233 (100%) |
| Period 5 | Significant | n = 18 (7.6)% | n = 65 (27.5%) | n = 0 (0%) | n = 83 (35.2%) |
| | Not significant | n = 56 (23.7)% | n = 96 (40.7%) | n = 1 (0.4%) | n = 153 (64.8%) |
| | All | n = 74 (31.4)% | n = 161 (68.2%) | n = 1 (0.4%) | n = 236 (100%) |

**Table B.12:** Distribution of the AmF7 trends, using only gauges that have a record length of at least 60 years

| | Signature: ADF magnitude | Positive trend | Negative trend | No trend | All |
|---|---|---|---|---|---|
| Period 1 | Significant | n = 0 (0.0)% | n = 107 (45.5%) | n = 0 (0%) | n = 107 (45.5%) |
| | Not significant | n = 7 (3.0)% | n = 121 (51.5%) | n = 0 (0.0%) | n = 128 (54.5%) |
| | All | n = 7 (3.0)% | n = 228 (97.0%) | n = 0 (0.0%) | n = 235 (100%) |
| Period 2 | Significant | n = 3 (1.3)% | n = 32 (13.6%) | n = 0 (0%) | n = 35 (14.9%) |
| | Not significant | n = 63 (26.8)% | n = 137 (58.3%) | n = 0 (0.0%) | n = 200 (85.1%) |
| | All | n = 66 (28.1)% | n = 169 (71.9%) | n = 0 (0.0%) | n = 235 (100%) |
| Period 3 | Significant | n = 1 (0.4)% | n = 157 (66.8%) | n = 0 (0%) | n = 158 (67.2%) |
| | Not significant | n = 7 (3.0)% | n = 70 (29.8%) | n = 0 (0.0%) | n = 77 (32.8%) |
| | All | n = 8 (3.4)% | n = 227 (96.6%) | n = 0 (0.0%) | n = 235 (100%) |
| Period 4 | Significant | n = 6 (2.6)% | n = 28 (12.0%) | n = 0 (0%) | n = 34 (14.6%) |
| | Not significant | n = 35 (15.0)% | n = 164 (70.4%) | n = 0 (0.0%) | n = 199 (85.4%) |
| | All | n = 41 (17.6)% | n = 192 (82.4%) | n = 0 (0.0%) | n = 233 (100%) |
| Period 5 | Significant | n = 6 (2.5)% | n = 39 (16.5%) | n = 0 (0%) | n = 45 (19.1%) |
| | Not significant | n = 48 (20.3)% | n = 143 (60.6%) | n = 0 (0.0%) | n = 191 (80.9%) |
| | All | n = 54 (22.9)% | n = 182 (77.1%) | n = 0 (0.0%) | n = 236 (100%) |

**Table B.13:** Distribution of the ADF trends, using only gauges that have a record length of at least 60 years

| | Signature: AMF magnitude | Positive trend | Negative trend | No trend | All |
|---|---|---|---|---|---|
| Period 1 | Significant | n = 2 (0.9)% | n = 25 (10.6%) | n = 0 (0%) | n = 27 (11.5%) |
| | Not significant | n = 34 (14.5)% | n = 173 (73.6%) | n = 1 (0.4%) | n = 208 (88.5%) |
| | All | n = 36 (15.3)% | n = 198 (84.3%) | n = 1 (0.4%) | n = 235 (100%) |
| Period 2 | Significant | n = 0 (0.0)% | n = 54 (23.0%) | n = 0 (0%) | n = 54 (23.0%) |
| | Not significant | n = 29 (12.3)% | n = 150 (63.8%) | n = 2 (0.9%) | n = 181 (77.0%) |
| | All | n = 29 (12.3)% | n = 204 (86.8%) | n = 2 (0.9%) | n = 235 (100%) |
| Period 3 | Significant | n = 1 (0.4)% | n = 99 (42.1%) | n = 0 (0%) | n = 100 (42.6%) |
| | Not significant | n = 24 (10.2)% | n = 109 (46.4%) | n = 2 (0.9%) | n = 135 (57.4%) |
| | All | n = 25 (10.6)% | n = 208 (88.5%) | n = 2 (0.9%) | n = 235 (100%) |
| Period 4 | Significant | n = 14 (6.0)% | n = 13 (5.6%) | n = 0 (0%) | n = 27 (11.6%) |
| | Not significant | n = 83 (35.6)% | n = 121 (51.9%) | n = 2 (0.9%) | n = 206 (88.4%) |
| | All | n = 97 (41.6)% | n = 134 (57.5%) | n = 2 (0.9%) | n = 233 (100%) |
| Period 5 | Significant | n = 32 (13.6)% | n = 11 (4.7%) | n = 0 (0%) | n = 43 (18.2%) |
| | Not significant | n = 99 (41.9)% | n = 92 (39.0%) | n = 2 (0.8%) | n = 193 (81.8%) |
| | All | n = 131 (55.5)% | n = 103 (43.6%) | n = 2 (0.8%) | n = 236 (100%) |

**Table B.14:** Distribution of the AMF trends, using only gauges that have a record length of at least 60 years

| | Signature: LFPC | Positive trend | Negative trend | No trend | All |
|---|---|---|---|---|---|
| Period 1 | Significant | n = 20 (8.5)% | n = 4 (1.7%) | n = 0 (0%) | n = 24 (10.2%) |
| | Not significant | n = 103 (43.8)% | n = 41 (17.4%) | n = 67 (28.5%) | n = 211 (89.8%) |
| | All | n = 123 (52.3)% | n = 45 (19.1%) | n = 67 (28.5%) | n = 235 (100%) |
| Period 2 | Significant | n = 21 (8.9)% | n = 20 (8.5%) | n = 0 (0%) | n = 41 (17.4%) |
| | Not significant | n = 47 (20.0)% | n = 51 (21.7%) | n = 96 (40.9%) | n = 194 (82.6%) |
| | All | n = 68 (28.9)% | n = 71 (30.2%) | n = 96 (40.9%) | n = 235 (100%) |
| Period 3 | Significant | n = 92 (39.1)% | n = 8 (3.4%) | n = 0 (0%) | n = 100 (42.6%) |
| | Not significant | n = 67 (28.5)% | n = 8 (3.4%) | n = 60 (25.5%) | n = 135 (57.4%) |
| | All | n = 159 (67.7)% | n = 16 (6.8%) | n = 60 (25.5%) | n = 235 (100%) |
| Period 4 | Significant | n = 54 (23.2)% | n = 9 (3.9%) | n = 0 (0%) | n = 63 (27.0%) |
| | Not significant | n = 55 (23.6)% | n = 22 (9.4%) | n = 93 (39.9%) | n = 170 (73.0%) |
| | All | n = 109 (46.8)% | n = 31 (13.3%) | n = 93 (39.9%) | n = 233 (100%) |
| Period 5 | Significant | n = 82 (34.7)% | n = 15 (6.4%) | n = 0 (0%) | n = 97 (41.1%) |
| | Not significant | n = 63 (26.7)% | n = 17 (7.2%) | n = 59 (25.0%) | n = 139 (58.9%) |
| | All | n = 145 (61.4)% | n = 32 (13.6%) | n = 59 (25.0%) | n = 236 (100%) |

**Table B.15:** Distribution of the LFPC trends, using only gauges that have a record length of at least 60 years

| | Signature: HFPC | Positive trend | Negative trend | No trend | All |
|---|---|---|---|---|---|
| Period 1 | Significant | n = 2 (0.9)% | n = 19 (8.1%) | n = 0 (0%) | n = 21 (8.9%) |
| | Not significant | n = 30 (12.8)% | n = 104 (44.3%) | n = 80 (34.0%) | n = 214 (91.1%) |
| | All | n = 32 (13.6)% | n = 123 (52.3%) | n = 80 (34.0%) | n = 235 (100%) |
| Period 2 | Significant | n = 21 (8.9)% | n = 4 (1.7%) | n = 0 (0%) | n = 25 (10.6%) |
| | Not significant | n = 60 (25.5)% | n = 33 (14.0%) | n = 117 (49.8%) | n = 210 (89.4%) |
| | All | n = 81 (34.5)% | n = 37 (15.7%) | n = 117 (49.8%) | n = 235 (100%) |
| Period 3 | Significant | n = 2 (0.9)% | n = 30 (12.8%) | n = 0 (0%) | n = 32 (13.6%) |
| | Not significant | n = 25 (10.6)% | n = 69 (29.4%) | n = 109 (46.4%) | n = 203 (86.4%) |
| | All | n = 27 (11.5)% | n = 99 (42.1%) | n = 109 (46.4%) | n = 235 (100%) |
| Period 4 | Significant | n = 33 (14.2)% | n = 15 (6.4%) | n = 0 (0%) | n = 48 (20.6%) |
| | Not significant | n = 55 (23.6)% | n = 20 (8.6%) | n = 110 (47.2%) | n = 185 (79.4%) |
| | All | n = 88 (37.8)% | n = 35 (15.0%) | n = 110 (47.2%) | n = 233 (100%) |
| Period 5 | Significant | n = 42 (17.8)% | n = 14 (5.9%) | n = 0 (0%) | n = 56 (23.7%) |
| | Not significant | n = 41 (17.4)% | n = 17 (7.2%) | n = 122 (51.7%) | n = 180 (76.3%) |
| | All | n = 83 (35.2)% | n = 31 (13.1%) | n = 122 (51.7%) | n = 236 (100%) |

**Table B.16:** Distribution of the HFPC trends, using only gauges that have a record length of at least 60 years

| | Signature: LFPD | Positive trend | Negative trend | No trend | All |
|---|---|---|---|---|---|
| Period 1 | Significant | n = 109 (46.4)% | n = 2 (0.9%) | n = 0 (0%) | n = 111 (47.2%) |
| | Not significant | n = 112 (47.7)% | n = 10 (4.3%) | n = 2 (0.9%) | n = 124 (52.8%) |
| | All | n = 221 (94.0)% | n = 12 (5.1%) | n = 2 (0.9%) | n = 235 (100%) |
| Period 2 | Significant | n = 27 (11.5)% | n = 10 (4.3%) | n = 0 (0%) | n = 37 (15.7%) |
| | Not significant | n = 129 (54.9)% | n = 59 (25.1%) | n = 10 (4.3%) | n = 198 (84.3%) |
| | All | n = 156 (66.4)% | n = 69 (29.4%) | n = 10 (4.3%) | n = 235 (100%) |
| Period 3 | Significant | n = 95 (40.4)% | n = 7 (3.0%) | n = 0 (0%) | n = 102 (43.4%) |
| | Not significant | n = 100 (42.6)% | n = 25 (10.6%) | n = 8 (3.4%) | n = 133 (56.6%) |
| | All | n = 195 (83.0)% | n = 32 (13.6%) | n = 8 (3.4%) | n = 235 (100%) |
| Period 4 | Significant | n = 54 (23.2)% | n = 10 (4.3%) | n = 0 (0%) | n = 64 (27.5%) |
| | Not significant | n = 88 (37.8)% | n = 62 (26.6%) | n = 19 (8.2%) | n = 169 (72.5%) |
| | All | n = 142 (60.9)% | n = 72 (30.9%) | n = 19 (8.2%) | n = 233 (100%) |
| Period 5 | Significant | n = 58 (24.6)% | n = 22 (9.3%) | n = 0 (0%) | n = 80 (33.9%) |
| | Not significant | n = 73 (30.9)% | n = 62 (26.3%) | n = 21 (8.9%) | n = 156 (66.1%) |
| | All | n = 131 (55.5)% | n = 84 (35.6%) | n = 21 (8.9%) | n = 236 (100%) |

**Table B.17:** Distribution of the LFPD trends, using only gauges that have a record length of at least 60 years

| | Signature: HFPD | Positive trend | Negative trend | No trend | All |
|---|---|---|---|---|---|
| Period 1 | Significant | n = 0 (0.0)% | n = 52 (22.1%) | n = 0 (0%) | n = 52 (22.1%) |
| | Not significant | n = 26 (11.1)% | n = 157 (66.8%) | n = 0 (0.0%) | n = 183 (77.9%) |
| | All | n = 26 (11.1)% | n = 209 (88.9%) | n = 0 (0.0%) | n = 235 (100%) |
| Period 2 | Significant | n = 3 (1.3)% | n = 19 (8.1%) | n = 0 (0%) | n = 22 (9.4%) |
| | Not significant | n = 78 (33.2)% | n = 132 (56.2%) | n = 3 (1.3%) | n = 213 (90.6%) |
| | All | n = 81 (34.5)% | n = 151 (64.3%) | n = 3 (1.3%) | n = 235 (100%) |
| Period 3 | Significant | n = 3 (1.3)% | n = 66 (28.1%) | n = 0 (0%) | n = 69 (29.4%) |
| | Not significant | n = 23 (9.8)% | n = 143 (60.9%) | n = 0 (0.0%) | n = 166 (70.6%) |
| | All | n = 26 (11.1)% | n = 209 (88.9%) | n = 0 (0.0%) | n = 235 (100%) |
| Period 4 | Significant | n = 5 (2.1)% | n = 24 (10.3%) | n = 0 (0%) | n = 29 (12.4%) |
| | Not significant | n = 66 (28.3)% | n = 136 (58.4%) | n = 2 (0.9%) | n = 204 (87.6%) |
| | All | n = 71 (30.5)% | n = 160 (68.7%) | n = 2 (0.9%) | n = 233 (100%) |
| Period 5 | Significant | n = 6 (2.5)% | n = 45 (19.1%) | n = 0 (0%) | n = 51 (21.6%) |
| | Not significant | n = 58 (24.6)% | n = 125 (53.0%) | n = 2 (0.8%) | n = 185 (78.4%) |
| | All | n = 64 (27.1)% | n = 170 (72.0%) | n = 2 (0.8%) | n = 236 (100%) |

**Table B.18:** Distribution of the HFPD trends, using only gauges that have a record length of at least 60 years